A *qualitative* introduction to gravitational waves

Enrico Barausse

SISSA (Trieste, Italy)

H2020-MSCA-RISE-2020
GRU 101007855

ERC-2018-COG GRAMS 815673

Lectures outline

- A semi-quantitative discussion of the two body problem in General Relativity and its implications for GW emission from binaries
- The post-merger ringdown signal
- The LIGO/Virgo detections (physics & astrophysics)
- LISA and pulsar timing arrays
- Selected exotica (applications to DM/QG)

General relativity in a nutshell

$$G_{\mu\nu} \equiv R_{\mu\nu} - \frac{1}{2} g_{\mu\nu} R = 8\pi T_{\mu\nu} \quad \Longleftrightarrow \quad \nabla^2 \phi = 4\pi G \rho.$$

$$T^{\mu\nu} = (\epsilon + p) u^\mu u^\nu + p g^{\mu\nu}$$

(perfect fluid)

$$\nabla_\nu G^{\mu\nu} = 0 \quad \Longrightarrow \quad \nabla_\nu T^{\mu\nu} = 0$$

$$a^\mu = -\frac{(g^{\mu\nu} + u^\mu u^\nu)\partial_\mu p}{p + \epsilon}$$

$$u^\mu \partial_\mu \epsilon = -(p + \epsilon) \nabla_\mu u^\mu$$

For dust (p=0) Euler equation gives geodesic equation

$$a^\mu \equiv \frac{du^\mu}{d\tau} + \Gamma^\mu_{\alpha\beta} u^\alpha u^\beta = 0$$

BHs in GR have no hair

$$G^{\mu\nu} = 0$$

$$ds^2 = -\left(1 - \frac{2M}{r}\right) dt^2 + \left(1 - \frac{2M}{r}\right)^{-1} dr^2 + r^2 d\Omega^2$$

$$d\Omega^2 = d\theta^2 + \sin^2\theta d\varphi^2$$

Schwarzschild BH (parametrized by mass alone)

$$\begin{aligned} ds^2 &= -\frac{(\Delta - a^2\sin^2\theta)}{\Sigma} dt^2 - 2a\sin^2\theta \frac{(r^2 + a^2 - \Delta)}{\Sigma} dt\, d\phi \\ &+ \left(\frac{(r^2 + a^2)^2 - \Delta a^2 \sin^2\theta}{\Sigma}\right) \sin^2\theta d\phi^2 + \frac{\Sigma}{\Delta} dr^2 + \Sigma d\theta^2 \end{aligned}$$

$$\begin{aligned} \Sigma &= r^2 + a^2\cos^2\theta \\ \Delta &= r^2 - 2Mr + a^2 \end{aligned}$$

$$a = \frac{J}{M}$$

Kerr BH (parametrized by mass and spin)

Electrically charged BHs (Reissner-Nordström, Kerr-Newman) probably irrelevant astrophysical

Geodesics in Schwarzschild

Metric is static and spherically symmetric

→

Conserved energy and orbital angular momentum (per unit particle mass) E and L

$$\theta = \frac{\pi}{2}$$

$$\left(1 - \frac{2GM}{r}\right)\frac{dt}{d\lambda} = E\ ,$$

$$r^2\frac{d\phi}{d\lambda} = L\ .$$

$$\epsilon = -g_{\mu\nu}\frac{dx^\mu}{d\lambda}\frac{dx^\nu}{d\lambda}$$

$$\frac{1}{2}\left(\frac{dr}{d\lambda}\right)^2 + V(r) = \frac{1}{2}E^2\ ,$$

$$V(r) = \frac{1}{2}\epsilon - \epsilon\frac{GM}{r} + \frac{L^2}{2r^2} - \frac{GML^2}{r^3}$$

Motion in 1D potential (Newtonian + corrections!)

Geodesics in Schwarzschild

Massive particles

$$\frac{1}{2}\left(\frac{dr}{d\lambda}\right)^2 + V(r) = \frac{1}{2}E^2 \, ,$$

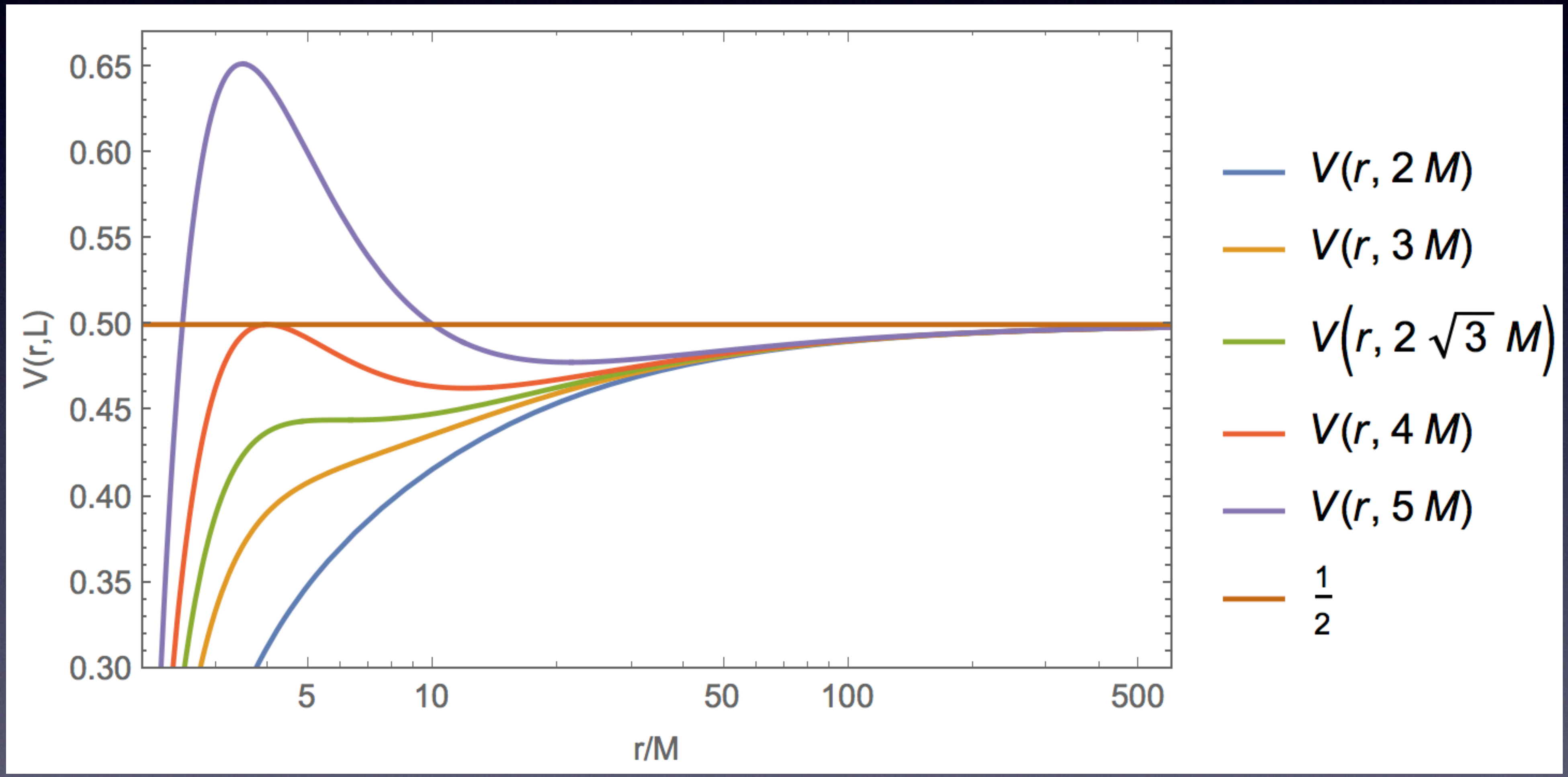

- Innermost stable circular orbit (ISCO) at r=6M
- Marginally bound orbit at r=4M
- Different than in Newtonian gravity

(circular orbits all the way down to r=0)

Geodesics in Schwarzschild

Dynamics of massless particles only depends on b=L/E

$$\frac{1}{E^2}\left(\frac{dr}{d\lambda}\right)^2 = -V = 1 - \frac{b^2}{r^2}\left(1 - \frac{2GM}{r}\right)$$

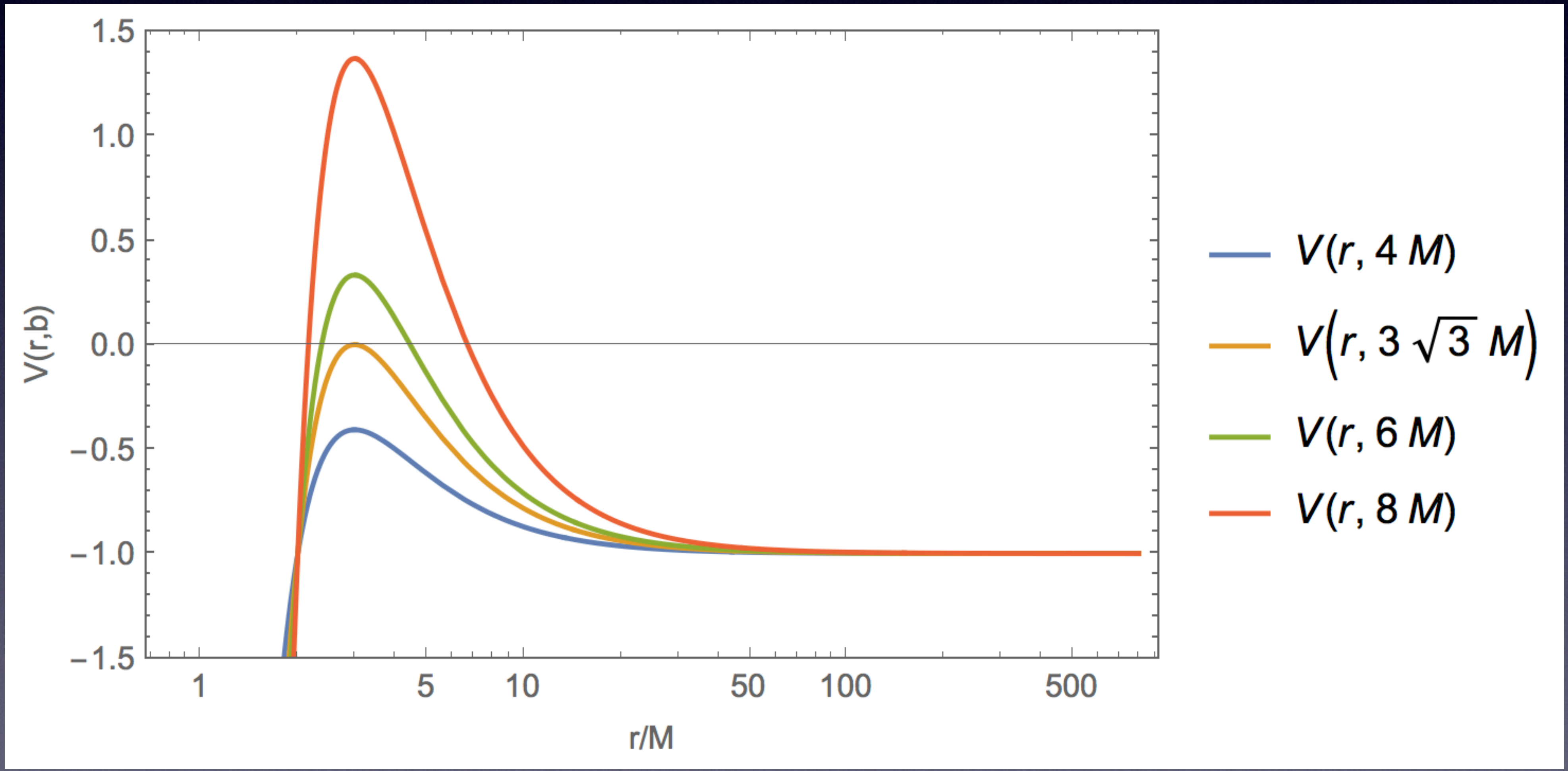

(Unstable) circular photon orbit (“light ring”) at r=3M

Peak of “potential barrier” at r=3M

Geodesics in Schwarzschild

Dynamics of massless particles only depends on b=L/E

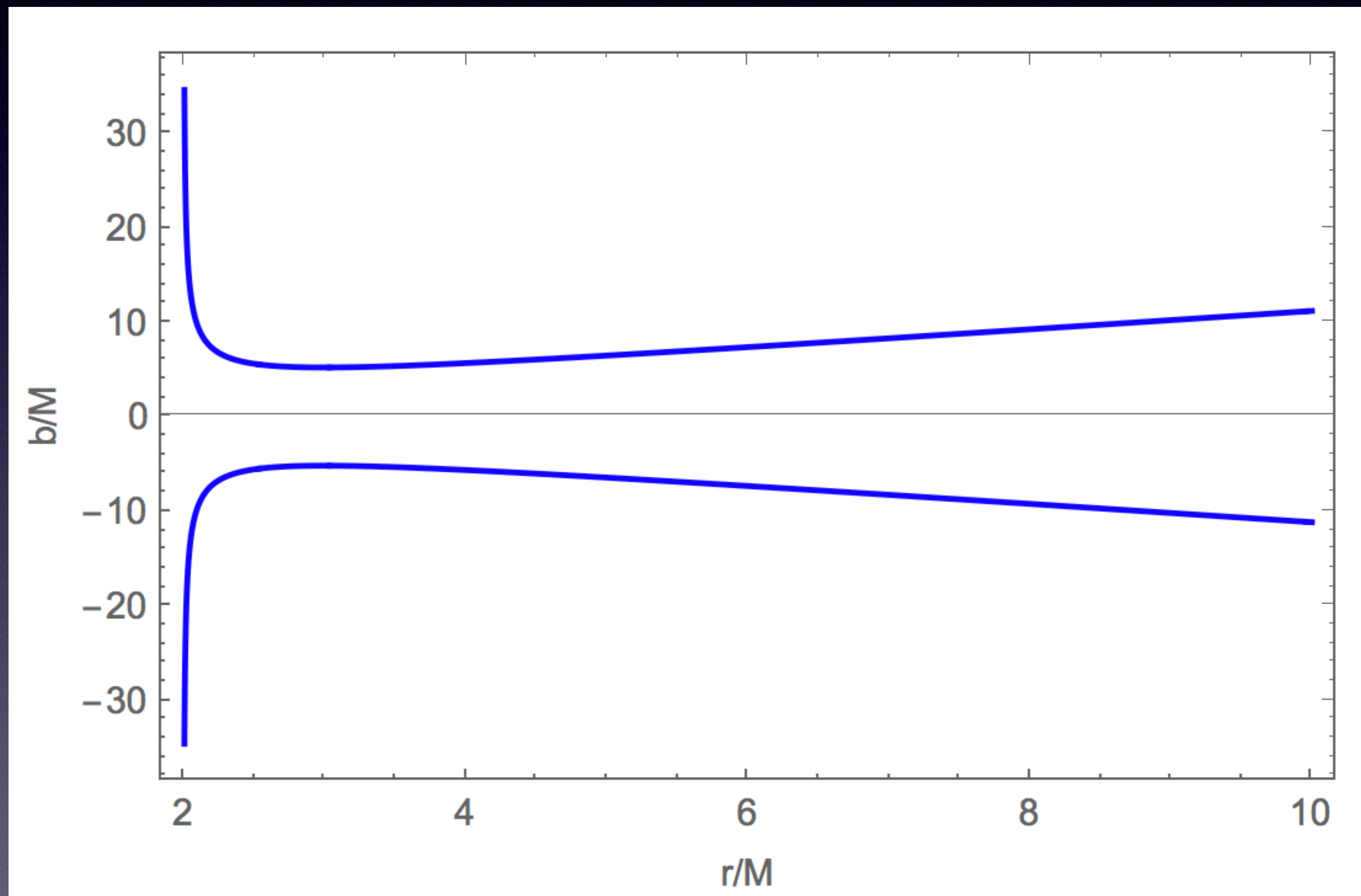

Below critical impact parameter $b = 3\sqrt{3}M$ photons fall into BH

Geodesics in Kerr

- "Separability" of geodesics equations not trivial, but possible due to presence of "hidden symmetry" that gives Carter constant Q

$$\left(\mu\frac{dr}{d\lambda}\right)^2 = V_r(r), \qquad \mu\frac{dt}{d\lambda} = V_t(r,\theta),$$

$$\left(\mu\frac{d\theta}{d\lambda}\right)^2 = V_\theta(\theta), \qquad \mu\frac{d\phi}{d\lambda} = V_\phi(r,\theta)\ ,$$

$$\Sigma \equiv r^2 + a^2\cos^2\theta, \qquad \Delta \equiv r^2 - 2Mr + a^2$$

$$\varpi^2 \equiv r^2 + a^2$$

$$V_t(r,\theta) \equiv E\left(\frac{\varpi^4}{\Delta} - a^2\sin^2\theta\right) + aL_z\left(1 - \frac{\varpi^2}{\Delta}\right),$$

$$V_r(r) \equiv \left(E\varpi^2 - aL_z\right)^2 - \Delta\left[\mu^2 r^2 + (L_z - aE)^2 + Q\right]$$

$$V_\theta(\theta) \equiv Q - L_z^2\cot^2\theta - a^2(\mu^2 - E^2)\cos^2\theta,$$

$$V_\phi(r,\theta) \equiv L_z\csc^2\theta + aE\left(\frac{\varpi^2}{\Delta} - 1\right) - \frac{a^2 L_z}{\Delta},$$

- Qualitatively same dynamics as in Schwarzschild ("light ring", ISCO, marginally bound orbits), but details depend on whether motion is prograde/retrograde

The effect of BH spins: frame-dragging in isolated BHs

Spin affects motion around BHs ("frame dragging")

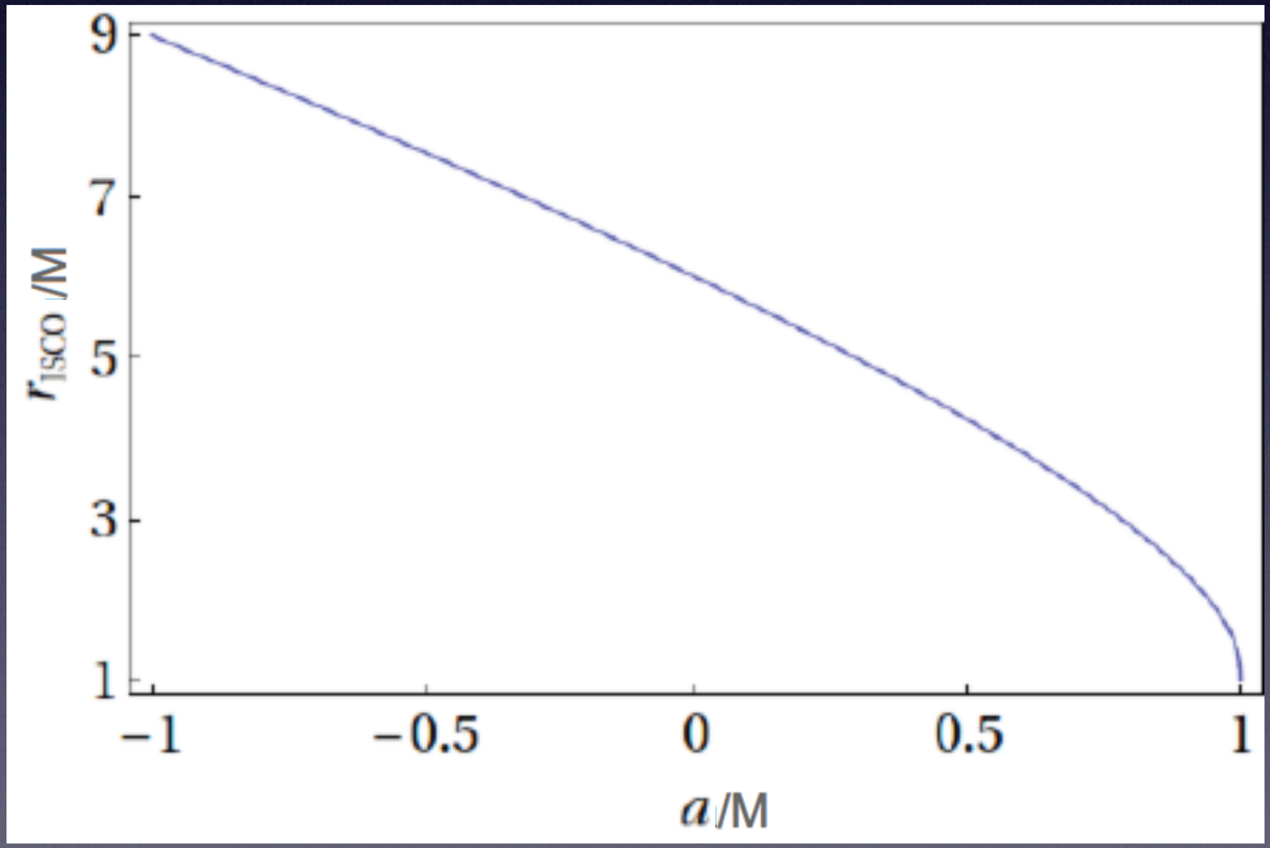

Innermost Stable Circular Orbit
(i.e. inner edge of thin disks)

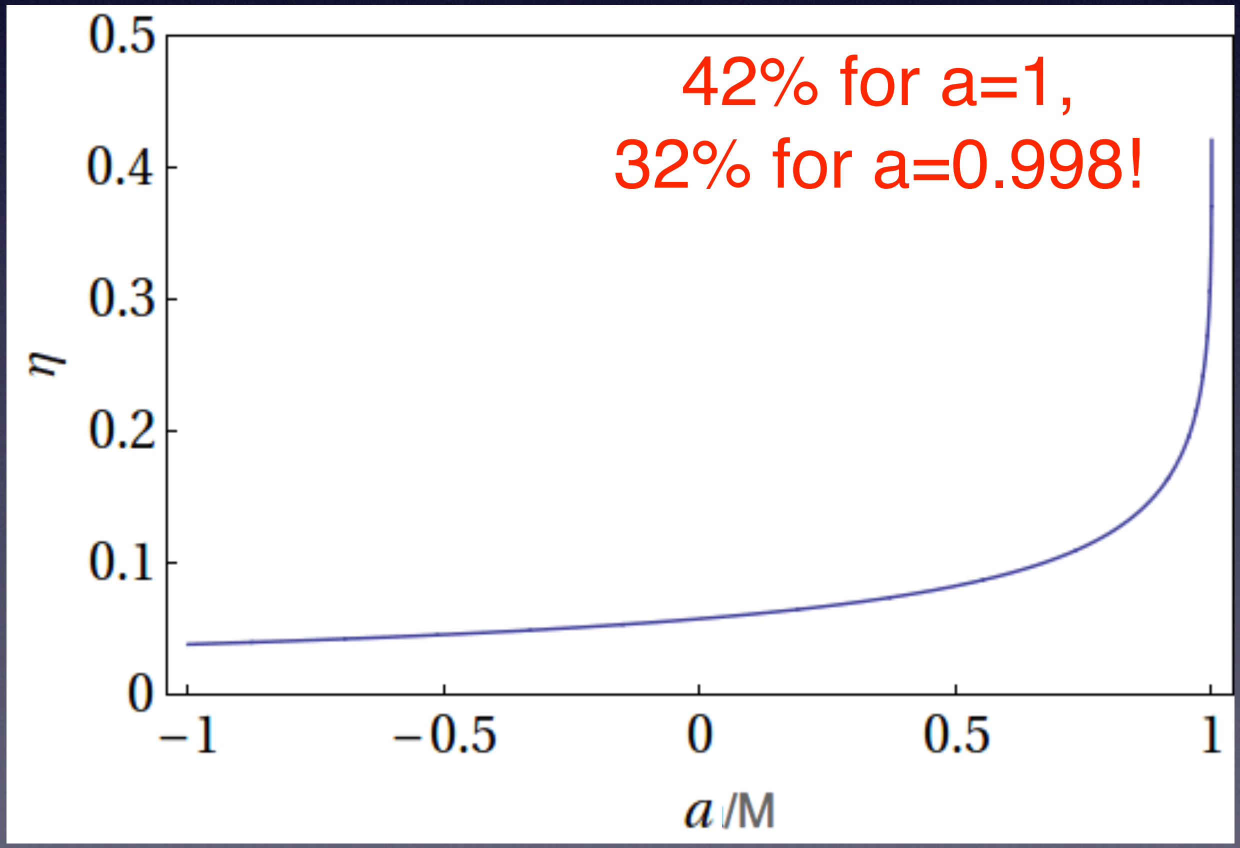

Efficiency of EM
emission from thin disks

The effect of BH spins: frame-dragging in isolated BHs

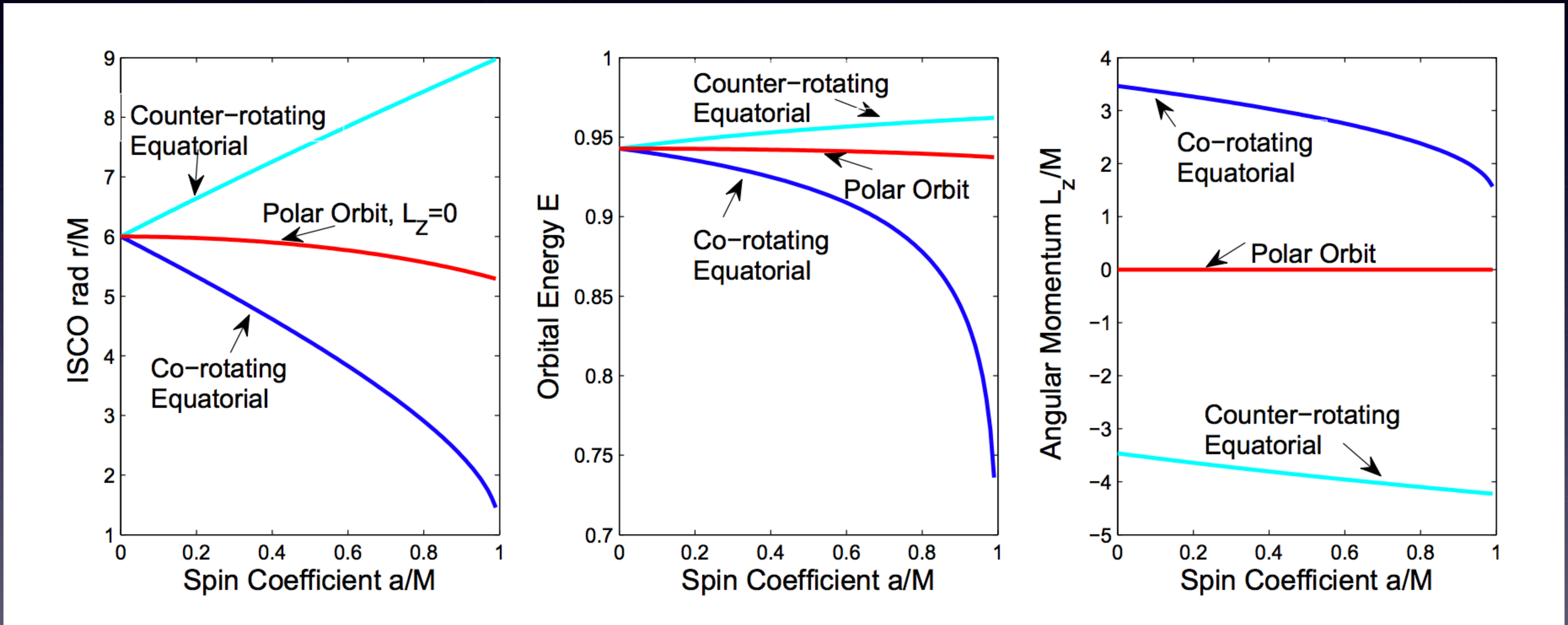

Figure from Mino & Brink 2008

EM BH spin measurements

Continuum fitting/iron-Kα lines

Binary System	$M/M_\odot$	a	Reference
4U 1543-47	9.4 ± 1.0	$0.75 - 0.85$	Shafee et al. (2006)
GRO J1655-40	6.30 ± 0.27	$0.65 - 0.75$	Shafee et al. (2006)
GRS 1915+105	14.0 ± 4.4	> 0.98	McClintock et al. (2006)
LMC X-3	$5 - 11$	< 0.26	Davis et al. (2006)
M33 X-7	15.65 ± 1.45	0.84 ± 0.05	Liu et al. (2008, 2010)
LMC X-1	10.91 ± 1.41	$0.92^{+0.05}_{-0.07}$	Gou et al. (2009)
XTE J1550-564	9.10 ± 0.61	$0.34^{+0.20}_{-0.28}$	Steiner et al. (2010b)

Stellar-mass BH spins

Object name	Galaxy type	z	L_X[erg s^{-1}]	$f_{\rm Edd}$	$\log(M_{\rm bh}[M_\odot])$	spin
1H0707-495	–	0.0411	3.7×10^{43}	1.0	6.70 ± 0.4	> 0.97
Mrk1018	S0	0.043	9.0×10^{43}	0.01	8.15	$0.58^{+0.36}_{-0.74}$
NGC4051	SAB(rs)bc	0.0023	3.0×10^{42}	0.03	6.28	> 0.99
NGC3783	SB(r)ab	0.0097	1.8×10^{44}	0.06	7.47 ± 0.08	> 0.88
1H0419-577	–	0.104	1.8×10^{44}	0.04	8.18 ± 0.05	> 0.89
3C120	S0	0.033	2.0×10^{44}	0.31	$7.74^{+0.20}_{-0.22}$	> 0.95
MCG-6-30-15	E/S0	0.008	1.0×10^{43}	0.4	6.65 ± 0.17	> 0.98
Ark564	SB	0.0247	1.4×10^{44}	0.11	< 6.90	$0.96^{+0.01}_{-0.06}$
TonS180	–	0.062	3.0×10^{44}	2.15	$7.30^{+0.60}_{-0.40}$	$0.91^{+0.02}_{-0.09}$
RBS1124	–	0.208	1.0×10^{45}	0.15	8.26	> 0.97
Mrk110	–	0.0355	1.8×10^{44}	0.16	7.40 ± 0.09	> 0.89
Mrk841	E	0.0365	8.0×10^{43}	0.44	7.90	> 0.52
Fairall9	Sc	0.047	3.0×10^{44}	0.05	8.41 ± 0.11	$0.52^{+0.19}_{-0.15}$
SWIFTJ2127.4+5654	SB0/a(s)	0.0147	1.2×10^{43}	0.18	7.18 ± 0.07	0.6 ± 0.2
Mrk79	SBb	0.0022	4.7×10^{43}	0.05	7.72 ± 0.14	0.7 ± 0.1
Mrk335	S0a	0.026	5.0×10^{43}	0.25	7.15 ± 0.13	$0.83^{+0.09}_{-0.13}$
Ark120	Sb/pec	0.0327	3.0×10^{45}	1.27	8.18 ± 0.12	$0.64^{+0.19}_{-0.11}$
Mrk359	pec	0.0174	6.0×10^{42}	0.25	6.04	$0.66^{+0.30}_{-0.54}$
IRAS13224-3809	–	0.0667	7.0×10^{43}	0.71	7.00	> 0.987
NGC1365	SB(s)b	0.0054	2.7×10^{42}	0.06	$6.60^{+1.40}_{-0.30}$	$0.97^{+0.01}_{-0.04}$

Compilations (Reynolds, Brenneman,...) of massive BH spins

The effect of BH spins: frame-dragging in binaries

- For large spins aligned with L, effective ISCO moves inward …

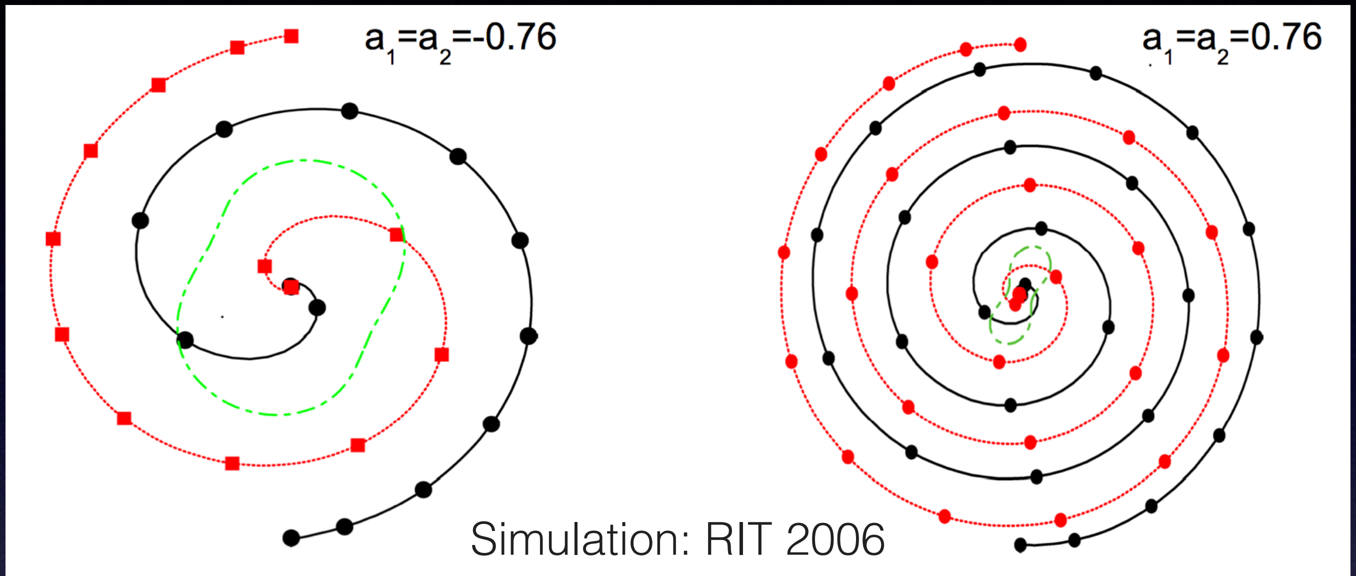

- ... and GW “efficiency” gets larger

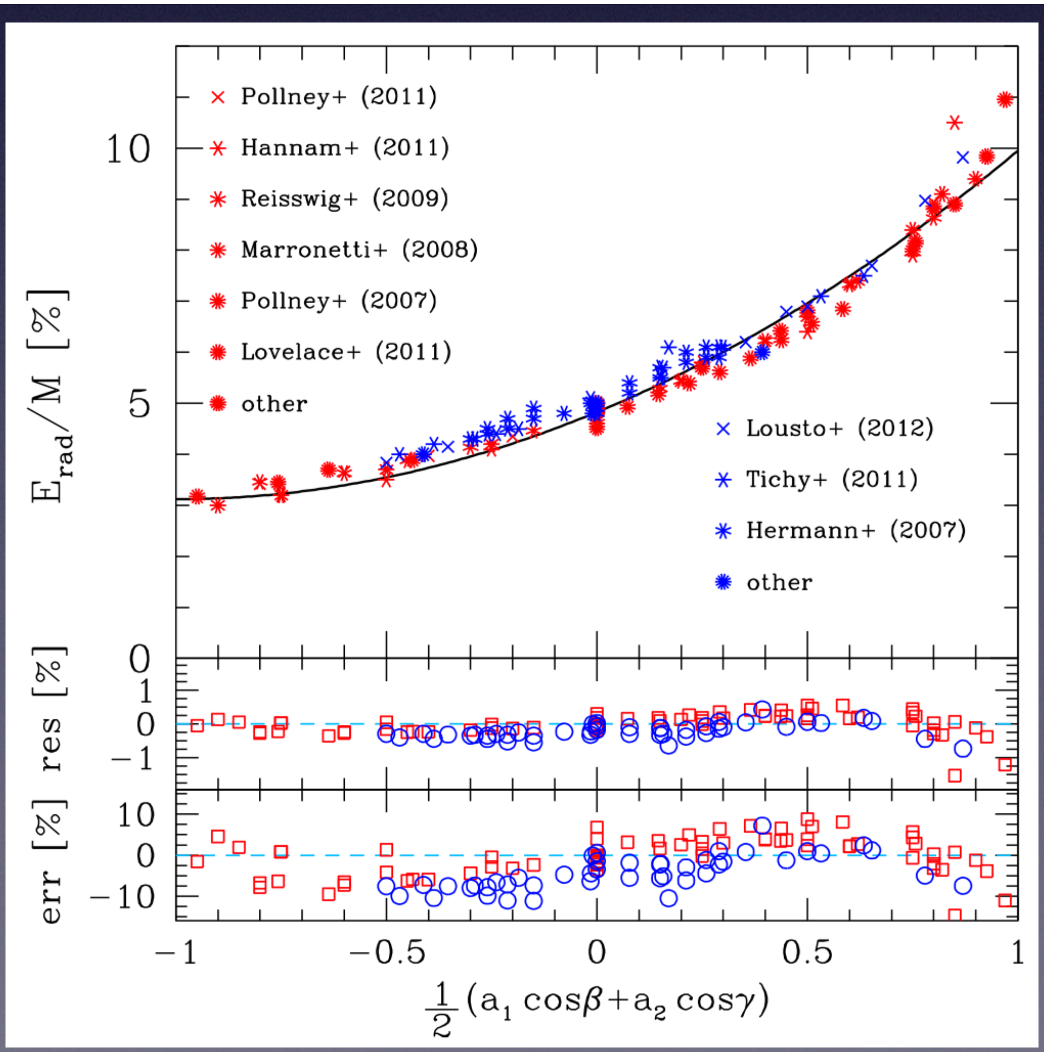

EB, Morozova & Rezzolla (2012)

Spins increase GW amplitudes

The effect of BH spins: frame-dragging in isolated BHs

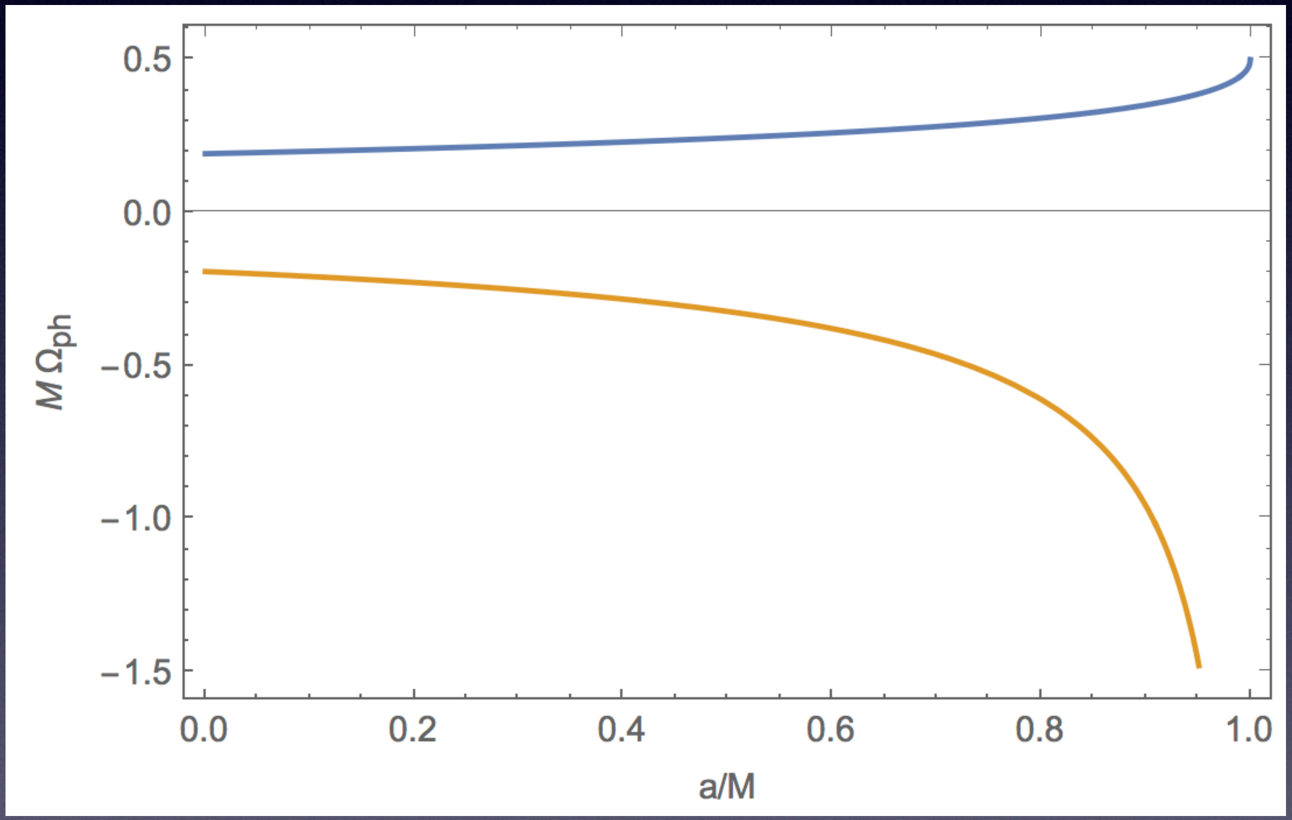

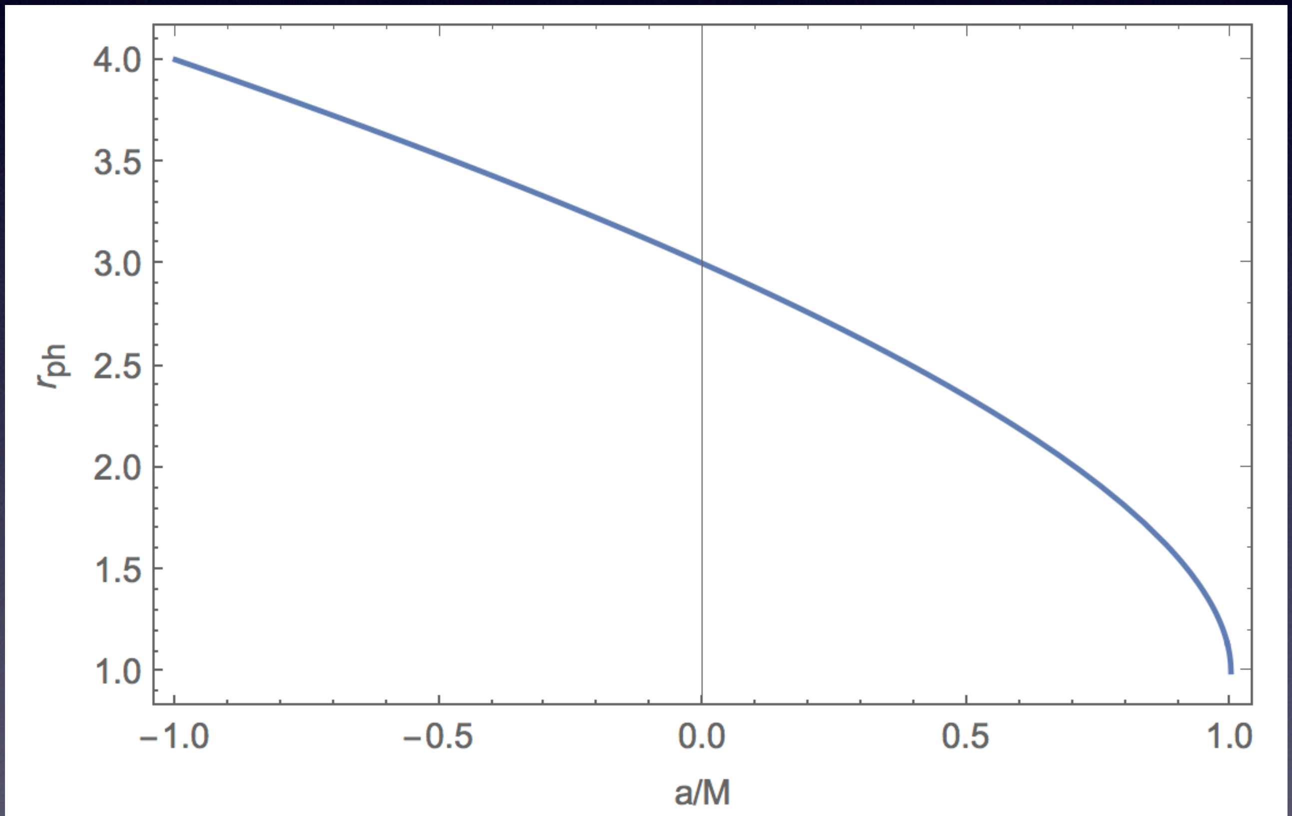

Orbital frequency of prograde circular photon orbit matches horizon's when a=M

BH shadows

Event Horizon Telescope
will image SgrA* and M87
via VLBI radio (mm wavelength)
observations

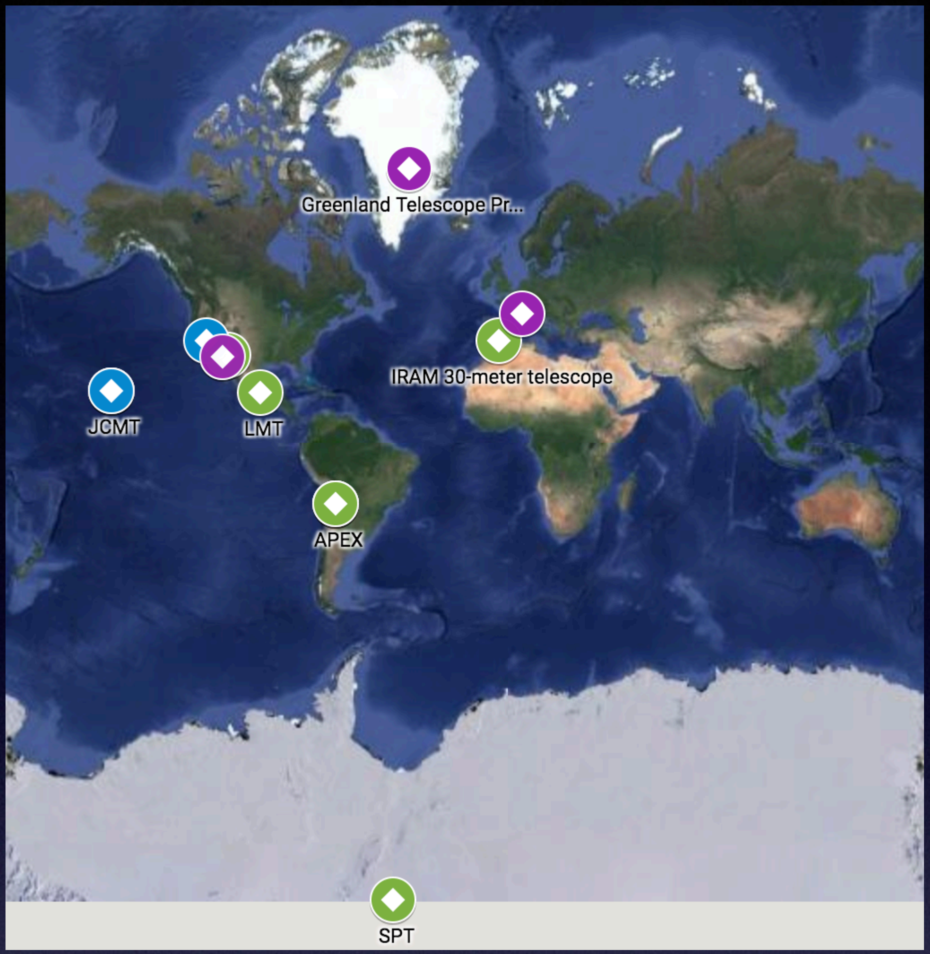

EHT collaboration 2019

BH binary dynamics

- We can rewrite geodesic motion in Schwarzschild/Kerr as Hamiltonian/Lagrangian

$$H = \beta^i P_i + \alpha\sqrt{m^2 + \gamma^{ij}\, P_i\, P_j}\,,$$

$$\begin{aligned}\alpha &= \frac{1}{\sqrt{-g^{tt}}}\,,\\ \beta^i &= \frac{g^{ti}}{g^{tt}}\,,\\ \gamma^{ij} &= g^{ij} - \frac{g^{ti}g^{tj}}{g^{tt}}\,,\end{aligned}$$

- How to go from test-particle limit to BH binary?
- In Newtonian gravity, one can go to center of mass frame and replace test-particle mass by binary's reduced mass
- At post-Newtonian orders ($O(v/c)^{2n}$ beyond Newton) things are more involved

The post-Newtonian Hamiltonian

$$H = m_1c^2 + m_2c^2 + H_N + H_{1PN} + H_{2PN} + H_{3PN} + \ldots$$

$$\hat{H} = (H - Mc^2)/\mu \qquad M = m_1 + m_2$$

$$\mu = m_1 m_2 / M \qquad \nu = \mu / M$$

$$p_r = (\mathbf{n}\cdot\mathbf{p}),\ \mathbf{q} = (\mathbf{x}_1 - \mathbf{x}_2)/GM,$$

$$\mathbf{p} = \mathbf{p}_1/\mu,\ r = r_{12} = |\mathbf{x}_1 - \mathbf{x}_2|,$$

$$\mathbf{n} = \mathbf{q}/|\mathbf{q}| \qquad \mathbf{p}_1 + \mathbf{p}_2 = 0$$

$$H^{1PN}_{S_1S_2} = \frac{G}{c^2}\sum_a \sum_{b\neq a} \frac{1}{2r_{ab}^3}\left[3(\mathbf{S}_a\cdot\mathbf{n}_{ab})(\mathbf{S}_b\cdot\mathbf{n}_{ab}) - (\mathbf{S}_a\cdot\mathbf{S}_b)\right]$$

$$H^{1PN}_{SO} = \frac{G}{c^2}\sum_a \sum_{b\neq a} \frac{1}{r_{ab}^2}(\mathbf{S}_a\times\mathbf{n}_{ab})\cdot\left[\frac{3m_b}{2m_a}\mathbf{p}_a - 2\mathbf{p}_b\right]$$

$$\begin{aligned}
\hat{H}_N &= \frac{p^2}{2} - \frac{1}{q},\\
c^2\hat{H}_{1PN} &= \frac{1}{8}(3\nu-1)p^4 - \frac{1}{2}[(3+\nu)p^2 + \nu p_r^2]\frac{1}{q} + \frac{1}{2q^2},\\
c^4\hat{H}_{2PN} &= \frac{1}{16}(1-5\nu+5\nu^2)p^6\\
&\quad + \frac{1}{8}[(5-20\nu-3\nu^2)p^4 - 2\nu^2p_r^2p^2 - 3\nu^2p_r^4]\frac{1}{q}\\
&\quad + \frac{1}{2}[(5+8\nu)p^2 + 3\nu p_r^2]\frac{1}{q^2} - \frac{1}{4}(1+3\nu)\frac{1}{q^3},\\
c^6\hat{H}_{3PN} &= \frac{1}{128}(-5+35\nu-70\nu^2+35\nu^3)p^8\\
&\quad + \frac{1}{16}\Big[(-7+42\nu-53\nu^2-5\nu^3)p^6 + (2-3\nu)\nu^2p_r^2p^4\\
&\qquad + 3(1-\nu)\nu^2p_r^4p^2 - 5\nu^3p_r^6\Big]\frac{1}{q}\\
&\quad + \Big[\frac{1}{16}(-27+136\nu+109\nu^2)p^4 + \frac{1}{16}(17+30\nu)\nu p_r^2p^2\\
&\qquad + \frac{1}{12}(5+43\nu)\nu p_r^4\Big]\frac{1}{q^2}\\
&\quad + \Big[\Big(-\frac{25}{8} + \Big(\frac{1}{64}\pi^2 - \frac{335}{48}\Big)\nu - \frac{23}{8}\nu^2\Big)p^2\\
&\qquad + \Big(-\frac{85}{16} - \frac{3}{64}\pi^2 - \frac{7}{4}\nu\Big)\nu p_r^2\Big]\frac{1}{q^3}\\
&\quad + \Big[\frac{1}{8} + \Big(\frac{109}{12} - \frac{21}{32}\pi^2\Big)\nu\Big]\frac{1}{q^4}.
\end{aligned}$$

The EOB formalism (Damour & Buonanno 1999)

- PN Hamiltonian is complicated, can we make sense of it?
- Newtonian binaries can be mapped to non-spinning test-particle with mass $\mu = m_1 m_2/M$ around mass $M=m_1+m_2$
- Energy levels of positronium ($e^+ - e^-$) can be mapped to those of hydrogen through

$$\frac{E_{\rm H}}{\mu c^2} = \frac{E_{\rm pos}^2 - m_1^2 c^4 - m_2^2 c^4}{2 m_1 m_2 c^4}$$

$m_1=m_2=m_e$

- Particle with mass $\mu = m_1 m_2/M$ around *deformed* Schwarzschild BH with $M=m_1+m_2$ ("effective one body'') has Hamiltonian related to PN Hamiltonian by

$$\frac{H_{\rm eff}}{\mu c^2} = \frac{H_{\rm PN}^2 - m_1^2 c^4 - m_2^2 c^4}{2 m_1 m_2 c^4}$$

(up to 3PN order)

EOB can be generalized to include BH spins and produce GW waveforms

PN/EOB ISCO

Qualitatively the same as Schwarzschild/Kerr

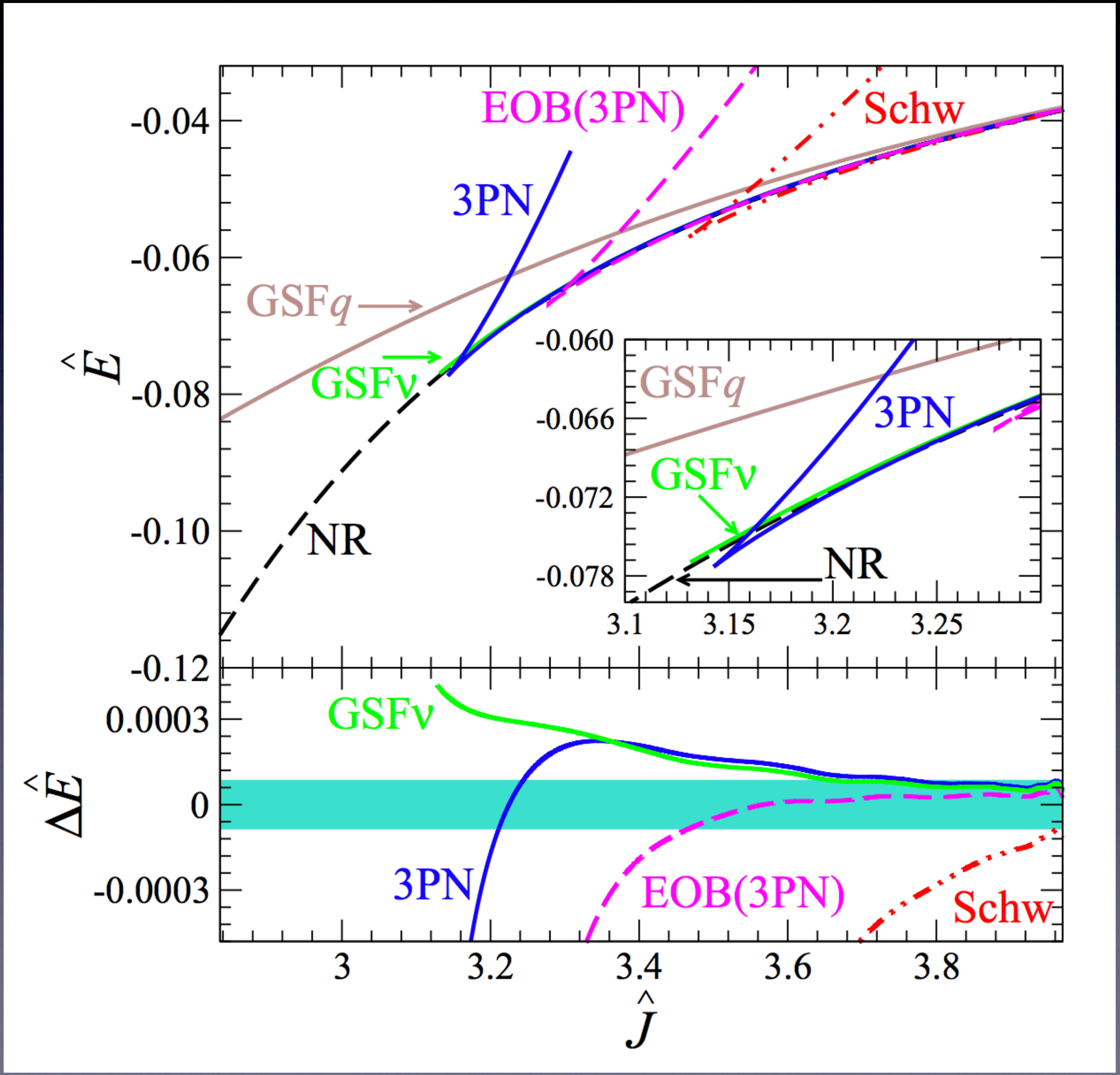

Le Tiec, EB, Buonanno 2011

BH spin precession

- Spin precesses around total angular momentum $J = L + S_1 + S_2$
- Precession-induced modulations observable with GW detectors:

  - Increase SNR and improve measurements of binary parameters (e.g. luminosity distance and sky localization)

  - Allow measurements of angle between spins

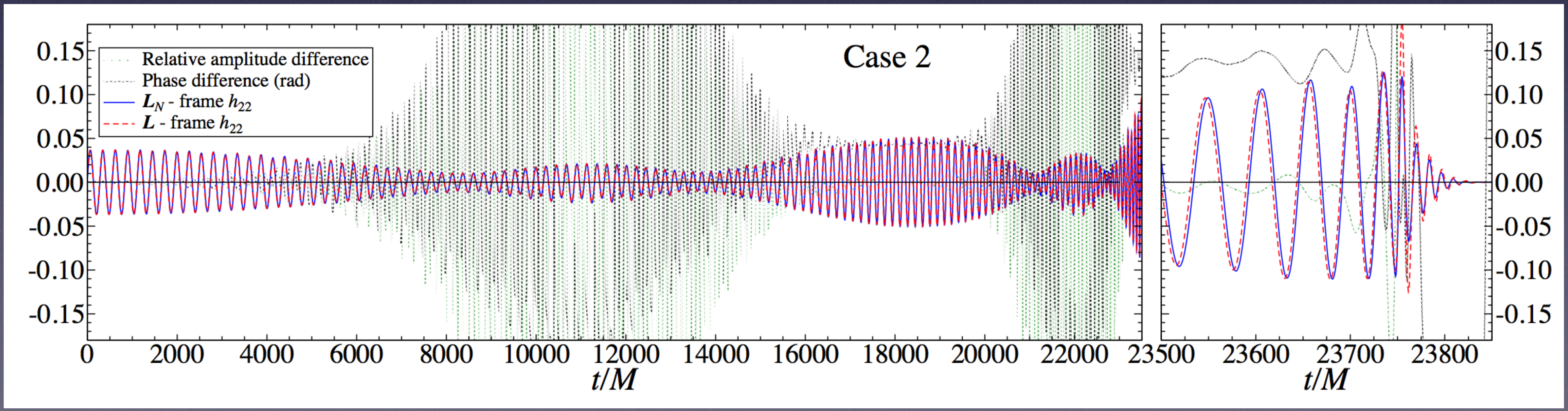

EOB waveforms for BH binary with mass ratio 1:6 and spins 0.6 and 0.8, from Pan et al (2013) [using spin-EOB model of EB & Buonanno 2010, 2011]

The PN formalism

Main idea: expand dynamics in powers of 1/c [i.e. of v/c, ∂_t/c, GM/(r c^2)]:

$$g_{00} = -\left(1 + 2\frac{\phi}{c^2}\right) ,$$
$$g_{0i} = \frac{\hat{\omega}_i}{c^3} ,$$
$$g_{ij} = \left(1 - 2\frac{\psi}{c^2}\right)\delta_{ij} + \frac{\hat{\chi}_{ij}}{c^2} ,$$

$$\hat{\omega}_i = \partial_i \omega + \omega_i ,$$

$$\hat{\chi}_{ij} = \left(\partial_{ij} - \frac{1}{3}\delta_{ij}\nabla^2\right)\chi + \partial_{(i}\chi_{j)} + \chi_{ij} ,$$

$$\partial_i \omega^i = \partial_i \chi^i = \partial_i \chi^{ij} = \chi^i_i = 0.$$

$$\omega = \chi = \chi_i = 0.$$

$$\partial_i \hat{\omega}^i = \partial_i \hat{\chi}^{ij} = 0$$

“Poisson gauge”

$$g_{00} = -\left(1 + 2\frac{\phi}{c^2}\right) ,$$
$$g_{0i} = \frac{\omega_i}{c^3} ,$$
$$g_{ij} = \left(1 - 2\frac{\psi}{c^2}\right)\delta_{ij} + \frac{\chi_{ij}}{c^2} ,$$

Einstein equations

$$\nabla^2\phi = \dots$$
$$\nabla^2\psi = \dots$$
$$\nabla^2\omega_i = \dots$$

$$\Box\chi_{ij} = \dots$$

The PN formalism

Expand Einstein eqs+perfect fluid in 1/c, over flat space:

$$\psi \equiv \phi + \frac{\delta\psi}{c^2}$$

$$\nabla^2\phi = 4\pi\left(3\frac{p}{c^2} + \rho\right) + \frac{2}{c^2}\phi_{,i}\phi_{,i} + 8\pi\rho\left(\frac{v}{c}\right)^2 - \frac{3}{c^2}\phi_{,tt}
+\frac{1}{c^4}\Big[-16\pi\rho\phi^2 - 8\pi\rho\delta\psi + \phi_{,i}\delta\psi_{,i} + \phi_{,i}{\omega^i}_{,t} - \frac{1}{2}{\omega^i}_{,j}{\omega^i}_{,j}
+\frac{1}{2}{\omega^i}_{,j}{\omega^j}_{,i} + 8\pi(p - 4\rho\phi)v^2 + 8\pi\rho v^4 + \phi_{,ij}\chi^{ij}
-3\delta\psi_{,tt}\Big] + \mathcal{O}\left(\frac{1}{c^6}\right),$$

$$\nabla^2\delta\psi = -12p\pi - 16\pi\rho\phi - \frac{7}{2}\phi_{,j}\phi_{,j}
- 4\pi\rho v^2 + 3\phi_{,tt} + \mathcal{O}\left(\frac{1}{c^2}\right).$$

$$\nabla^2\omega^i = 4(4\pi\rho v^i + \phi_{,ti}) + \frac{2}{c^2}\Big[\phi_{,j}{\omega^j}_{,i} - \phi_{,ij}\omega^j
+2\left(\phi_{,t}\phi_{,i} + \delta\psi_{,it} + 4p\pi v^i - 16\pi\rho\phi v^i + 4\pi\rho v^2 v^i + 2\pi\rho\omega^i\right)\Big]
+\mathcal{O}\left(\frac{1}{c^4}\right).$$

The PN formalism

Expand Einstein eqs+perfect fluid in 1/c, over flat space:

$$\psi \equiv \phi + \frac{\delta\psi}{c^2}$$

$$\nabla^2\phi = 4\pi\left(3\frac{p}{c^2} + \rho\right) + \frac{2}{c^2}\phi_{,i}\phi_{,i} + 8\pi\rho\left(\frac{v}{c}\right)^2 - \frac{3}{c^2}\phi_{,tt}$$
$$+\frac{1}{c^4}\Big[-16\pi\rho\phi^2 - 8\pi\rho\delta\psi + \phi_{,i}\delta\psi_{,i} + \phi_{,i}\omega^i{}_{,t} - \frac{1}{2}\omega^i{}_{,j}\omega^i{}_{,j}$$
$$+\frac{1}{2}\omega^i{}_{,j}\omega^j{}_{,i} + 8\pi(p - 4\rho\phi)v^2 + 8\pi\rho v^4 + \phi_{,ij}\chi^{ij}$$
$$-3\delta\psi_{,tt}\Big] + \mathcal{O}\left(\frac{1}{c^6}\right),$$

$$\nabla^2\delta\psi = -12p\pi - 16\pi\rho\phi - \frac{7}{2}\phi_{,j}\phi_{,j}$$
$$- 4\pi\rho v^2 + 3\phi_{,tt} + \mathcal{O}\left(\frac{1}{c^2}\right).$$

a=a_N

$$\nabla^2\omega^i = 4(4\pi\rho v^i + \phi_{,ti}) + \frac{2}{c^2}\Big[\phi_{,j}\omega^j{}_{,i} - \phi_{,ij}\omega^j$$
$$+2\left(\phi_{,t}\phi_{,i} + \delta\psi_{,it} + 4p\pi v^i - 16\pi\rho\phi v^i + 4\pi\rho v^2 v^i + 2\pi\rho\omega^i\right)\Big]$$
$$+\mathcal{O}\left(\frac{1}{c^4}\right).$$

The PN formalism

Expand Einstein eqs+perfect fluid in 1/c, over flat space:

$$\psi \equiv \phi + \frac{\delta\psi}{c^2}$$

$$\nabla^2\phi = 4\pi\left(3\frac{p}{c^2} + \rho\right) + \frac{2}{c^2}\phi_{,i}\phi_{,i} + 8\pi\rho\left(\frac{v}{c}\right)^2 - \frac{3}{c^2}\phi_{,tt}$$
$$+\frac{1}{c^4}\Big[-16\pi\rho\phi^2 - 8\pi\rho\delta\psi + \phi_{,i}\delta\psi_{,i} + \phi_{,i}\omega^i{}_{,t} - \frac{1}{2}\omega^i{}_{,j}\omega^i{}_{,j}$$
$$+\frac{1}{2}\omega^i{}_{,j}\omega^j{}_{,i} + 8\pi(p - 4\rho\phi)v^2 + 8\pi\rho v^4 + \phi_{,ij}\chi^{ij}$$
$$-3\delta\psi_{,tt}\Big] + \mathcal{O}\left(\frac{1}{c^6}\right),$$

$$\nabla^2\delta\psi = -12p\pi - 16\pi\rho\phi - \frac{7}{2}\phi_{,j}\phi_{,j}$$
$$- 4\pi\rho v^2 + 3\phi_{,tt} + \mathcal{O}\left(\frac{1}{c^2}\right).$$

a=aN(1+1PN/c²)

$$\nabla^2\omega^i = 4(4\pi\rho v^i + \phi_{,ti}) + \frac{2}{c^2}\Big[\phi_{,j}\omega^j{}_{,i} - \phi_{,ij}\omega^j$$
$$+2\left(\phi_{,t}\phi_{,i} + \delta\psi_{,it} + 4p\pi v^i - 16\pi\rho\phi v^i + 4\pi\rho v^2 v^i + 2\pi\rho\omega^i\right)\Big]$$
$$+\mathcal{O}\left(\frac{1}{c^4}\right).$$

The PN formalism

Expand Einstein eqs+perfect fluid in 1/c, over flat space:

$$\psi \equiv \phi + \frac{\delta\psi}{c^2}$$

$$\nabla^2\phi = 4\pi\left(3\frac{p}{c^2} + \rho\right) + \frac{2}{c^2}\phi_{,i}\phi_{,i} + 8\pi\rho\left(\frac{v}{c}\right)^2 - \frac{3}{c^2}\phi_{,tt}$$
$$+\frac{1}{c^4}\Big[-16\pi\rho\phi^2 - 8\pi\rho\delta\psi + \phi_{,i}\delta\psi_{,i} + \phi_{,i}\omega^i{}_{,t} - \frac{1}{2}\omega^i{}_{,j}\omega^i{}_{,j}$$
$$+\frac{1}{2}\omega^i{}_{,j}\omega^j{}_{,i} + 8\pi(p - 4\rho\phi)v^2 + 8\pi\rho v^4 + \phi_{,ij}\chi^{ij}$$
$$-3\delta\psi_{,tt}\Big] + \mathcal{O}\left(\frac{1}{c^6}\right),$$

$$\nabla^2\delta\psi = -12p\pi - 16\pi\rho\phi - \frac{7}{2}\phi_{,j}\phi_{,j}$$
$$- 4\pi\rho v^2 + 3\phi_{,tt} + \mathcal{O}\left(\frac{1}{c^2}\right).$$

a=a$_N$(1+1PN/c^2+2PN/c^4+…)

$$\nabla^2\omega^i = 4(4\pi\rho v^i + \phi_{,ti}) + \frac{2}{c^2}\Big[\phi_{,j}\omega^j{}_{,i} - \phi_{,ij}\omega^j$$
$$+2\left(\phi_{,t}\phi_{,i} + \delta\psi_{,it} + 4p\pi v^i - 16\pi\rho\phi v^i + 4\pi\rho v^2 v^i + 2\pi\rho\omega^i\right)\Big]$$
$$+\mathcal{O}\left(\frac{1}{c^4}\right).$$

PN effects are not only relevant for BH binaries

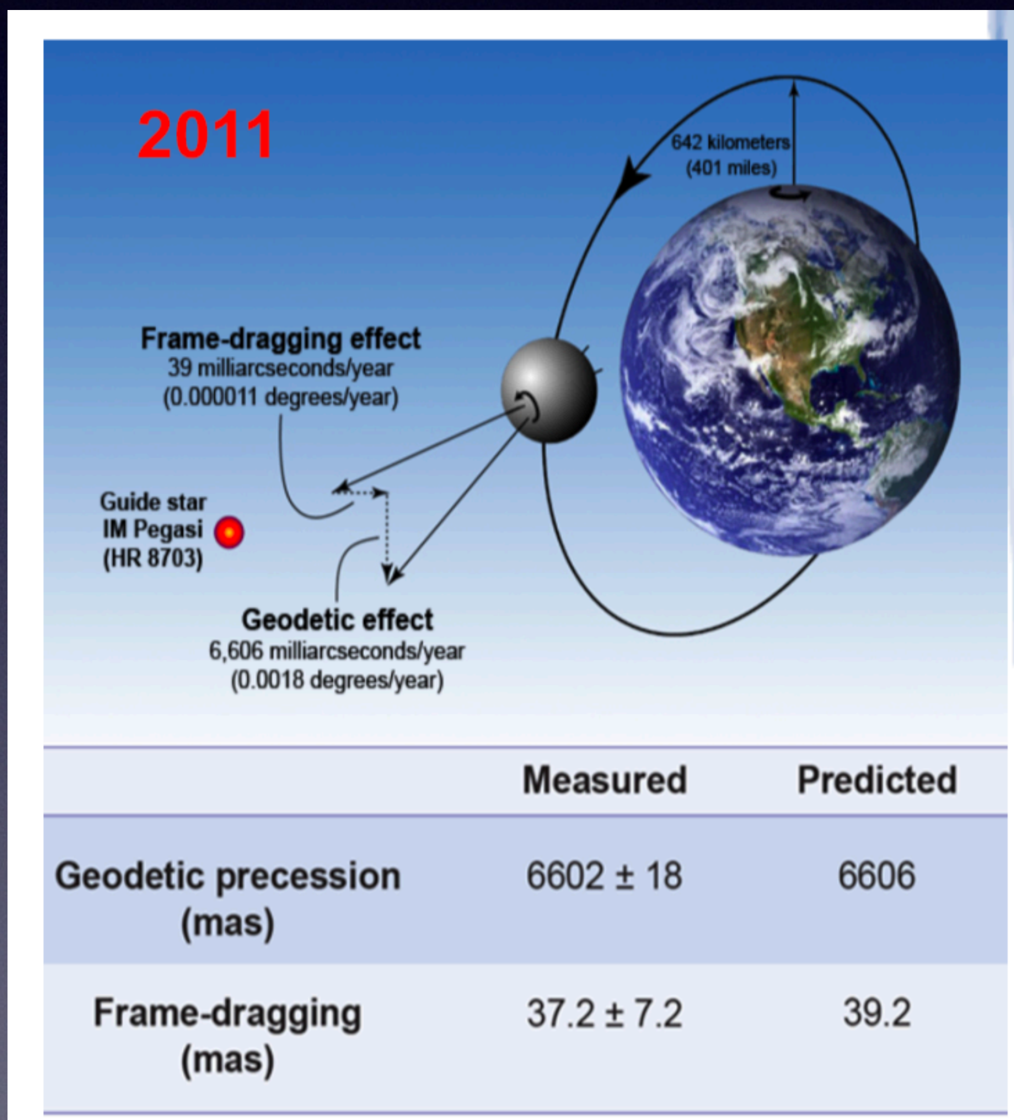

	Measured	Predicted
Geodetic precession (mas)	6602 ± 18	6606
Frame-dragging (mas)	37.2 ± 7.2	39.2

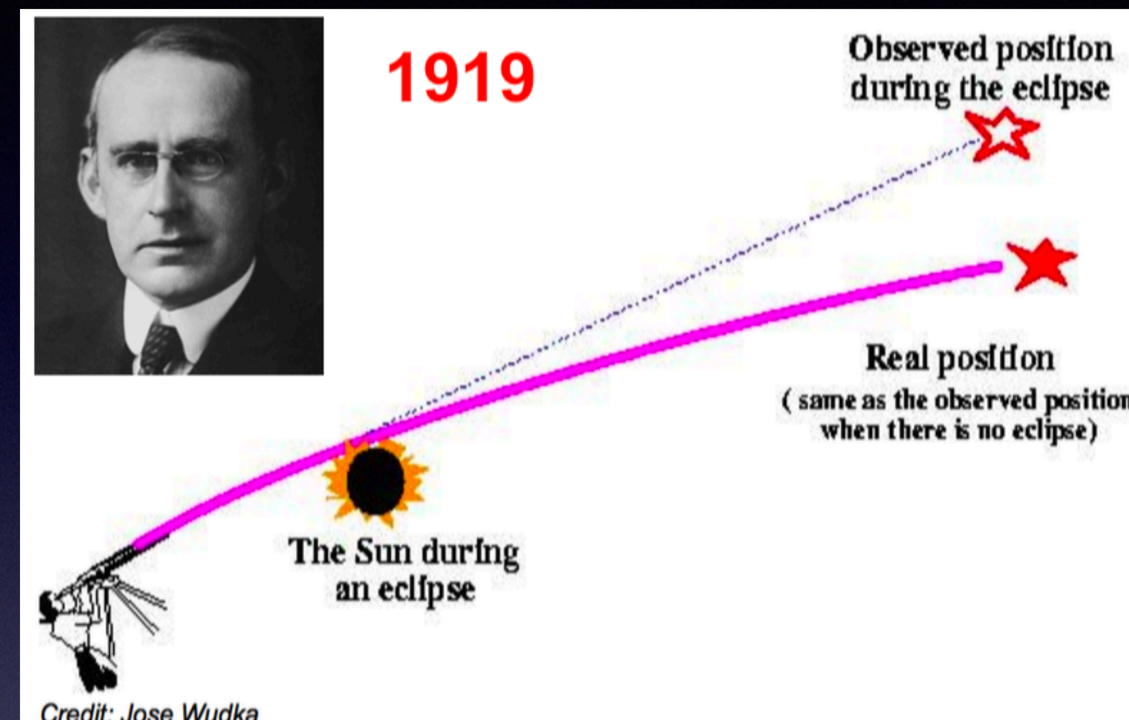

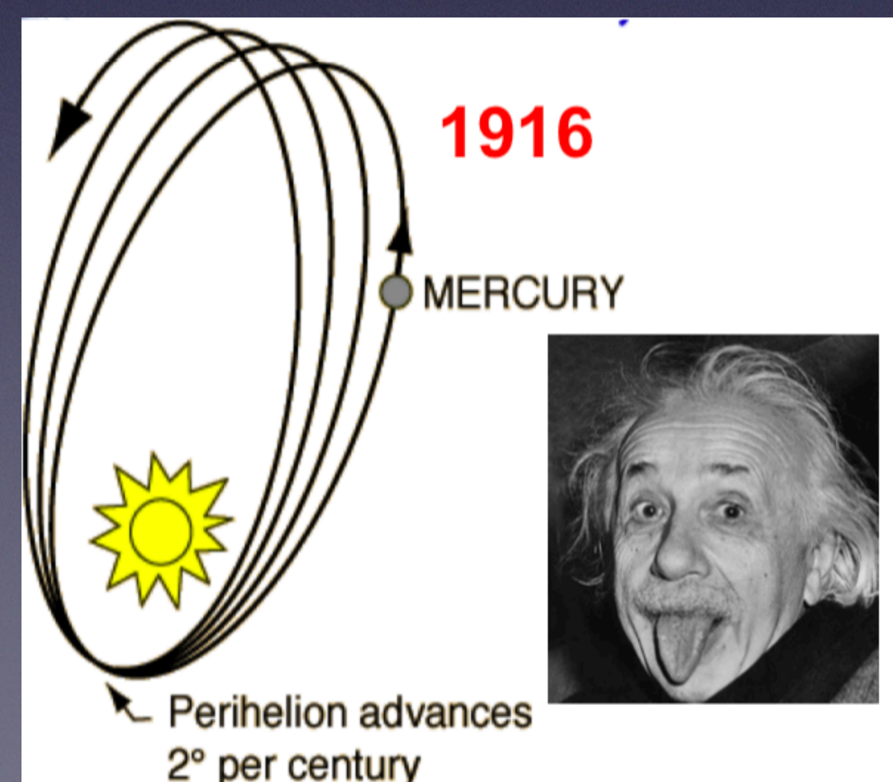

How about the TT term?

Keep time derivatives even though
they carry factor 1/c, because for GWs $\partial_t/c \sim \partial_x$)

$$\Box\chi_{ij} \approx -16\pi\sigma_{ij}$$

$$\sigma_{ij} = P_i^k P_j^l T_{kl} - P_{ij}P^{kl}T_{kl}/2$$

$$P_{ij} = \delta_{ij} - \frac{\partial_i\partial_j}{\nabla^2}$$

$$\begin{aligned}
\chi_{ij} &= -16\pi\Box^{-1}\sigma_{ij} = -16\pi\Box^{-1}\left(P_i^k P_j^l - \frac{1}{2}P_{ij}P^{kl}\right)T_{kl} \\
&= -16\pi\left(P_i^k P_j^l - \frac{1}{2}P_{ij}P^{kl}\right)\Box^{-1}T_{kl} \\
&= 4\left(P_i^k P_j^l - \frac{1}{2}P_{ij}P^{kl}\right)\int\frac{T_{ij}\left(t-|\boldsymbol{x}-\boldsymbol{x}'|,\boldsymbol{x}'\right)}{|\boldsymbol{x}-\boldsymbol{x}'|}\mathrm{d}^3x' \\
&\approx \frac{4}{r}\left(P_i^k P_j^l - \frac{1}{2}P_{ij}P^{kl}\right)\int T_{ij}(t-r,\boldsymbol{x}')\mathrm{d}^3x'
\end{aligned}$$

How about the TT term?

Keep time derivatives even though they carry factor 1/c, because for GWs $\partial_t/c \sim \partial_x$)

$$\Box \chi_{ij} \approx -16\pi\sigma_{ij}$$

$$\sigma_{ij} = P_i^k P_j^l T_{kl} - P_{ij} P^{kl} T_{kl}/2$$

$$P_{ij} = \delta_{ij} - \frac{\partial_i \partial_j}{\nabla^2}$$

$$\begin{aligned}
\chi_{ij} &= -16\pi \Box^{-1} \sigma_{ij} = -16\pi \Box^{-1} \left(P_i^k P_j^l - \frac{1}{2} P_{ij} P^{kl} \right) T_{kl} \\
&= -16\pi \left(P_i^k P_j^l - \frac{1}{2} P_{ij} P^{kl} \right) \Box^{-1} T_{kl} \\
&= 4 \left(P_i^k P_j^l - \frac{1}{2} P_{ij} P^{kl} \right) \int \frac{T_{ij}\left(t - |\boldsymbol{x} - \boldsymbol{x}'|, \boldsymbol{x}'\right)}{|\boldsymbol{x} - \boldsymbol{x}'|} \mathrm{d}^3 x' \\
&\approx \frac{4}{r} \left(P_i^k P_j^l - \frac{1}{2} P_{ij} P^{kl} \right) \int T_{ij}(t - r, \boldsymbol{x}') \mathrm{d}^3 x'
\end{aligned}$$

The quadrupole formula

$$\partial_t^2\left(T^{tt}x^ix^j\right)=\partial_k\partial_l\left(T^{kl}x^ix^j\right)-2\partial_k\left(T^{ik}x^j+T^{kj}x^i\right)+2T^{ij}$$

$$\frac{4}{r}\int d^3x'\,T_{ij}=\frac{4}{r}\int d^3x'\left[\frac{1}{2}\partial_t^2\left(T^{tt}x'^ix'^j\right)+\partial_k\left(T^{ik}x'^j+T^{kj}x'^i\right)\;-\frac{1}{2}\partial_k\partial_l\left(T^{kl}x'^ix'^j\right)\right]$$

$$=\frac{2}{r}\int d^3x'\,\partial_t^2\left(T^{tt}x'^ix'^j\right)\;=\frac{2}{r}\frac{\partial^2}{\partial t^2}\int d^3x'\,\rho\,x'^ix'^j\;=\frac{2}{r}\frac{d^2I_{ij}(t-r)}{dt^2}$$

$$I_{ij}(t)=\int d^3x'\,\rho(t,\mathbf{x}')\,x'^ix'^j$$

$$\chi_{ij}\;\approx\frac{4}{r}\left(P_i^kP_j^l-\frac{1}{2}P_{ij}P^{kl}\right)\int T_{ij}(t-r,\boldsymbol{x}')\mathrm{d}^3x'$$

$$=\frac{2}{r}\frac{d^2\mathcal{I}_{kl}(t-r)}{dt^2}\left[P_{ik}(\mathbf{n})P_{jl}(\mathbf{n})-\frac{1}{2}P_{kl}(\mathbf{n})P_{ij}(\mathbf{n})\right]\frac{G}{c^4}$$

$$P_{ij}=\delta_{ij}-n_in_j\qquad\mathcal{I}_{ij}=I_{ij}-\frac{1}{3}\delta_{ij}I,$$

Quadrupole tensor

small number!

The quadrupole formula

Binary moving on circular orbit on x,y plane
with orbital frequency Ω, GW traveling along z

$$\chi_{ij} = h \times \begin{bmatrix} \cos 2\Omega t & \sin 2\Omega t & 0 \\ \sin 2\Omega t & -\cos 2\Omega t & 0 \\ 0 & 0 & 0 \end{bmatrix}$$

$$h = \frac{4\mu\Omega^2 R^2}{r} = \frac{4\mu(M\Omega)^{2/3}}{r} = \frac{4M_c^{5/3}\Omega^{2/3}}{r} \qquad M_c = M\nu^{3/5} \quad \nu = \frac{\mu}{M}$$

$$h \approx 1.9 \times 10^{-21} \left(\frac{f_{\rm gw}}{100Hz}\right)^{2/3} \left(\frac{M_{c,z}}{30M_\odot}\right)^{5/3} \left(\frac{400{\rm Mpc}}{d_L}\right)$$

$$\approx 3.5 \times 10^{-18} \left(\frac{f_{\rm gw}}{10{\rm mHz}}\right)^{2/3} \left(\frac{M_{c,z}}{10^6 M_\odot}\right)^{5/3} \left(\frac{16{\rm Gpc}}{d_L}\right)$$

$h_{Sun} \sim G\,M_{sun}/R_{sun}\,c^2$
$\sim 2 \times 10^{-6}$

$$M_{c,z} = M_c(1+z) \qquad f_{\rm gw} = \frac{2f_{\rm orb}}{1+z} = \frac{\Omega}{\pi(1+z)} \qquad d_L(z=2) \approx 16 \text{ Gpc}$$

GW detectors

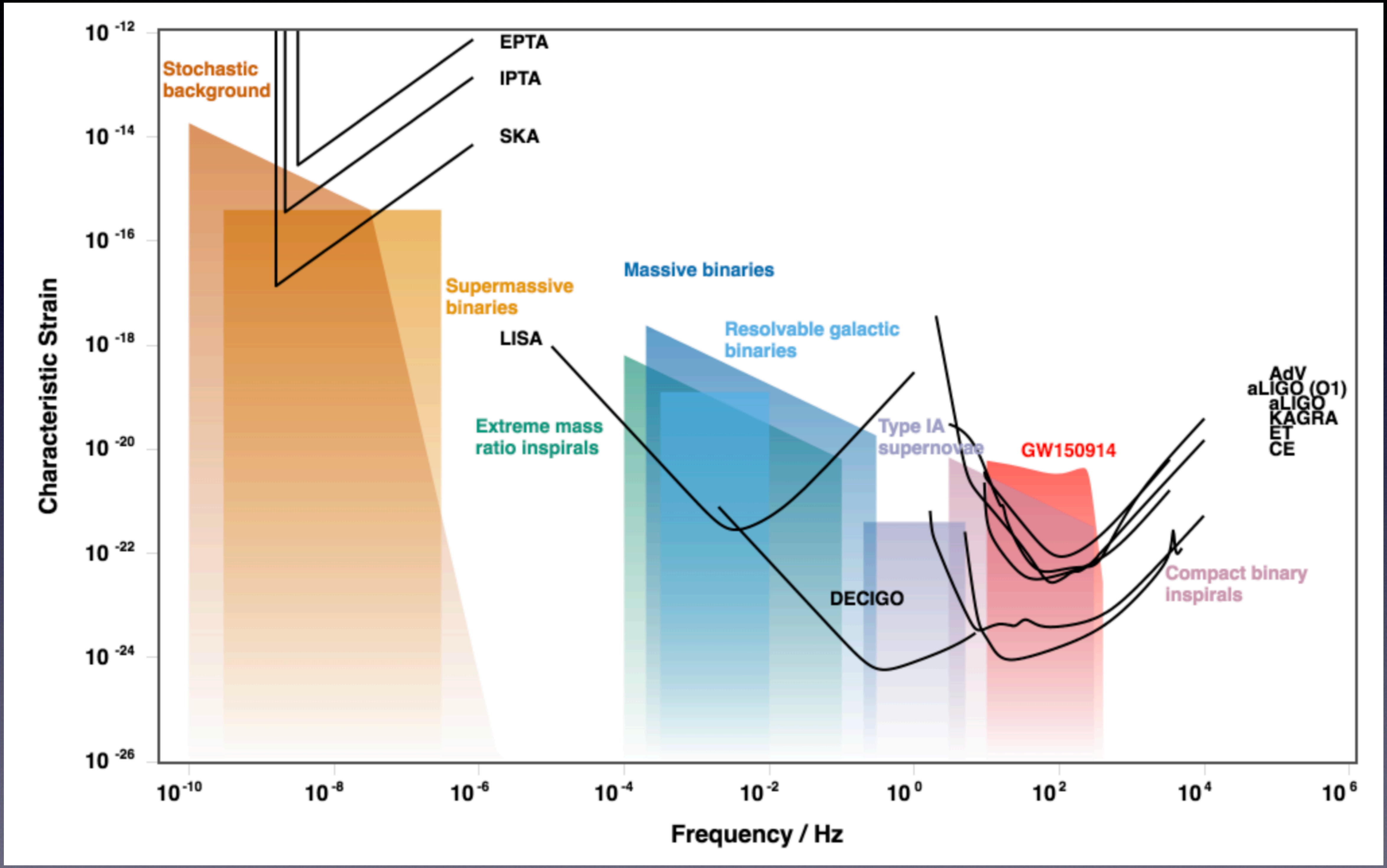

Figure generated by http://gwplotter.com/

Wrong+wrong=right

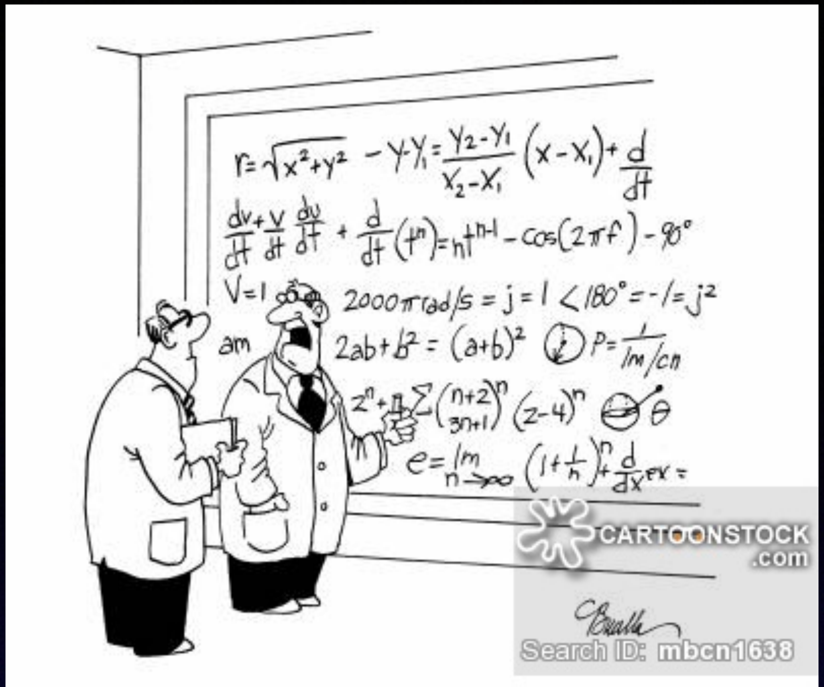

"It's a government funded study to find out how many wrongs make a right."

- We have started from linearized theory over Minkowski
- This implies that stress energy tensor is conserved wrt to Minkowski metric ...
- … and that is used to go from "Green formula" to "quadrupole formula"
- This is inconsistent as a binary system in GW-dominated regimes does NOT move on Minkowski geodesics (i.e. straight lines)
- Exercise: compute GWs from Green formula for a system of two equal masses on Keplerian orbits one around the other and verify that the GW amplitudes differ by a factor 2 (assume propagation along z axis)
- Which one is correct? Quadrupole or Green?
- One would expect Green, but actually the quadrupole formula is the correct one

A (more) correct derivation

$$\bar{H}^{\mu\nu} \equiv \eta^{\mu\nu} - (-g)^{1/2} g^{\mu\nu} \qquad \partial_\beta \bar{H}^{\alpha\beta} = 0$$ harmonic gauge

$$\rightarrow \quad \Box_{\text{flat}} \bar{H}^{\alpha\beta} = -16\pi\tau^{\alpha\beta} \qquad \tau^{\alpha\beta} = (-g)T^{\alpha\beta} + (16\pi)^{-1}\Lambda^{\alpha\beta}$$

Full Einstein equations!

$$\Lambda^{\alpha\beta} = 16\pi(-g)t^{\alpha\beta}_{\text{LL}} + (\bar{H}^{\alpha\mu}{}_{,\nu}\, \bar{H}^{\beta\nu}{}_{,\mu} - \bar{H}^{\alpha\beta}{}_{,\mu\nu}\, \bar{H}^{\mu\nu})$$

$$16\pi(-g)t^{\alpha\beta}_{\text{LL}} \equiv g_{\lambda\mu} g^{\nu\rho} \bar{H}^{\alpha\lambda}_{,\nu} \bar{H}^{\beta\mu}_{,\rho}$$
$$+\frac{1}{2} g_{\lambda\mu} g^{\alpha\beta} \bar{H}^{\lambda\nu}_{,\rho} \bar{H}^{\rho\mu}_{,\nu} - 2 g_{\mu\nu} g^{\lambda(\alpha} \bar{H}^{\beta)\nu}_{,\rho} \bar{H}^{\rho\mu}_{,\lambda}$$
$$+\frac{1}{8}(2g^{\alpha\lambda}g^{\beta\mu} - g^{\alpha\beta}g^{\lambda\mu})(2g_{\nu\rho}g_{\sigma\tau} - g_{\rho\sigma}g_{\nu\tau})\bar{H}^{\nu\tau}_{,\lambda} \bar{H}^{\rho\sigma}_{,\mu}$$

From gauge condition,

$$\tau^{\alpha\beta}{}_{,\beta} = 0$$

= geodesic motion in curved metric *g*

$$\bar{H}^{\mu\nu} \approx \bar{h}^{\mu\nu} \equiv h^{\mu\nu} - \frac{1}{2} h \eta^{\mu\nu}$$

→ Proceed as before but with T replaced by τ

A (more) correct derivation

$$
\begin{aligned}
g_{00} &= -1 - 2\frac{\phi}{c^2} + O(1/c^4) & \tau^{00} &= T^{00} + O(1/c^0)\\
g_{0i} &= O(1/c^3) & \tau^{0i} &= T^{0i} + O(1/c^1)\\
g_{ij} &= \left(1 - 2\frac{\phi}{c^2}\right)\delta_{ij} + O(1/c^4) & \tau^{ij} &= T^{ij} + \frac{1}{4\pi G}\left(\partial^i\phi\partial^j\phi - \frac{1}{2}\delta^{ij}\partial_k\phi\partial^k\phi\right) + O(1/c^2),
\end{aligned}
$$

- Non-linear terms are important in τ_{ij} but not τ_{00}
- Non-linear terms in Green formula account for discrepancy with quadrupole formula for circular Keplerian binaries
- Quadrupole formula is correct, Green's is not

GW "backreact" on geometry at 2nd order

Figure from Kip Thorne's website

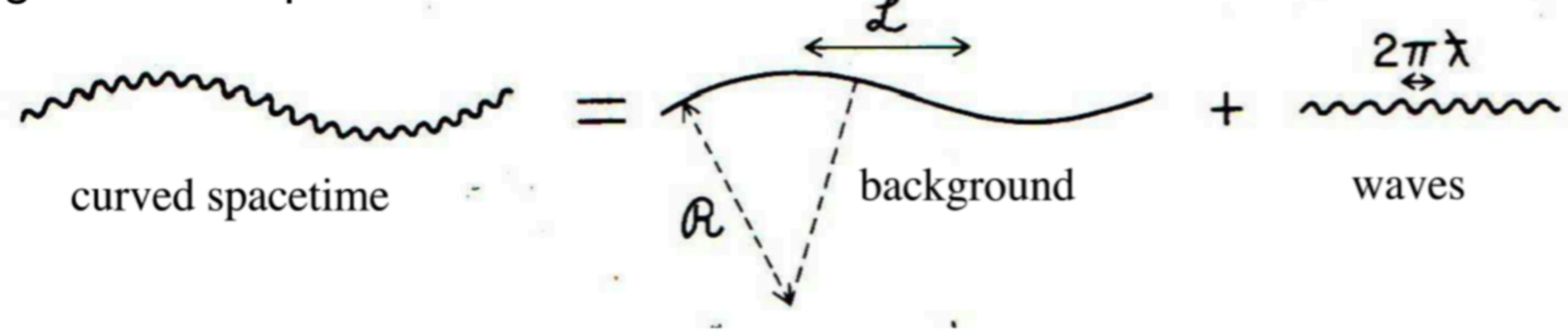

geometric-optics regime

$$g^{\rm B}_{\alpha\beta} \equiv \langle g_{\alpha\beta} \rangle \qquad g_{\alpha\beta} = g^{\rm B}_{\alpha\beta} + \varepsilon h_{\alpha\beta} + \varepsilon^2 j_{\alpha\beta} + O(\varepsilon^3)$$

$$\begin{aligned} 0 &= G_{\alpha\beta} \\ &= G_{\alpha\beta}[g^{\rm B}_{cd}] + \varepsilon G^{(1)}_{\alpha\beta}[h_{cd}; g^{\rm B}_{ef}] + \varepsilon^2 G^{(1)}_{\alpha\beta}[j_{cd}; g^{\rm B}_{ef}] + \varepsilon^2 G^{(2)}_{\alpha\beta}[h_{cd}; g^{\rm B}_{ef}] \\ &\quad + O(\varepsilon^3) \, . \end{aligned}$$

$$G_{\alpha\beta}[g^{\rm B}_{cd}] = 0, \qquad G^{(1)}_{\alpha\beta}[h_{cd}; g^{\rm B}_{ef}] = 0 \, , \qquad G^{(1)}_{\alpha\beta}[j_{cd}; g^{\rm B}_{ef}] = -G^{(2)}_{\alpha\beta}[h_{cd}; g^{\rm B}_{ef}]$$

GWs carry energy and momentum

Average Einstein equations on scale >> λ and << L

$$\Delta j_{\alpha\beta} = j_{\alpha\beta} - \langle j_{\alpha\beta} \rangle$$

$$G^{(1)}_{\alpha\beta}[\langle j_{cd}\rangle; g^{\mathrm{B}}_{ef}] = -\langle G^{(2)}_{\alpha\beta}[h_{cd}; g^{\mathrm{B}}_{ef}]\rangle$$

$$G^{(1)}_{\alpha\beta}[\Delta j_{cd}] = -G^{(2)}_{\alpha\beta}[h_{cd}; g^{\mathrm{B}}_{ef}] + \langle G^{(2)}_{\alpha\beta}[h_{cd}; g^{\mathrm{B}}_{ef}]\rangle$$

$$G_{\alpha\beta}[g^{\mathrm{B}}_{cd} + \varepsilon^2 \langle j_{cd}\rangle] = 8\pi G\, T^{\mathrm{GW,eff}}_{\alpha\beta} + O(\varepsilon^3) \qquad T^{\mathrm{GW,eff}}_{\alpha\beta} = -\frac{1}{8\pi G}\langle G^{(2)}_{\alpha\beta}[h_{cd}; g^{\mathrm{B}}_{ef}]\rangle$$

Using gauge freedom and integrating by parts:

$$T^{\mathrm{GW,eff}}_{\alpha\beta} = \frac{1}{32\pi G}\left\langle \nabla^{\mathrm{B}}_{\alpha} h^{\mathrm{TT}}_{\rho\sigma}\, \nabla^{\mathrm{B}}_{\beta} h^{\rho\sigma}_{\mathrm{TT}} \right\rangle$$

$$L_{\text{mass quadrupole}} \equiv \frac{1}{5}\frac{G}{c^5}\langle\, \dddot{I}\, \rangle^2 = \frac{1}{5}\frac{G}{c^5}\langle \dddot{I\!\!\!-}_{jk} \dddot{I\!\!\!-}_{jk}\rangle^2$$

$$\dddot{I\!\!\!-}_{jk} \sim \frac{(\text{mass of the system in motion}) \times (\text{size of the system})^2}{(\text{time scale})^3} \sim \frac{MR^2}{\tau^3} \sim \frac{Mv^2}{\tau}$$

BH binaries inspiral till (effective) ISCO

From energy balance: $$\frac{\dot{P}_b}{P_b} = -\frac{3}{2}\frac{\dot{E}_b}{E_b}$$

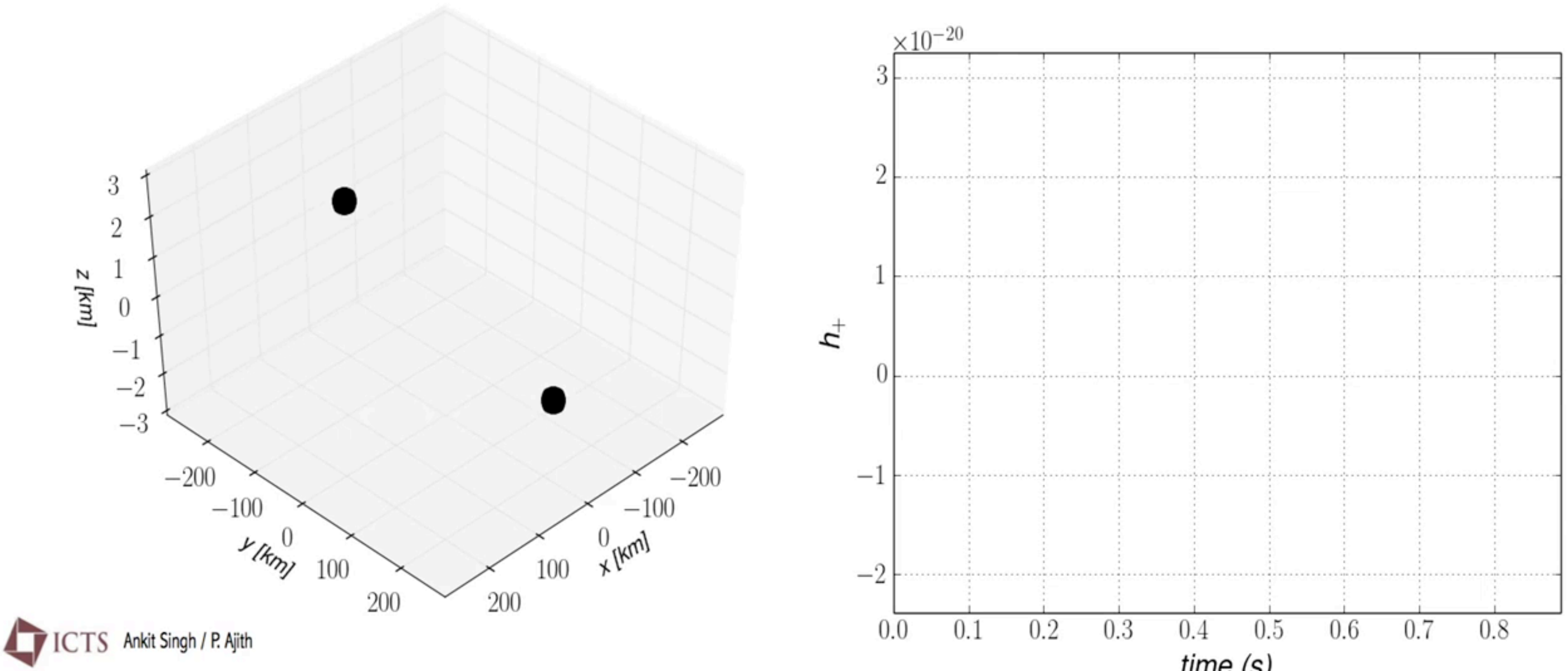

GWs from binary BHs

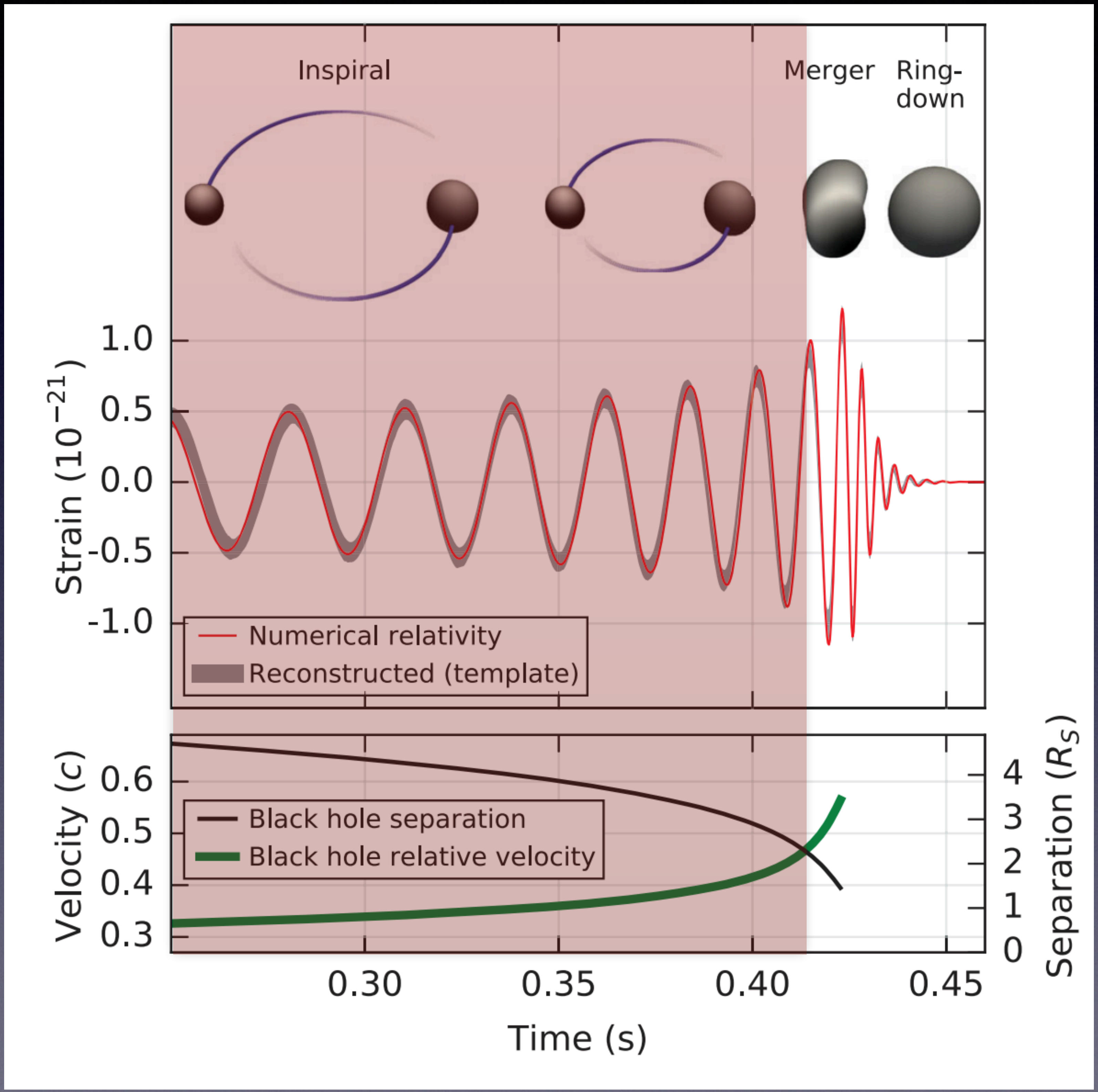

LSC collaboration 2015

Extracting the BH masses

$$\mathcal{M} = \frac{(m_1 m_2)^{3/5}}{(m_1+m_2)^{1/5}} = \frac{c^3}{G}\left[\frac{5}{96}\pi^{-8/3} f^{-11/3}\dot{f}\right]^{3/5}$$

$$\mathcal{M} \simeq 30 M_\odot$$

$$M = m_1 + m_2 \gtrsim 70 M_\odot$$

$$2GM/c^2 \gtrsim 210 \text{ km}$$

$f_{gw}\sim$ 150 Hz corresponds to $r_{12}\sim$350 km

Objects in GW150914 must be BHs (not WDs or NSs)

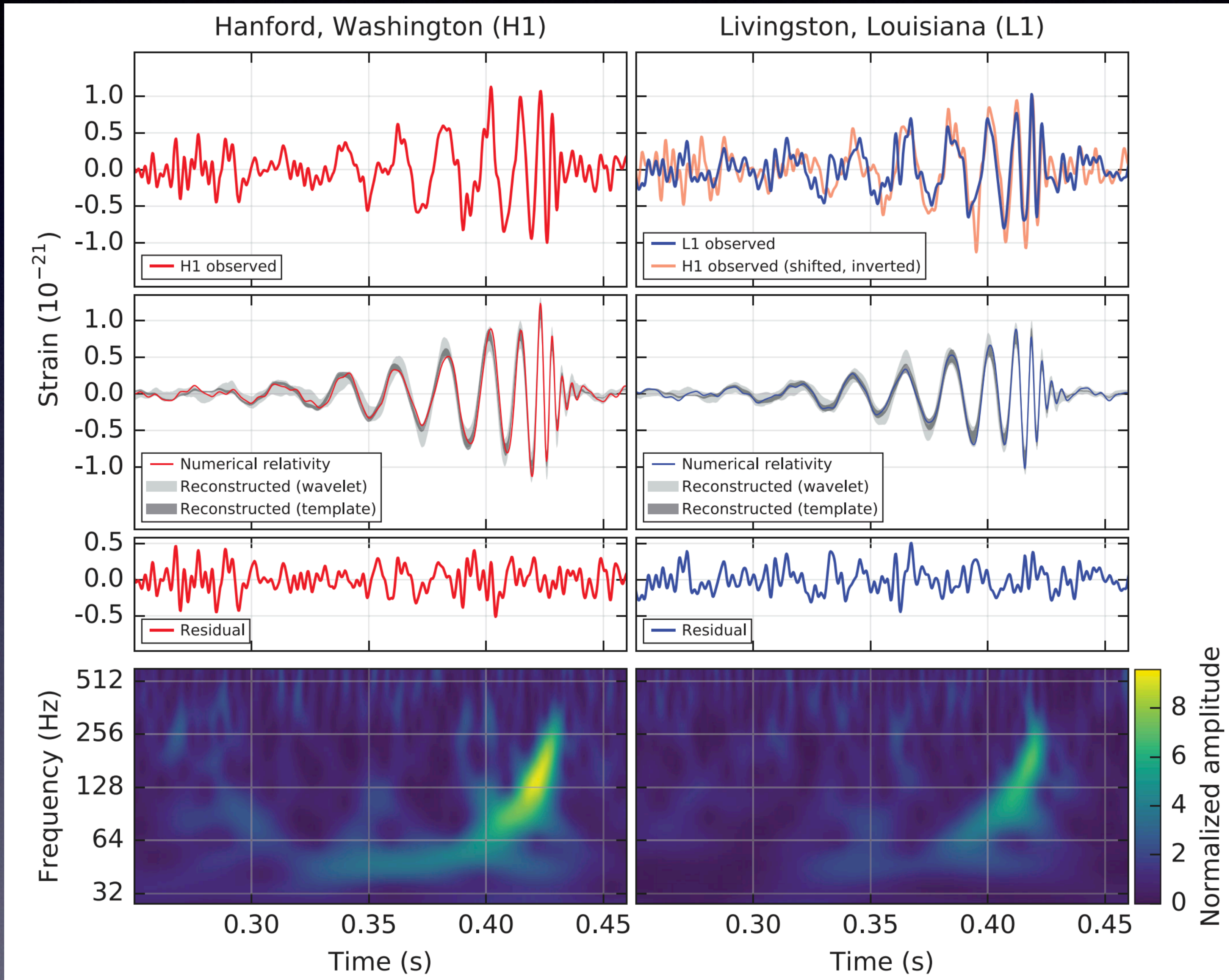

LSC collaboration 2015

Extracting the component masses

Name	$\mathbf{FAR}_{\rm min}$ (yr^{-1})	$p_{\rm astro}$	$m_1/M_\odot$	$m_2/M_\odot$	$\mathcal{M}/M_\odot$	$\chi_{\rm eff}$	First appears in
GW150914	$< 1 \times 10^{-5}$	> 0.99	$35.6^{+4.7}_{-3.1}$	$30.6^{+3.0}_{-4.4}$	$28.6^{+1.7}_{-1.5}$	$-0.01^{+0.12}_{-0.13}$	[13]
GW151012	7.92×10^{-3}	> 0.99	$23.2^{+14.9}_{-5.5}$	$13.6^{+4.1}_{-4.8}$	$15.2^{+2.1}_{-1.2}$	$0.05^{+0.31}_{-0.20}$	[14]
GW151226	$< 1 \times 10^{-5}$	> 0.99	$13.7^{+8.8}_{-3.2}$	$7.7^{+2.2}_{-2.5}$	$8.9^{+0.3}_{-0.3}$	$0.18^{+0.20}_{-0.12}$	[15]
GW170104	$< 1 \times 10^{-5}$	> 0.99	$30.8^{+7.3}_{-5.6}$	$20.0^{+4.9}_{-4.6}$	$21.4^{+2.2}_{-1.8}$	$-0.04^{+0.17}_{-0.21}$	[16]
GW170608	$< 1 \times 10^{-5}$	> 0.99	$11.0^{+5.5}_{-1.7}$	$7.6^{+1.4}_{-2.2}$	$7.9^{+0.2}_{-0.2}$	$0.03^{+0.19}_{-0.07}$	[17]
GW170729	1.80×10^{-1}	0.98	$50.2^{+16.2}_{-10.2}$	$34.0^{+9.1}_{-10.1}$	$35.4^{+6.5}_{-4.8}$	$0.37^{+0.21}_{-0.25}$	[2]
GW170809	$< 1 \times 10^{-5}$	> 0.99	$35.0^{+8.3}_{-5.9}$	$23.8^{+5.1}_{-5.2}$	$24.9^{+2.1}_{-1.7}$	$0.08^{+0.17}_{-0.17}$	[2]
GW170814	$< 1 \times 10^{-5}$	> 0.99	$30.6^{+5.6}_{-3.0}$	$25.2^{+2.8}_{-4.0}$	$24.1^{+1.4}_{-1.1}$	$0.07^{+0.12}_{-0.12}$	[18]
GW170817	$< 1 \times 10^{-5}$	> 0.99	$1.46^{+0.12}_{-0.10}$	$1.27^{+0.09}_{-0.09}$	$1.186^{+0.001}_{-0.001}$	$0.00^{+0.02}_{-0.01}$	[19]
GW170818	$< 1 \times 10^{-5}$	> 0.99	$35.4^{+7.5}_{-4.7}$	$26.7^{+4.3}_{-5.2}$	$26.5^{+2.1}_{-1.7}$	$-0.09^{+0.18}_{-0.21}$	[2]
GW170823	$< 1 \times 10^{-5}$	> 0.99	$39.5^{+11.2}_{-6.7}$	$29.0^{+6.7}_{-7.8}$	$29.2^{+4.6}_{-3.6}$	$0.09^{+0.22}_{-0.26}$	[2]
GW190408_181802	$< 1 \times 10^{-5}$	> 0.99	$24.6^{+5.1}_{-3.4}$	$18.4^{+3.3}_{-3.6}$	$18.3^{+1.9}_{-1.2}$	$-0.03^{+0.14}_{-0.19}$	[3]
GW190412_053044	$< 1 \times 10^{-5}$	> 0.99	$30.1^{+4.7}_{-5.1}$	$8.3^{+1.6}_{-0.9}$	$13.3^{+0.4}_{-0.3}$	$0.25^{+0.08}_{-0.11}$	[20]

LSC 2021

GW190413_134308	1.81×10^{-1}	0.99	$47.5^{+13.5}_{-10.7}$	$31.8^{+11.7}_{-10.8}$	$33.0^{+8.2}_{-5.4}$	$-0.03^{+0.25}_{-0.29}$	[3]
GW190421_213856	2.83×10^{-3}	>0.99	$41.3^{+10.4}_{-6.9}$	$31.9^{+8.0}_{-8.8}$	$31.2^{+5.9}_{-4.2}$	$-0.06^{+0.22}_{-0.27}$	[3]
GW190425_081805	3.38×10^{-2}	0.78	$2.0^{+0.6}_{-0.3}$	$1.4^{+0.3}_{-0.3}$	$1.44^{+0.02}_{-0.02}$	$0.06^{+0.11}_{-0.05}$	[21]
GW190503_185404	$<1\times10^{-5}$	>0.99	$43.3^{+9.2}_{-8.1}$	$28.4^{+7.7}_{-8.0}$	$30.2^{+4.2}_{-4.2}$	$-0.03^{+0.20}_{-0.26}$	[3]
GW190512_180714	$<1\times10^{-5}$	>0.99	$23.3^{+5.3}_{-5.8}$	$12.6^{+3.6}_{-2.5}$	$14.6^{+1.3}_{-1.0}$	$0.03^{+0.12}_{-0.13}$	[3]
GW190513_205428	$<1\times10^{-5}$	>0.99	$35.7^{+9.5}_{-9.2}$	$18.0^{+7.7}_{-4.1}$	$21.6^{+3.8}_{-1.9}$	$0.11^{+0.28}_{-0.17}$	[3]
GW190517_055101	3.47×10^{-4}	>0.99	$37.4^{+11.7}_{-7.6}$	$25.3^{+7.0}_{-7.3}$	$26.6^{+4.0}_{-4.0}$	$0.52^{+0.19}_{-0.19}$	[3]
GW190519_153544	$<1\times10^{-5}$	>0.99	$66.0^{+10.7}_{-12.0}$	$40.5^{+11.0}_{-11.1}$	$44.5^{+6.4}_{-7.1}$	$0.31^{+0.20}_{-0.22}$	[3]
GW190521_030229	$<1\times10^{-5}$	>0.99	$95.3^{+28.7}_{-18.9}$	$69.0^{+22.7}_{-23.1}$	$69.2^{+17.0}_{-10.6}$	$0.03^{+0.32}_{-0.39}$	[22]
GW190521_074359	1.00×10^{-2}	>0.99	$42.2^{+5.9}_{-4.8}$	$32.8^{+5.4}_{-6.4}$	$32.1^{+3.2}_{-2.5}$	$0.09^{+0.10}_{-0.13}$	[22]
GW190527_092055	2.28×10^{-1}	0.85	$36.5^{+16.4}_{-9.0}$	$22.6^{+10.5}_{-8.1}$	$24.3^{+9.1}_{-4.2}$	$0.11^{+0.28}_{-0.28}$	[3]
GW190602_175927	$<1\times10^{-5}$	>0.99	$69.1^{+15.7}_{-13.0}$	$47.8^{+14.3}_{-17.4}$	$49.1^{+9.1}_{-8.5}$	$0.07^{+0.25}_{-0.24}$	[3]
GW190620_030421	1.12×10^{-2}	0.99	$57.1^{+16.0}_{-12.7}$	$35.5^{+12.2}_{-12.3}$	$38.3^{+8.3}_{-6.5}$	$0.33^{+0.22}_{-0.25}$	[3]
GW190630_185205	$<1\times10^{-5}$	>0.99	$35.1^{+6.9}_{-5.6}$	$23.7^{+5.2}_{-5.1}$	$24.9^{+2.1}_{-2.1}$	$0.10^{+0.12}_{-0.13}$	[3]
GW190701_203306	5.71×10^{-3}	0.99	$53.9^{+11.8}_{-8.0}$	$40.8^{+8.7}_{-12.0}$	$40.3^{+5.4}_{-4.9}$	$-0.07^{+0.23}_{-0.29}$	[3]
GW190706_222641	$<1\times10^{-5}$	>0.99	$67.0^{+14.6}_{-16.2}$	$38.2^{+14.6}_{-13.3}$	$42.7^{+10.0}_{-7.0}$	$0.28^{+0.26}_{-0.29}$	[3]
GW190707_093326	$<1\times10^{-5}$	>0.99	$11.6^{+3.3}_{-1.7}$	$8.4^{+1.4}_{-1.7}$	$8.5^{+0.6}_{-0.5}$	$-0.05^{+0.10}_{-0.08}$	[3]
GW190708_232457	3.09×10^{-4}	>0.99	$17.6^{+4.7}_{-2.3}$	$13.2^{+2.0}_{-2.7}$	$13.2^{+0.9}_{-0.6}$	$0.02^{+0.10}_{-0.08}$	[3]
GW190720_000836	$<1\times10^{-5}$	>0.99	$13.4^{+6.7}_{-3.0}$	$7.8^{+2.3}_{-2.2}$	$8.9^{+0.5}_{-0.8}$	$0.18^{+0.14}_{-0.12}$	[3]
GW190727_060333	$<1\times10^{-5}$	>0.99	$38.0^{+9.5}_{-6.2}$	$29.4^{+7.1}_{-8.4}$	$28.6^{+5.3}_{-3.7}$	$0.11^{+0.26}_{-0.25}$	[3]
GW190728_064510	$<1\times10^{-5}$	>0.99	$12.3^{+7.2}_{-2.2}$	$8.1^{+1.7}_{-2.6}$	$8.6^{+0.5}_{-0.3}$	$0.12^{+0.20}_{-0.07}$	[3]
GW190803_022701	7.32×10^{-2}	0.94	$37.3^{+10.6}_{-7.0}$	$27.3^{+7.8}_{-8.2}$	$27.3^{+5.7}_{-4.1}$	$-0.03^{+0.24}_{-0.27}$	[3]
GW190814_211039	$<1\times10^{-5}$	>0.99	$23.2^{+1.1}_{-1.0}$	$2.59^{+0.08}_{-0.09}$	$6.09^{+0.06}_{-0.06}$	$0.00^{+0.06}_{-0.06}$	[23]
GW190828_063405	$<1\times10^{-5}$	>0.99	$32.1^{+5.8}_{-4.0}$	$26.2^{+4.6}_{-4.8}$	$25.0^{+3.4}_{-2.1}$	$0.19^{+0.15}_{-0.16}$	[3]
GW190828_065509	$<1\times10^{-5}$	>0.99	$24.1^{+7.0}_{-7.2}$	$10.2^{+3.6}_{-2.1}$	$13.3^{+1.2}_{-1.0}$	$0.08^{+0.16}_{-0.16}$	[3]
GW190910_112807	2.87×10^{-3}	>0.99	$43.9^{+7.6}_{-6.1}$	$35.6^{+6.3}_{-7.2}$	$34.3^{+4.1}_{-4.1}$	$0.02^{+0.18}_{-0.18}$	[3]
GW190915_235702	$<1\times10^{-5}$	>0.99	$35.3^{+9.5}_{-6.4}$	$24.4^{+5.6}_{-6.1}$	$25.3^{+3.2}_{-2.7}$	$0.02^{+0.20}_{-0.25}$	[3]
GW190924_021846	$<1\times10^{-5}$	>0.99	$8.9^{+7.0}_{-2.0}$	$5.0^{+1.4}_{-1.9}$	$5.8^{+0.2}_{-0.2}$	$0.03^{+0.30}_{-0.09}$	[3]
GW190925_232845	7.20×10^{-3}	0.99	$21.2^{+6.9}_{-3.1}$	$15.6^{+2.6}_{-3.6}$	$15.8^{+1.1}_{-1.0}$	$0.11^{+0.17}_{-0.14}$	[4]
GW190929_012149	1.55×10^{-1}	0.87	$80.8^{+33.0}_{-33.2}$	$24.1^{+19.3}_{-10.6}$	$35.8^{+14.9}_{-8.2}$	$0.01^{+0.34}_{-0.33}$	[3]
GW190930_133541	1.23×10^{-2}	>0.99	$12.3^{+12.4}_{-2.3}$	$7.8^{+1.7}_{-3.3}$	$8.5^{+0.5}_{-0.5}$	$0.14^{+0.31}_{-0.15}$	[3]
GW191105_143521	1.18×10^{-2}	>0.99	$10.7^{+3.7}_{-1.6}$	$7.7^{+1.4}_{-1.9}$	$7.82^{+0.61}_{-0.45}$	$-0.02^{+0.13}_{-0.09}$	[1]
GW191109_010717	1.80×10^{-4}	>0.99	65^{+11}_{-11}	47^{+15}_{-13}	$47.5^{+9.6}_{-7.5}$	$-0.29^{+0.42}_{-0.31}$	[1]
GW191127_050227	2.49×10^{-1}	0.49	53^{+47}_{-20}	24^{+17}_{-14}	$29.9^{+11.7}_{-9.1}$	$0.18^{+0.34}_{-0.36}$	[1]
GW191129_134029	$<1\times10^{-5}$	>0.99	$10.7^{+4.1}_{-2.1}$	$6.7^{+1.5}_{-1.7}$	$7.31^{+0.43}_{-0.28}$	$0.06^{+0.16}_{-0.08}$	[1]
GW191204_171526	$<1\times10^{-5}$	>0.99	$11.9^{+3.3}_{-1.8}$	$8.2^{+1.4}_{-1.6}$	$8.55^{+0.38}_{-0.27}$	$0.16^{+0.08}_{-0.05}$	[1]
GW191215_223052	$<1\times10^{-5}$	>0.99	$24.9^{+7.1}_{-4.1}$	$18.1^{+3.8}_{-4.1}$	$18.4^{+2.2}_{-1.7}$	$-0.04^{+0.17}_{-0.21}$	[1]
GW191216_213338	$<1\times10^{-5}$	>0.99	$12.1^{+4.6}_{-2.3}$	$7.7^{+1.6}_{-1.9}$	$8.33^{+0.22}_{-0.19}$	$0.11^{+0.13}_{-0.06}$	[1]
GW191222_033537	$<1\times10^{-5}$	>0.99	$45.1^{+10.9}_{-8.0}$	$34.7^{+9.3}_{-10.5}$	$33.8^{+7.1}_{-5.0}$	$-0.04^{+0.20}_{-0.25}$	[1]
GW191230_180458	5.02×10^{-2}	0.95	$49.4^{+14.0}_{-9.6}$	37^{+11}_{-12}	$36.5^{+8.2}_{-5.6}$	$-0.05^{+0.26}_{-0.31}$	[1]
GW200105_162426	2.04×10^{-1}	0.36	$8.9^{+1.2}_{-1.5}$	$1.9^{+0.3}_{-0.2}$	$3.41^{+0.08}_{-0.07}$	$-0.01^{+0.11}_{-0.15}$	[10]
GW200112_155838	$<1\times10^{-5}$	>0.99	$35.6^{+6.7}_{-4.5}$	$28.3^{+4.4}_{-5.9}$	$27.4^{+2.6}_{-2.1}$	$0.06^{+0.15}_{-0.15}$	[1]
GW200115_042309	$<1\times10^{-5}$	>0.99	$5.9^{+2.0}_{-2.5}$	$1.44^{+0.85}_{-0.29}$	$2.43^{+0.05}_{-0.07}$	$-0.15^{+0.24}_{-0.42}$	[10]
GW200128_022011	4.29×10^{-3}	>0.99	$42.2^{+11.6}_{-8.1}$	$32.6^{+9.5}_{-9.2}$	$32.0^{+7.5}_{-5.5}$	$0.12^{+0.24}_{-0.25}$	[1]
GW200129_065458	$<1\times10^{-5}$	>0.99	$34.5^{+9.9}_{-3.2}$	$28.9^{+3.4}_{-9.3}$	$27.2^{+2.1}_{-2.3}$	$0.11^{+0.11}_{-0.16}$	[1]
GW200202_154313	$<1\times10^{-5}$	>0.99	$10.1^{+3.5}_{-1.4}$	$7.3^{+1.1}_{-1.7}$	$7.49^{+0.24}_{-0.20}$	$0.04^{+0.13}_{-0.06}$	[1]
GW200208_130117	3.11×10^{-4}	>0.99	$37.8^{+9.2}_{-6.2}$	$27.4^{+6.1}_{-7.4}$	$27.7^{+3.6}_{-3.1}$	$-0.07^{+0.22}_{-0.27}$	[1]
GW200209_085452	4.64×10^{-2}	0.95	$35.6^{+10.5}_{-6.8}$	$27.1^{+7.8}_{-7.8}$	$26.7^{+6.0}_{-4.2}$	$-0.12^{+0.24}_{-0.30}$	[1]
GW200219_094415	9.94×10^{-4}	>0.99	$37.5^{+10.1}_{-6.9}$	$27.9^{+7.4}_{-8.4}$	$27.6^{+5.6}_{-3.8}$	$-0.08^{+0.23}_{-0.29}$	[1]
GW200224_222234	$<1\times10^{-5}$	>0.99	$40.0^{+6.9}_{-4.5}$	$32.5^{+5.0}_{-7.2}$	$31.1^{+3.2}_{-2.6}$	$0.10^{+0.15}_{-0.15}$	[1]
GW200225_060421	$<1\times10^{-5}$	>0.99	$19.3^{+5.0}_{-3.0}$	$14.0^{+2.8}_{-3.5}$	$14.2^{+1.5}_{-1.4}$	$-0.12^{+0.17}_{-0.28}$	[1]
GW200302_015811	1.12×10^{-1}	0.91	$37.8^{+8.7}_{-8.5}$	$20.0^{+8.1}_{-5.7}$	$23.4^{+4.7}_{-3.0}$	$0.01^{+0.25}_{-0.26}$	[1]
GW200311_115853	$<1\times10^{-5}$	>0.99	$34.2^{+6.4}_{-3.8}$	$27.7^{+4.1}_{-5.9}$	$26.6^{+2.4}_{-2.0}$	$-0.02^{+0.16}_{-0.20}$	[1]

LSC 2021

GW200316_215756	$< 1 \times 10^{-5}$	> 0.99	$13.1^{+10.2}_{-2.9}$	$7.8^{+1.9}_{-2.9}$	$8.75^{+0.62}_{-0.55}$	$0.13^{+0.27}_{-0.10}$	[1]
GW190413_052954	8.17×10^{-1}	0.93	$34.7^{+12.6}_{-8.1}$	$23.7^{+7.3}_{-6.7}$	$24.6^{+5.5}_{-4.1}$	$-0.01^{+0.29}_{-0.34}$	[3]
GW190426_152155	9.12×10^{-1}	0.14	$5.7^{+3.9}_{-2.3}$	$1.5^{+0.8}_{-0.5}$	$2.41^{+0.08}_{-0.08}$	$-0.03^{+0.32}_{-0.30}$	[3]
GW190719_215514	6.31×10^{-1}	0.92	$36.5^{+18.0}_{-10.3}$	$20.8^{+9.0}_{-7.2}$	$23.5^{+6.5}_{-4.0}$	$0.32^{+0.29}_{-0.31}$	[3]
GW190725_174728	4.58×10^{-1}	0.96	$11.5^{+6.2}_{-2.7}$	$6.4^{+2.0}_{-2.0}$	$7.4^{+0.6}_{-0.5}$	$-0.04^{+0.26}_{-0.14}$	[24]
GW190731_140936	3.35×10^{-1}	0.78	$41.5^{+12.2}_{-9.0}$	$28.8^{+9.7}_{-9.5}$	$29.5^{+7.1}_{-5.2}$	$0.06^{+0.24}_{-0.24}$	[3]
GW190805_211137	6.28×10^{-1}	0.95	$48.2^{+17.5}_{-12.5}$	$32.0^{+13.4}_{-11.4}$	$33.5^{+10.1}_{-7.0}$	$0.35^{+0.3}_{-0.36}$	[4]
GW190917_114630	6.56×10^{-1}	0.77	$9.3^{+3.4}_{-4.4}$	$2.1^{+1.5}_{-0.5}$	$3.7^{+0.2}_{-0.2}$	$-0.11^{+0.24}_{-0.49}$	[4]
GW191103_012549	4.58×10^{-1}	0.94	$11.8^{+6.2}_{-2.2}$	$7.9^{+1.7}_{-2.4}$	$8.34^{+0.66}_{-0.57}$	$0.21^{+0.16}_{-0.10}$	[1]
GW200216_220804	3.50×10^{-1}	0.77	51^{+22}_{-13}	30^{+14}_{-16}	$32.9^{+9.3}_{-8.5}$	$0.10^{+0.34}_{-0.36}$	[1]

TABLE I: A table of GW events that meet the criteria for inclusion in this work. Events are separated by a horizontal line into sections of $\mathrm{FAR}_{\min} < 0.25\,\mathrm{yr}^{-1}$ and $1\,\mathrm{yr}^{-1} \geq FAR_{\min} \geq 0.25\,\mathrm{yr}^{-1}$ (lower), where $\mathrm{FAR}_{\min}$ is the smallest FAR reported over all pipelines. Within these sections, events are listed by the date they were detected. Columns provide the FAR, p_{astro} (from the pipeline with the smallest FAR), and previously-reported estimates of selected parameters. These previously-reported parameters may adopt different priors than our work and do not precisely correspond to our inputs; see Section III for details. The low-significance event GW190531 is not included, lacking parameter inferences.

LSC 2021

Extracting the masses

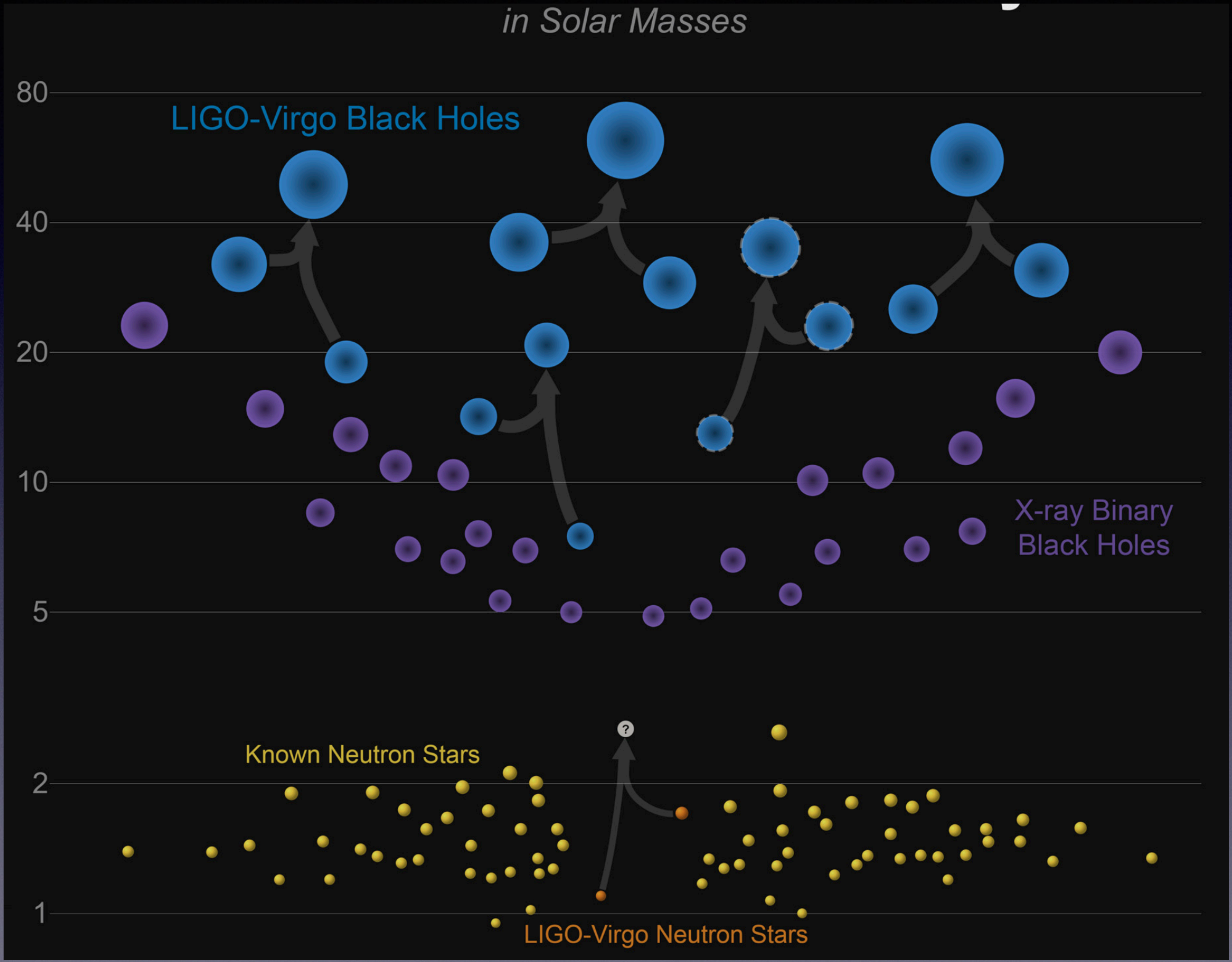

Figure: LSC collaboration 2018

2021 update

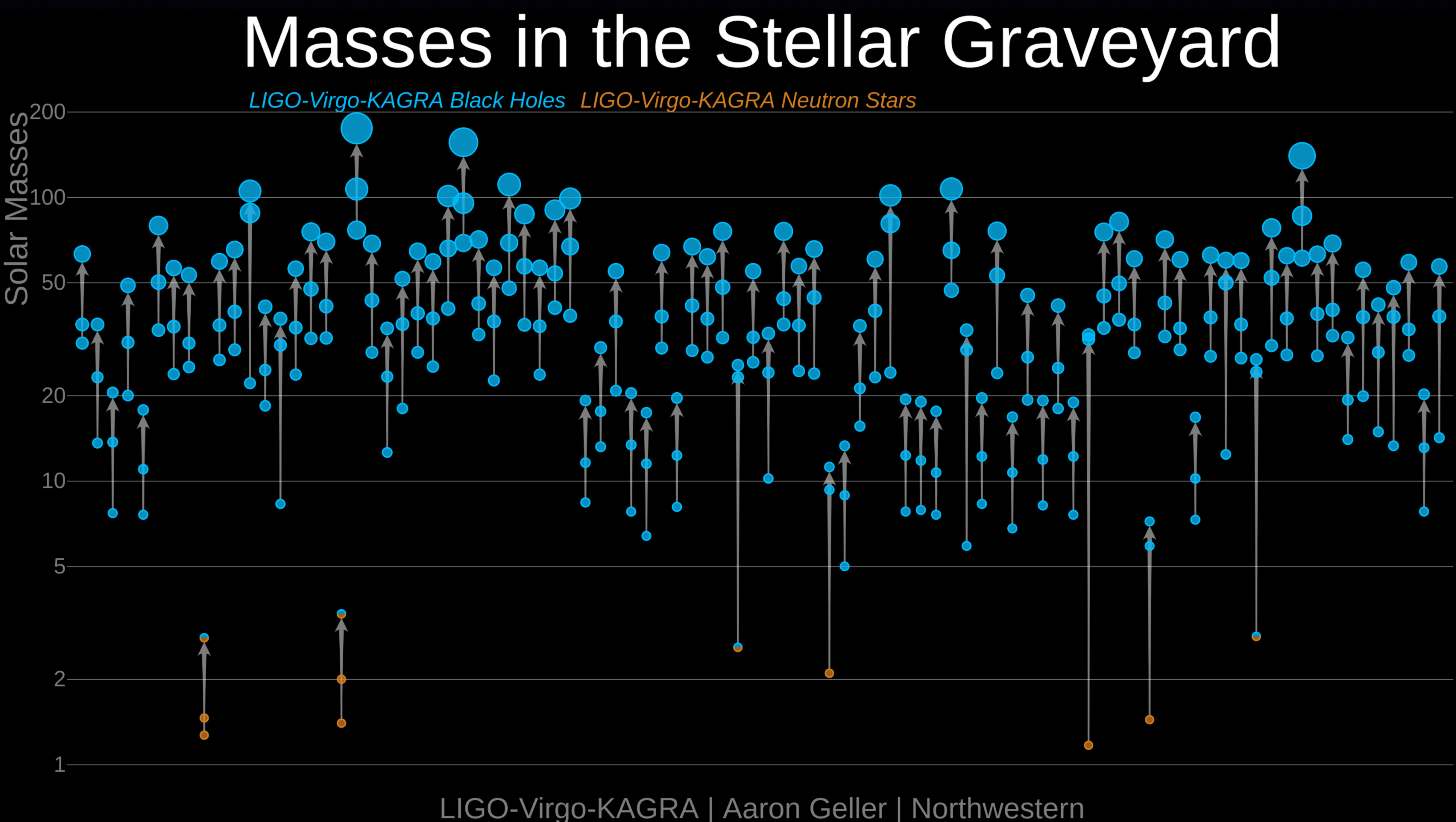
Masses in the Stellar Graveyard
LIGO-Virgo-KAGRA Black Holes
LIGO-Virgo-KAGRA Neutron Stars
Solar Masses
200
100
50
20
10
5
2
1
LIGO-Virgo-KAGRA | Aaron Geller | Northwestern

Measuring BH spins

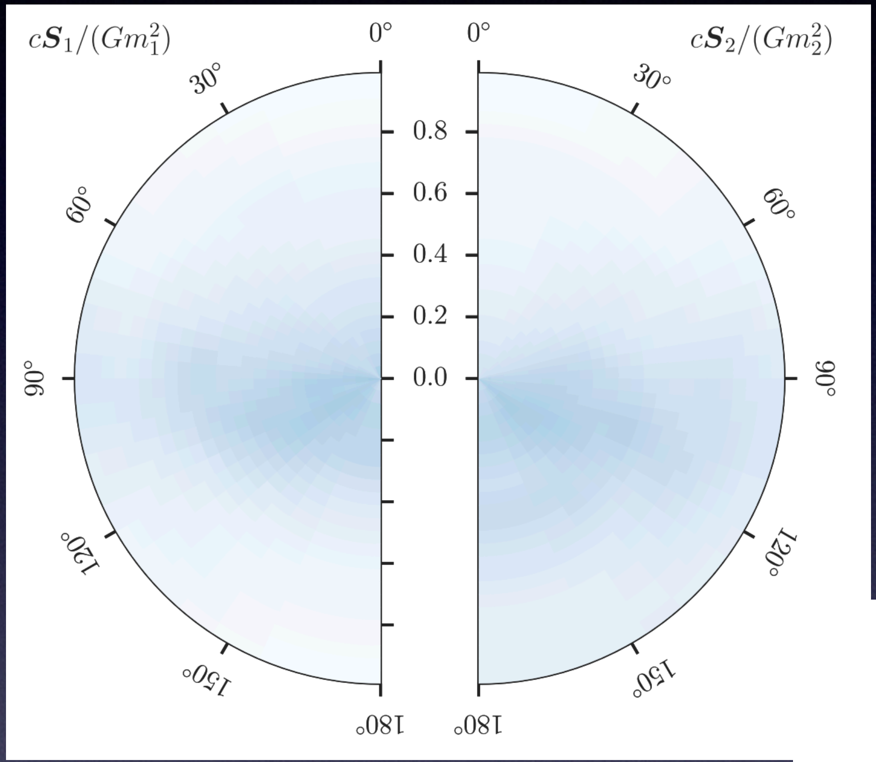

GW150914

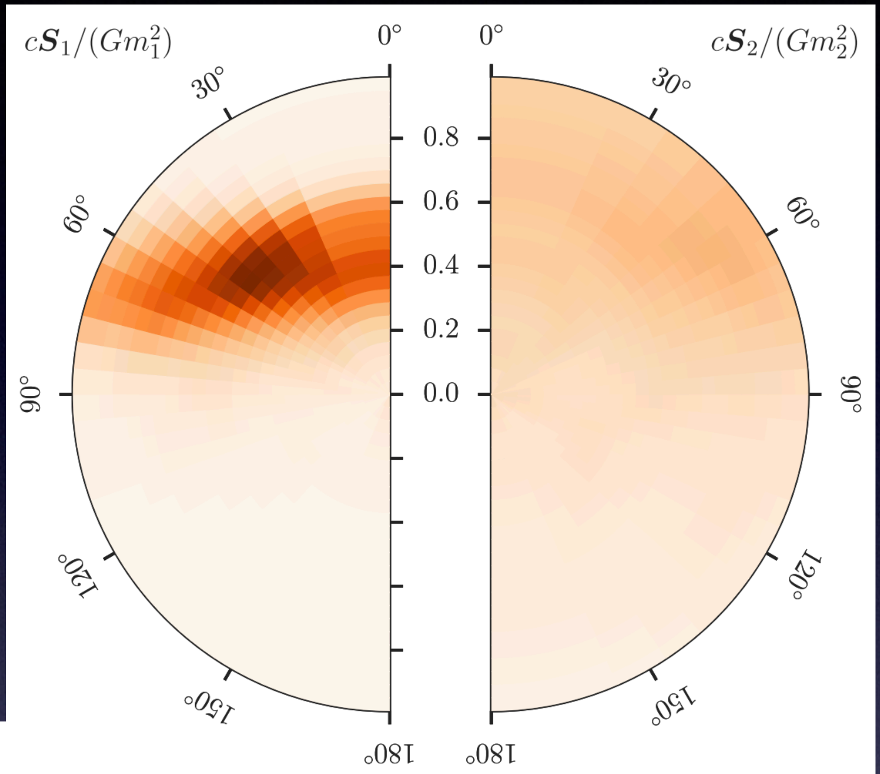

GW151226

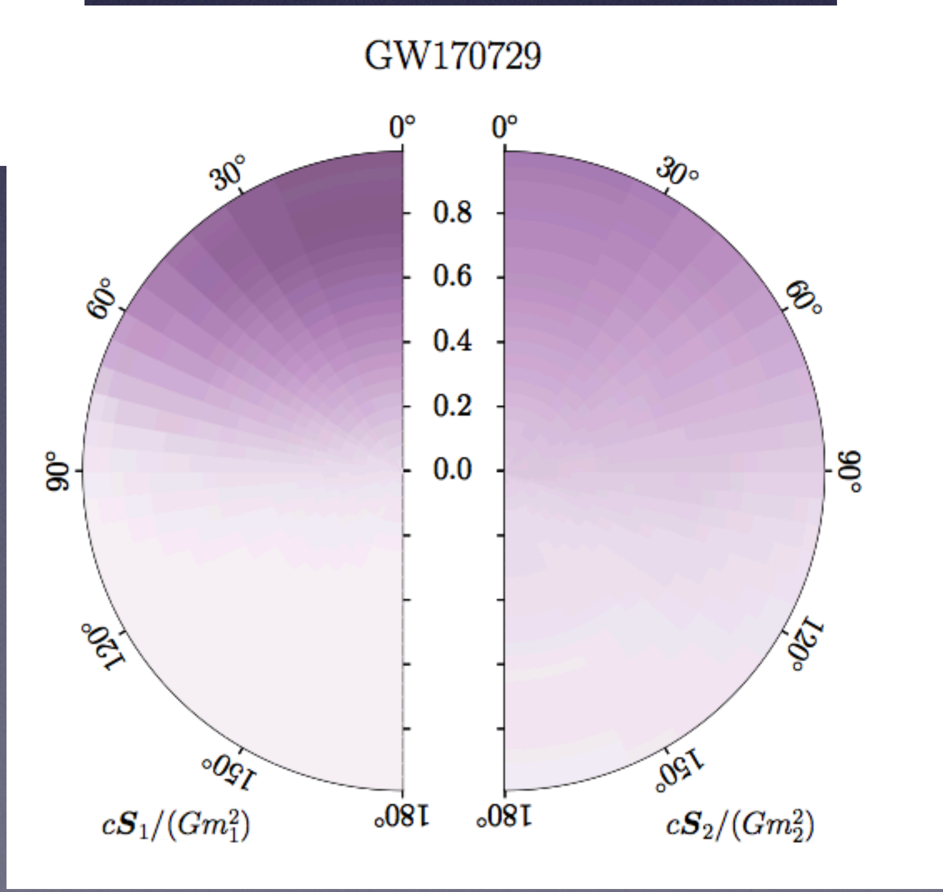

Figures: LSC collaboration 2016, 2018

O3a updates

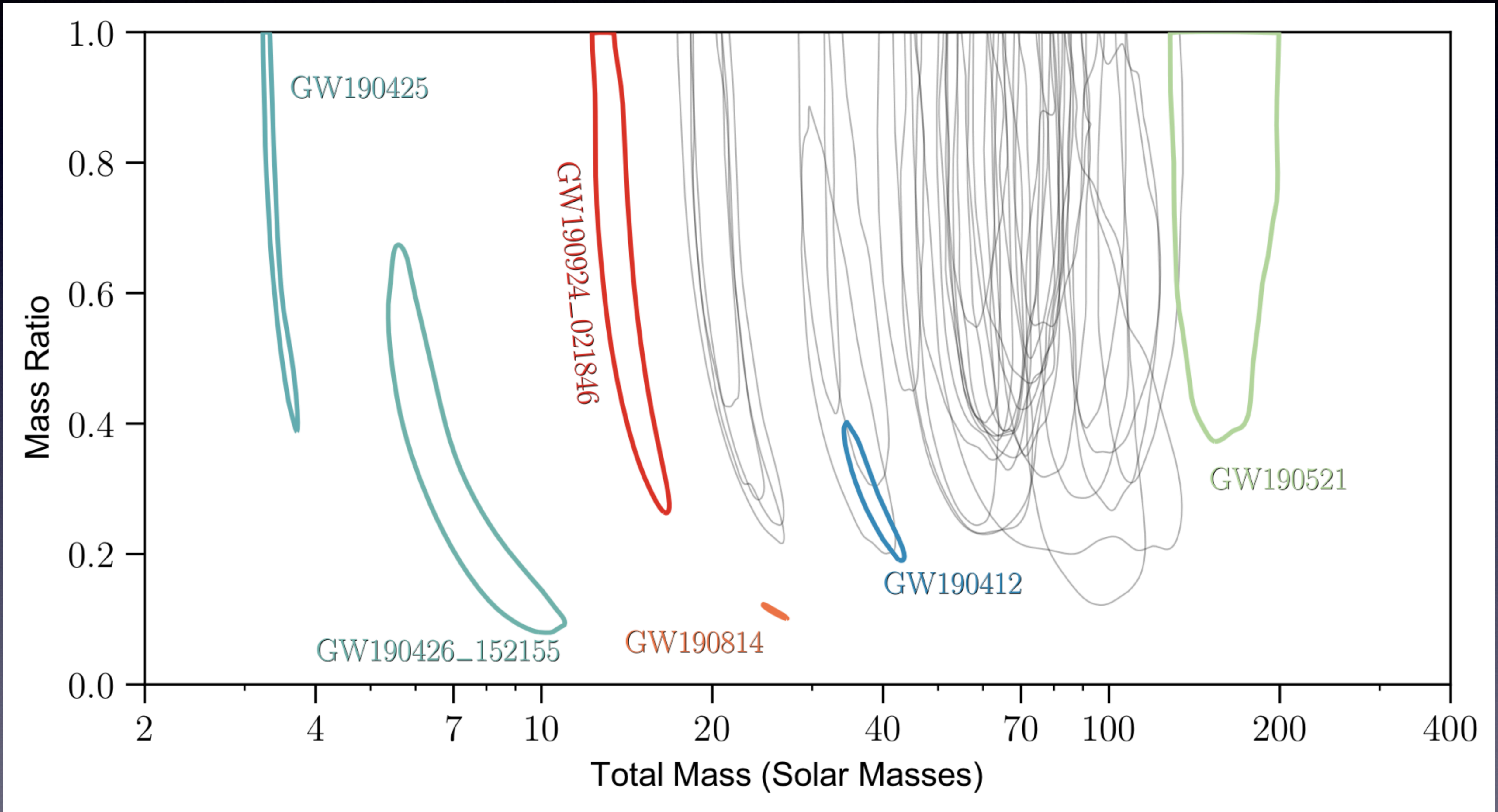

Mass Ratio
1.0
0.8
0.6
0.4
0.2
0.0
GW190425
GW190426_152155
GW190924_021846
GW190814
GW190412
GW190521
2
4
7
10
20
40
70
100
200
400
Total Mass (Solar Masses)

O3b updates

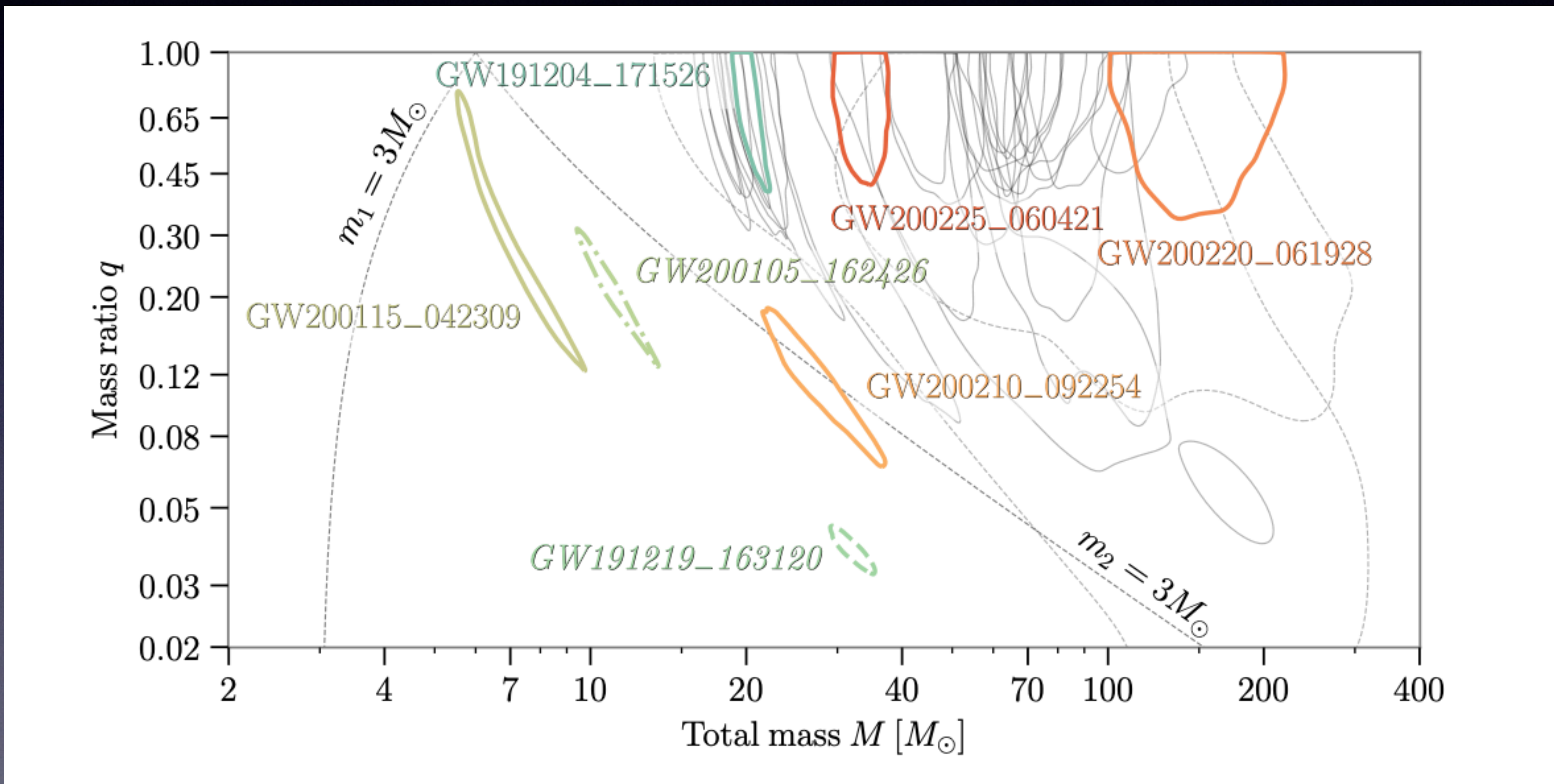

GW191204_171526
GW200225_060421
GW200220_061928
GW200105_162426
GW200115_042309
GW200210_092254
GW191219_163120
$m_1 = 3M_\odot$
$m_2 = 3M_\odot$
Mass ratio q
1.00
0.65
0.45
0.30
0.20
0.12
0.08
0.05
0.03
0.02
2
4
7
10
20
40
70
100
200
400
Total mass M [$M_\odot$]

O3a updates

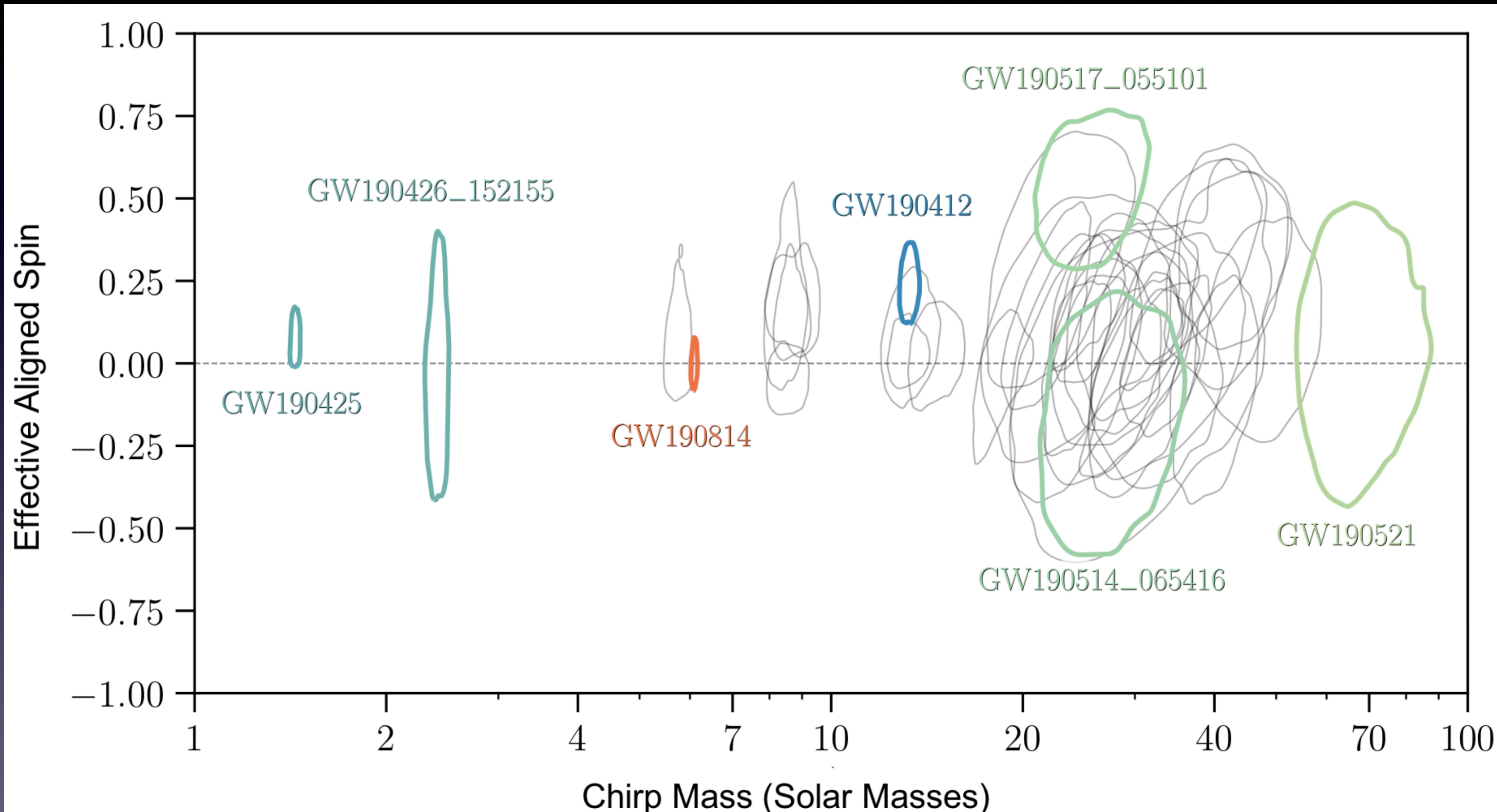

$$\chi_{\rm eff} = \frac{c}{GM}\left(\frac{\boldsymbol{S}_1}{m_1} + \frac{\boldsymbol{S}_2}{m_2}\right)\cdot\frac{\boldsymbol{L}}{|\mathbf{L}|}$$

O3b updates

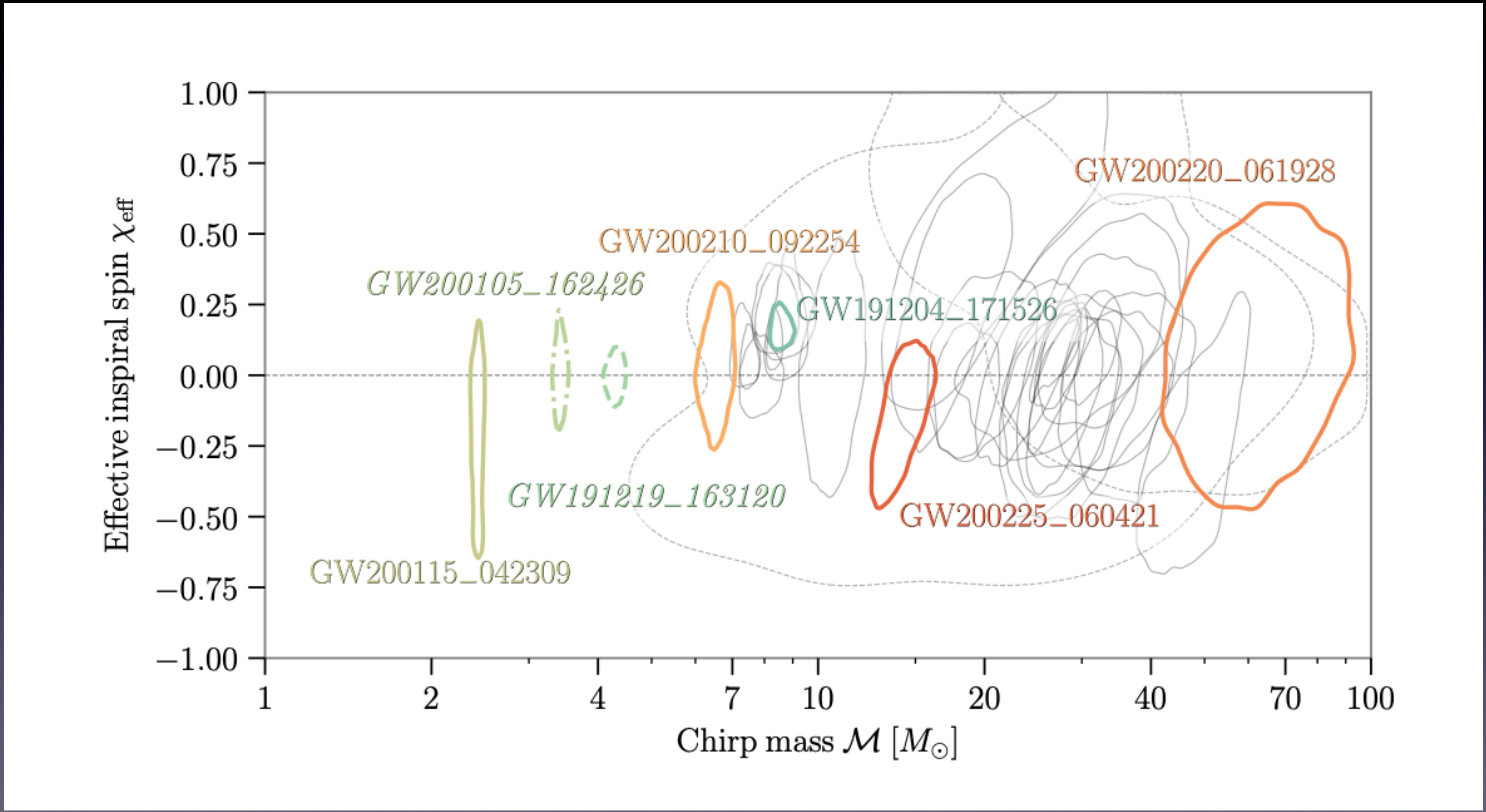

$$\chi_{\mathrm{eff}} = \frac{c}{GM}\left(\frac{\boldsymbol{S}_1}{m_1} + \frac{\boldsymbol{S}_2}{m_2}\right) \cdot \frac{\boldsymbol{L}}{|\mathbf{L}|}$$

GW170817 (NS binary)

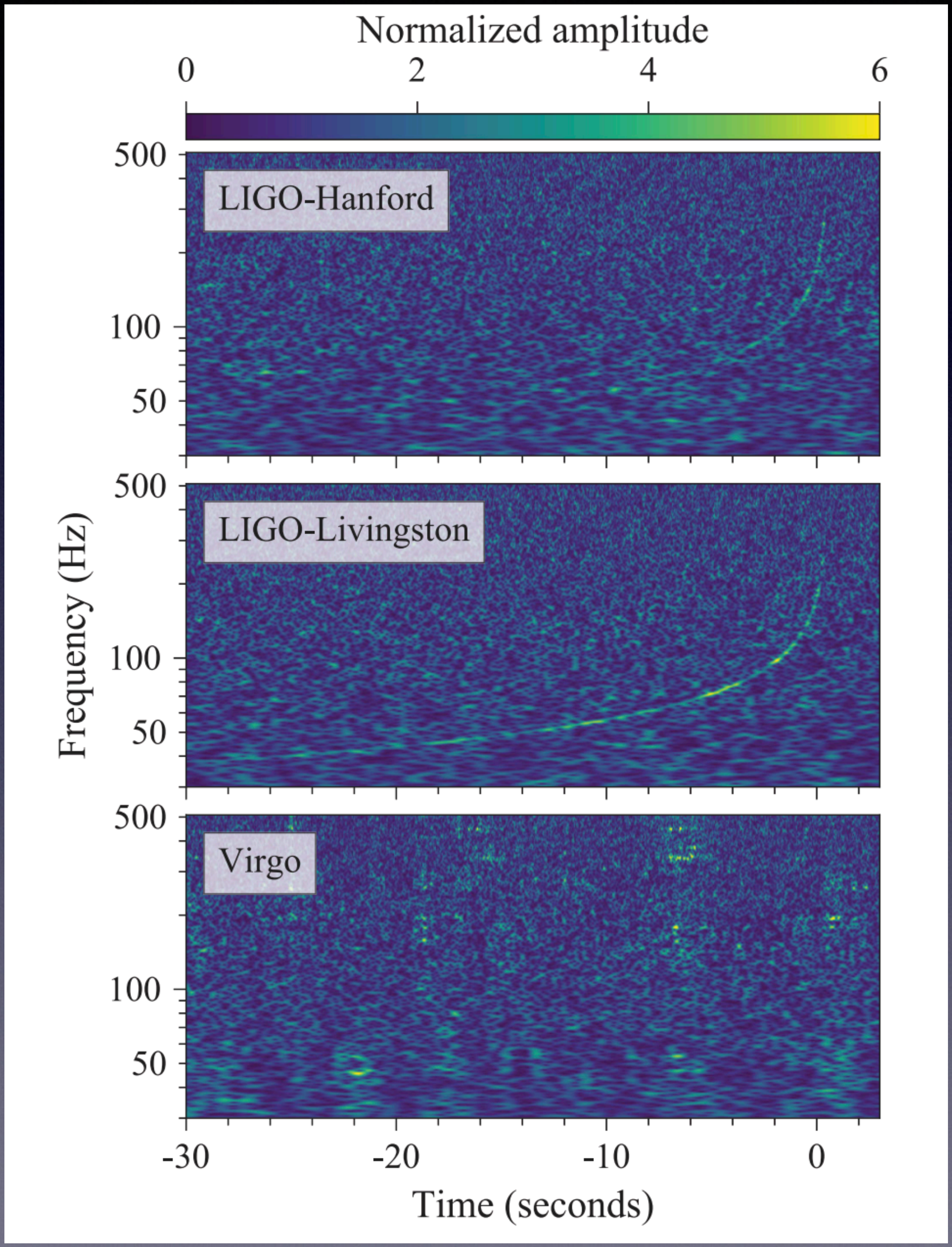

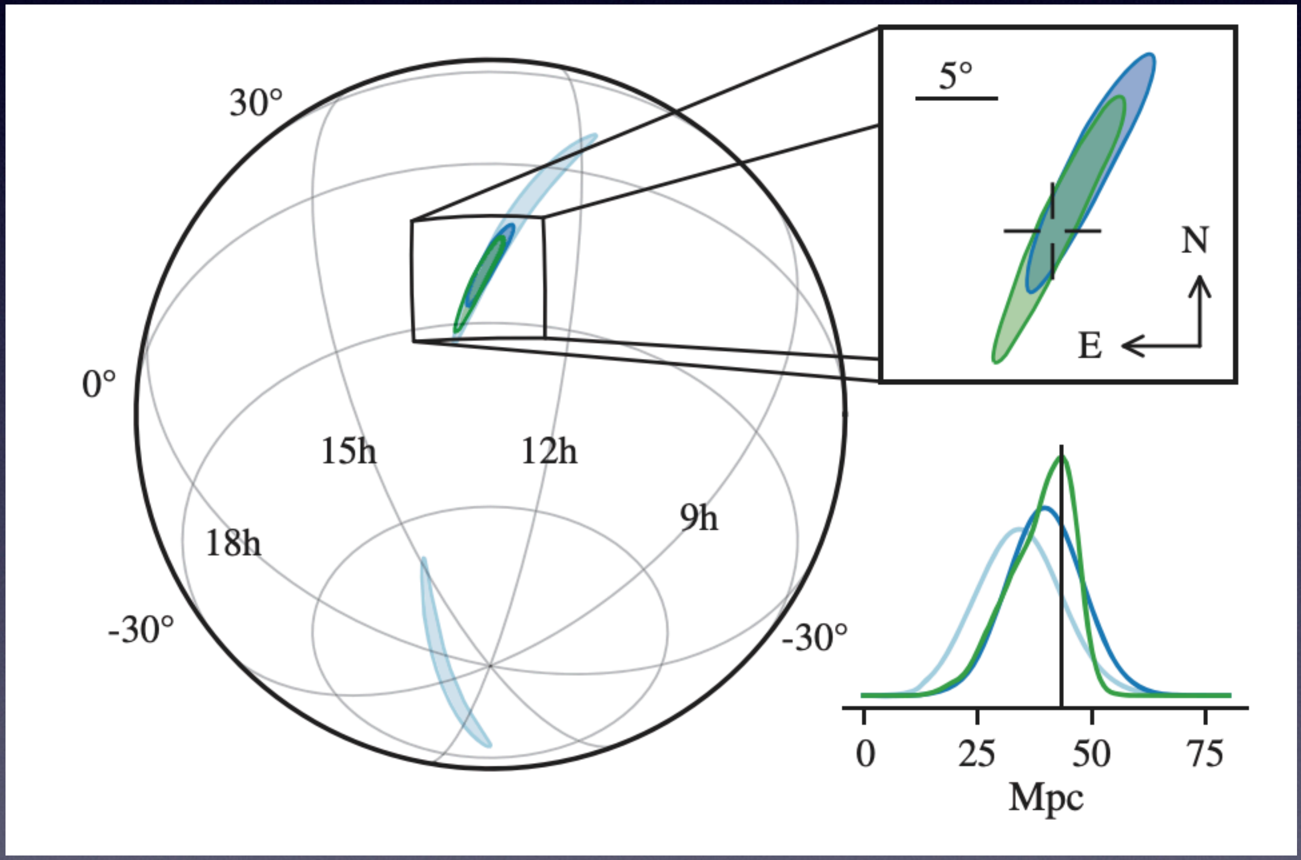

GW170817 (NS binary)

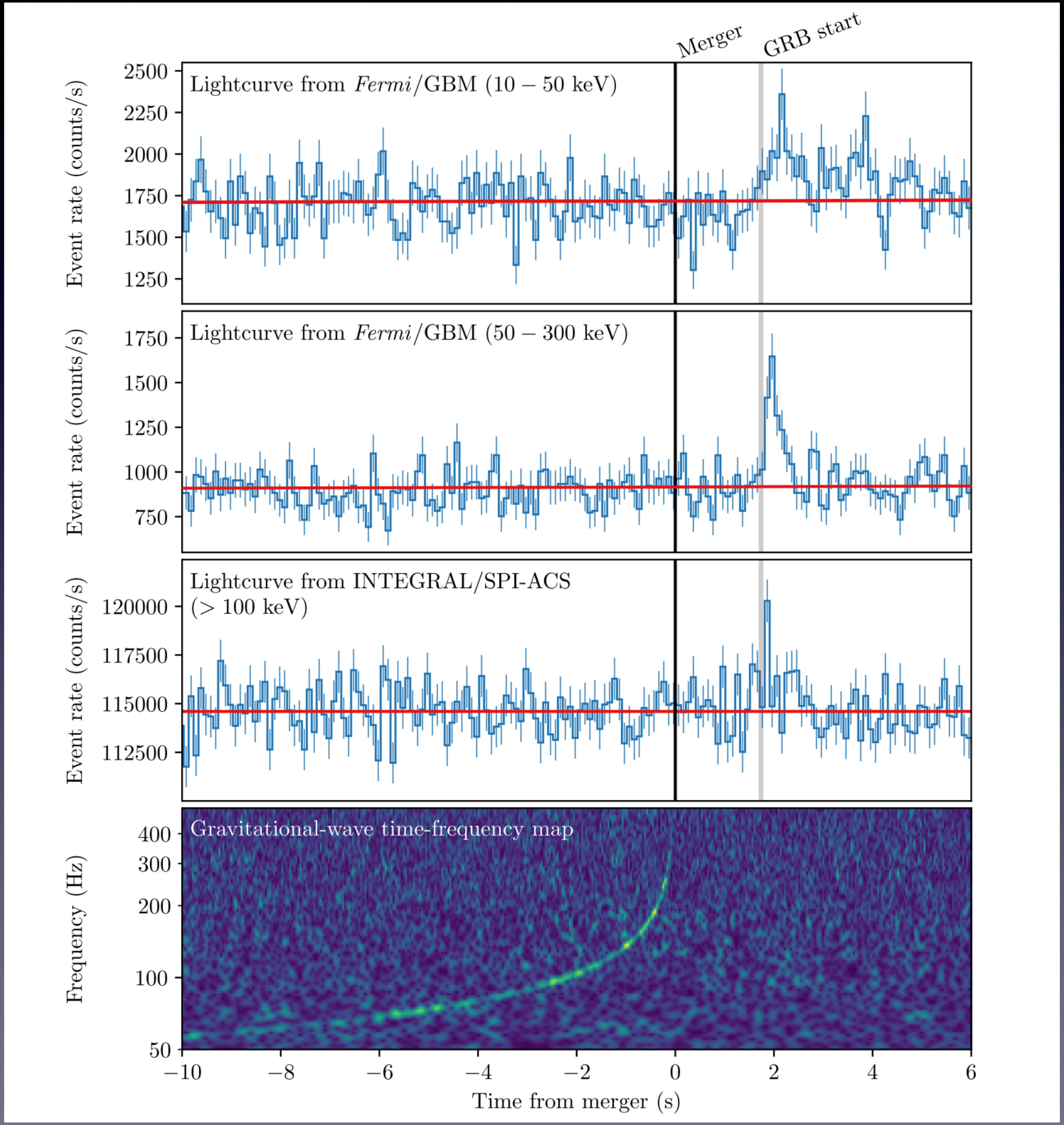

Coincident detection implies

$$\frac{|c_{gw} - c|}{c} \lesssim 10^{-15}$$

GW170817 (NS binary)

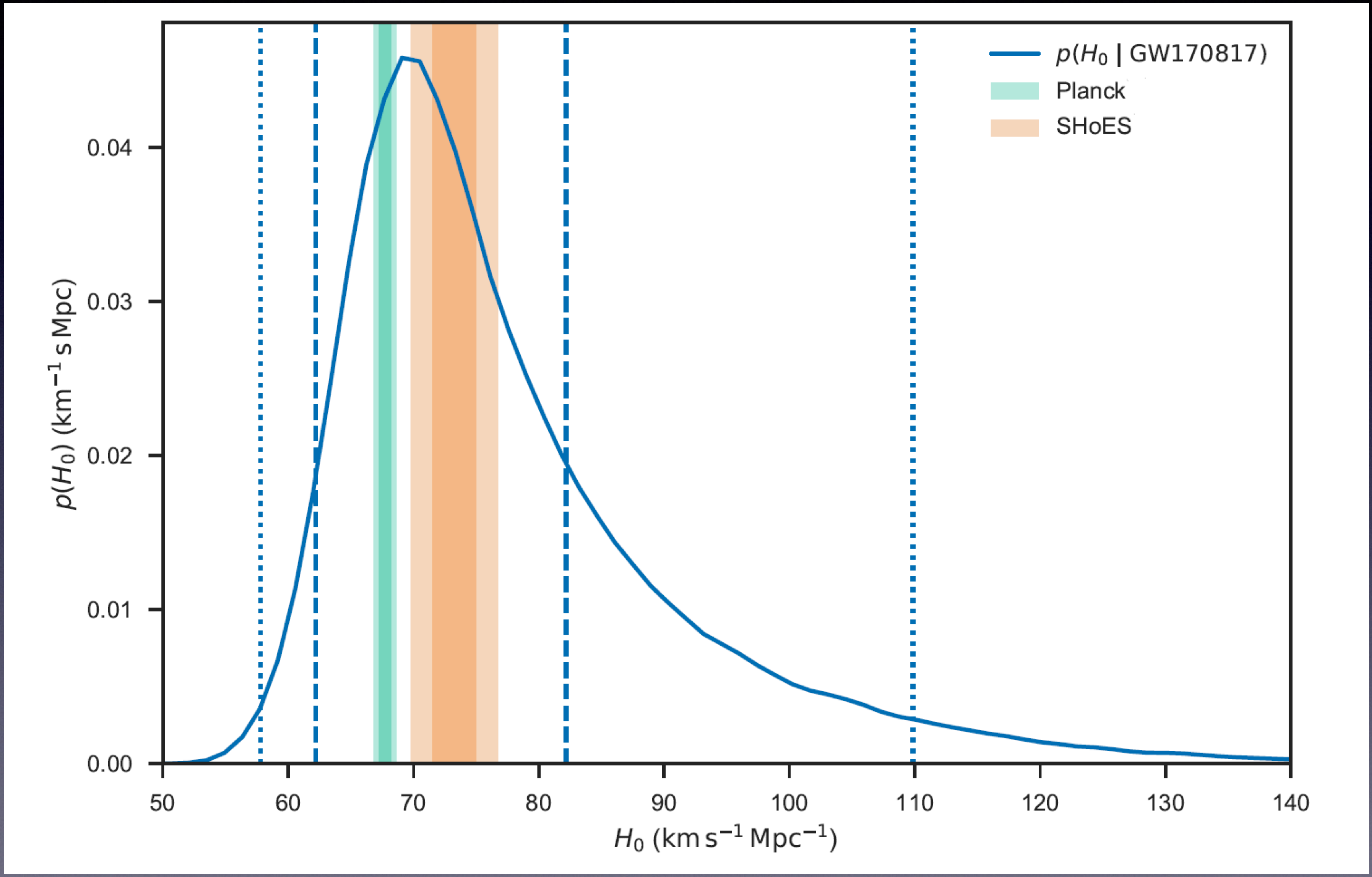

LSC 2018

GW170817 (NS binary)

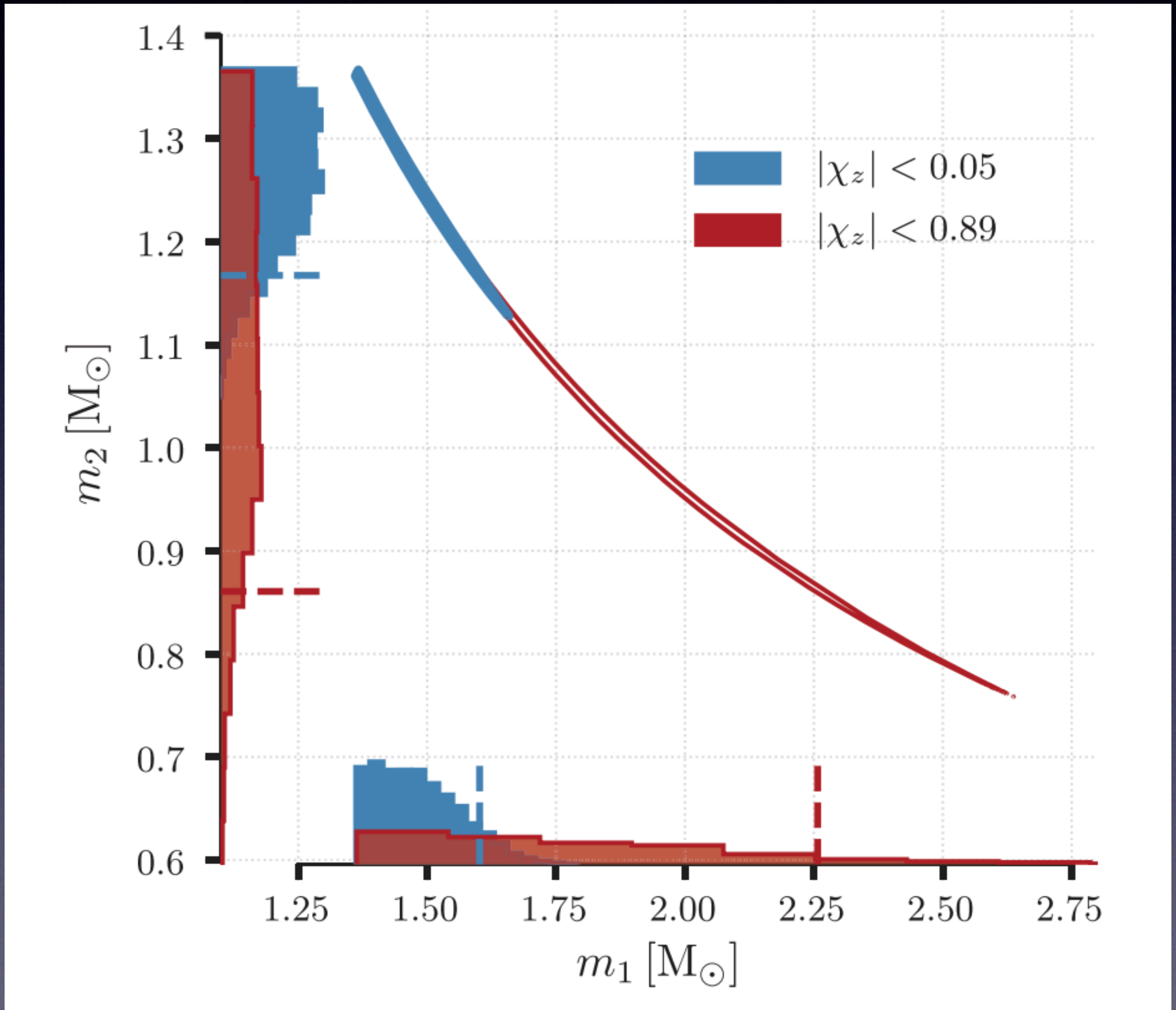

Up to 5PN order, inspiral is the same as for BHs

GW170817 (NS binary)

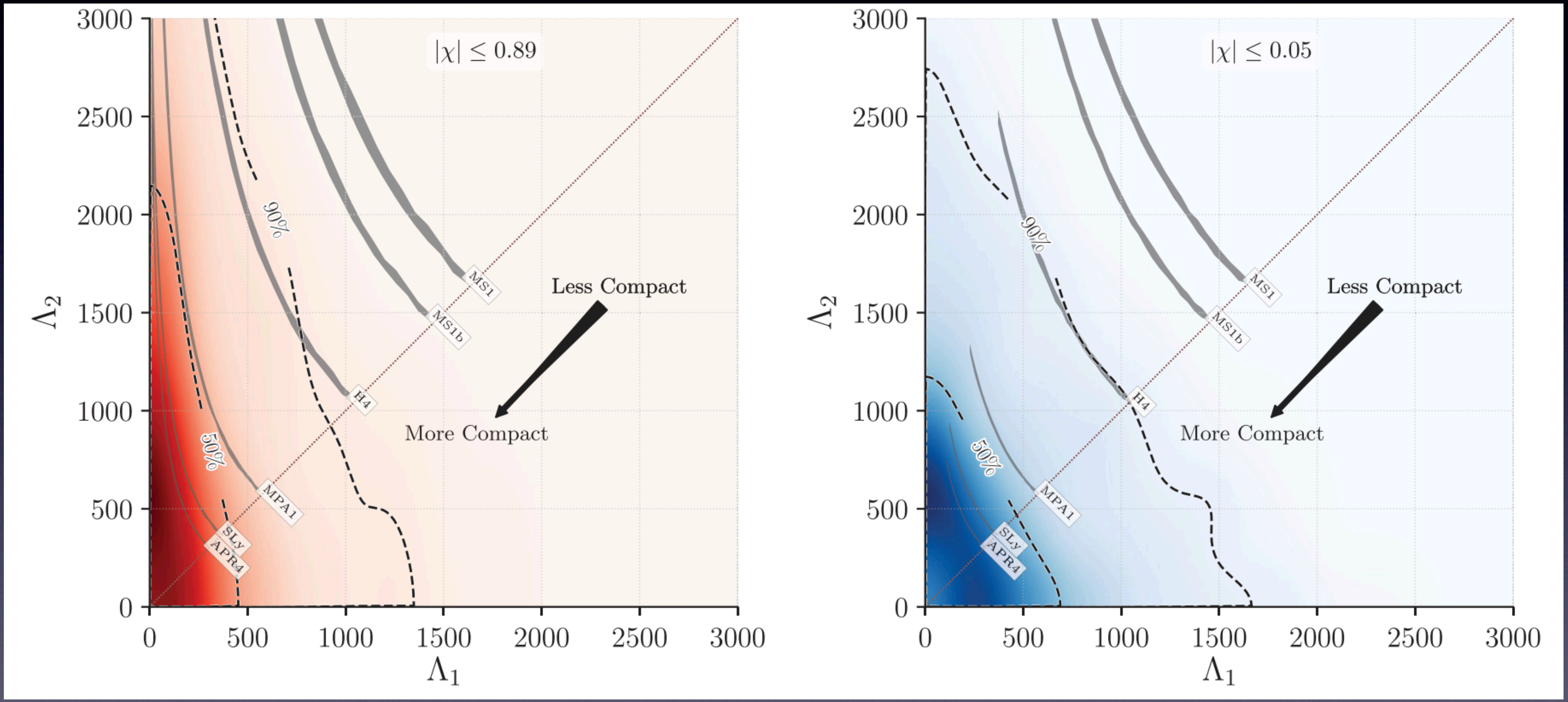

Tidal effects constrain EOS of nuclear matter

Two NS-BH mergers

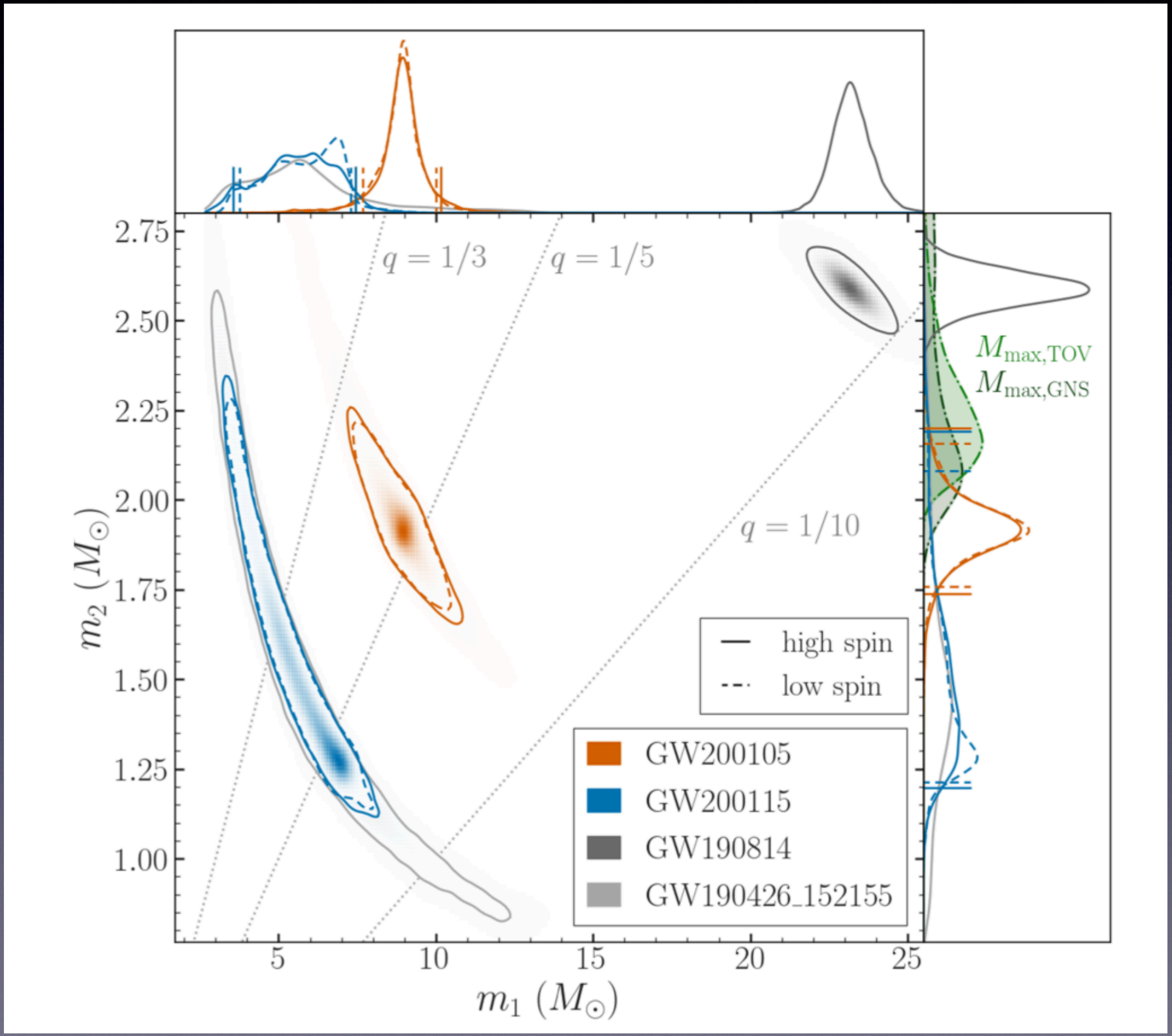

The formation of stellar-mass BHs

- Stellar-mass BH form from massive stars
- Difficult problem: stellar evolution needed to understand mass loss from stellar winds, and explosion mechanism (core collapse SN, direct collapse to BH)
- Evolution depends on mass, metallicity, rotation

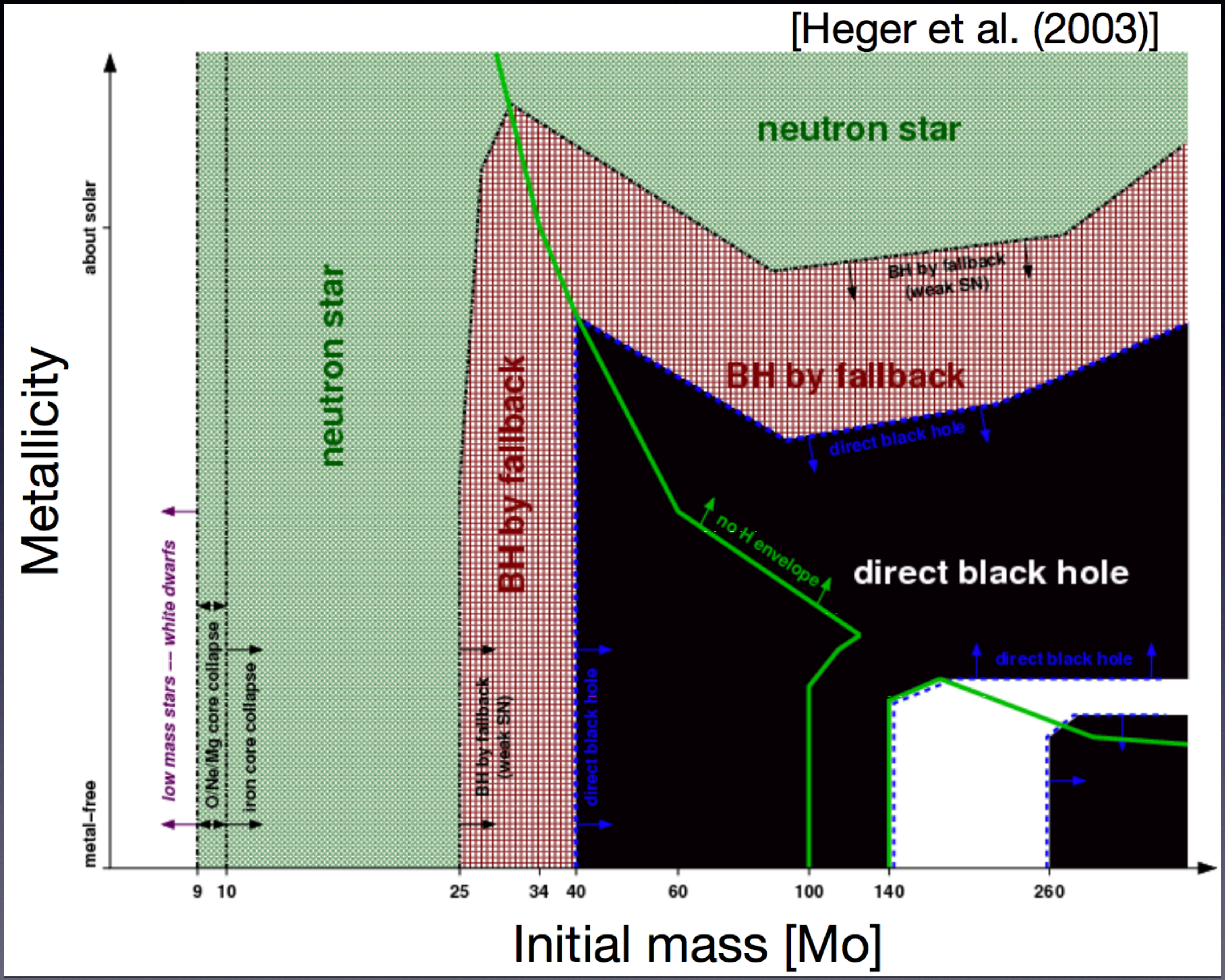

The role of metallicity and stellar winds

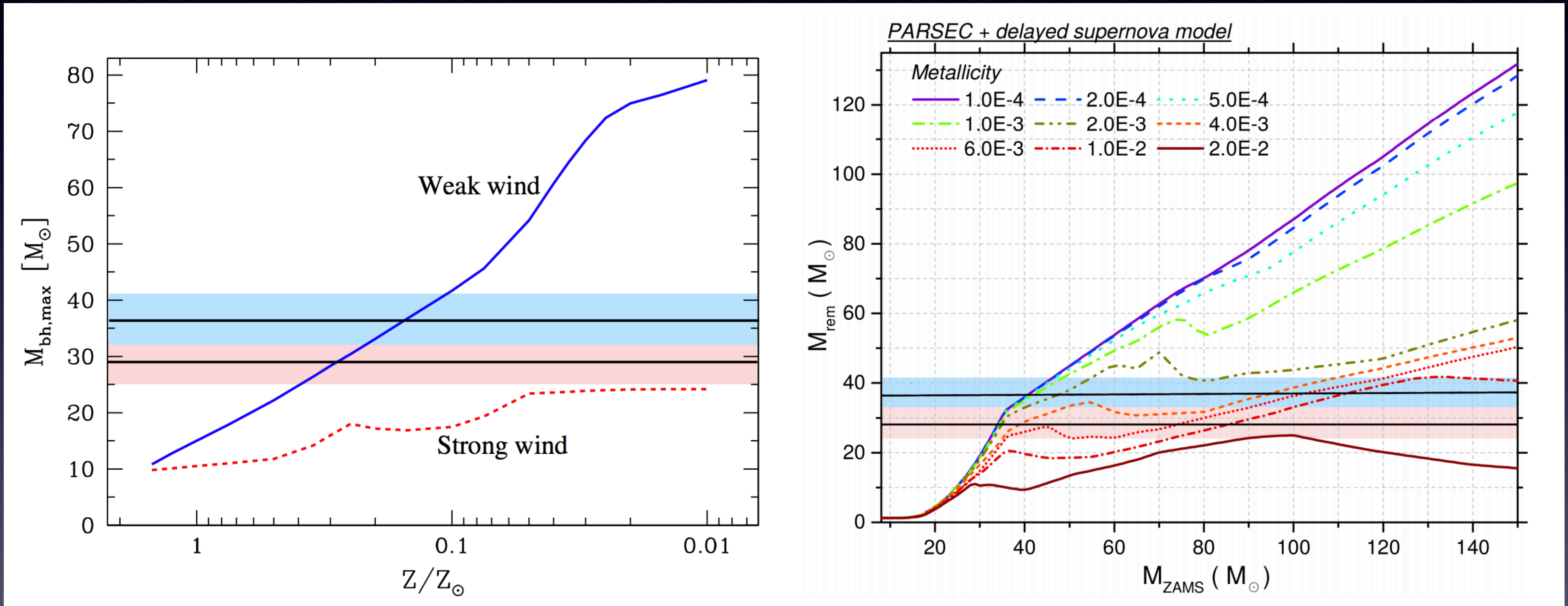

LSC 2015; Belczynski et al 2010; Spera et al 2015

The role of metallicity and stellar winds

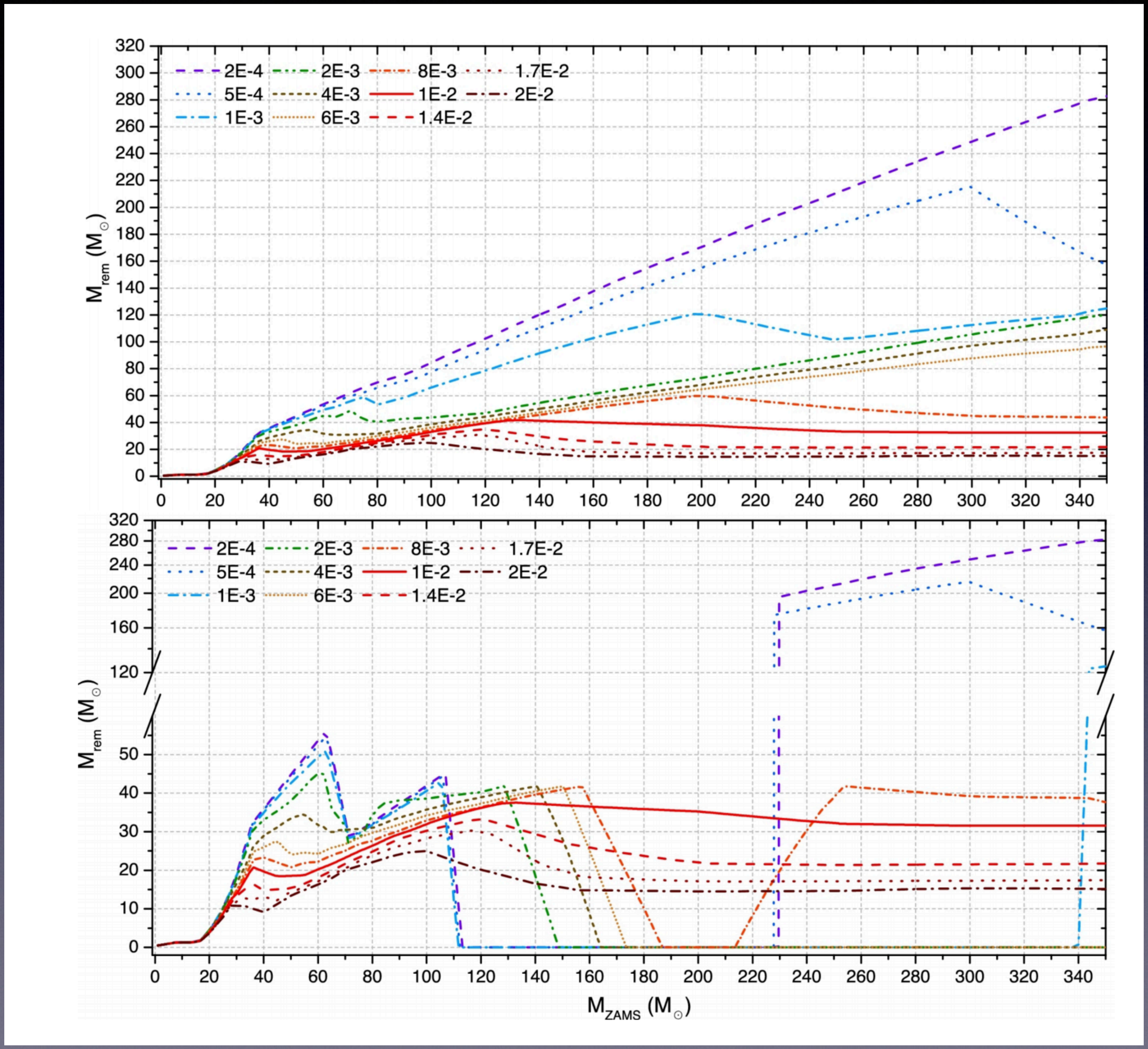

Mapelli 2018;
Spera & Mapelli 2017

Pair instability SN

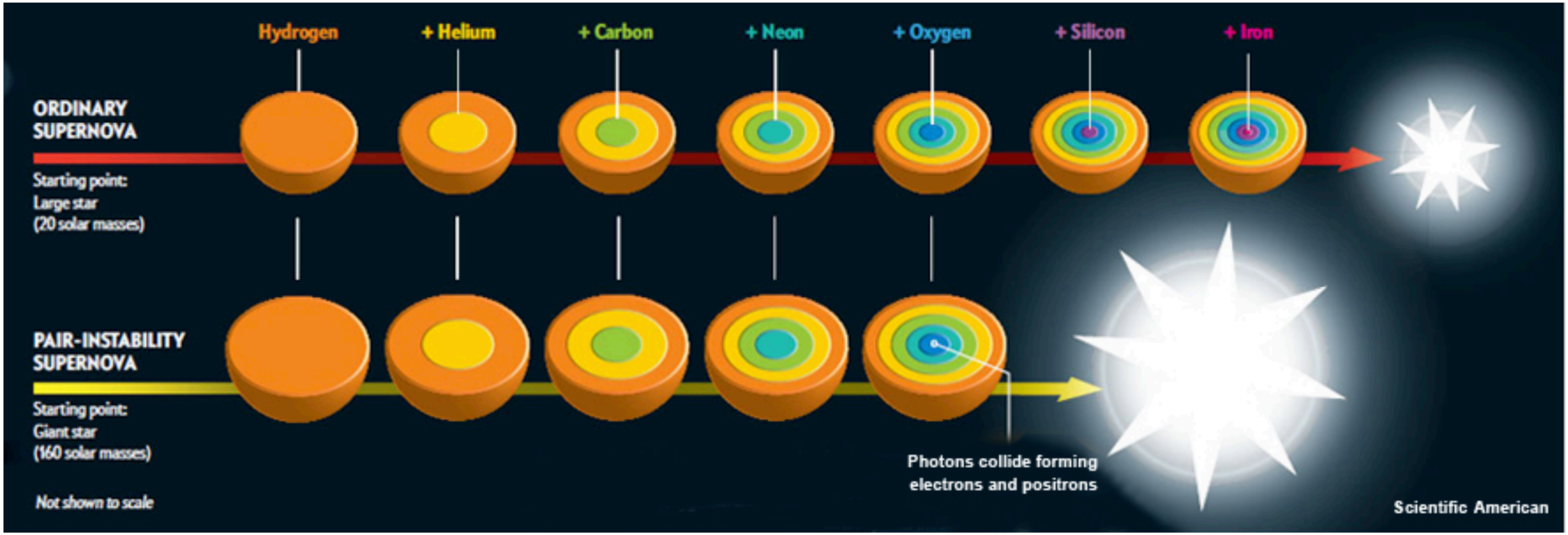

Mass at birth (solar masses)	Helium core mass (solar masses)	Compact remnant	Event
10–95	2–40	Neutron star, black hole	Ordinary supernova
95–130	40–60	Neutron star, black hole	Pulsational pair-instability supernova
130–260	60–137	Explosion, no remnant	Pair-instability supernova
>260	>137	Black hole	?

Woosley, Blinnikov, Heger (2007)

A cutoff at 40 Msun?

Mass at birth (solar masses)	Helium core mass (solar masses)	Compact remnant	Event
10–95	2–40	Neutron star, black hole	Ordinary supernova
95–130	40–60	Neutron star, black hole	Pulsational pair-instability supernova
130–260	60–137	Explosion, no remnant	Pair-instability supernova
>260	>137	Black hole	?

Woosley, Blinnikov, Heger (2007)

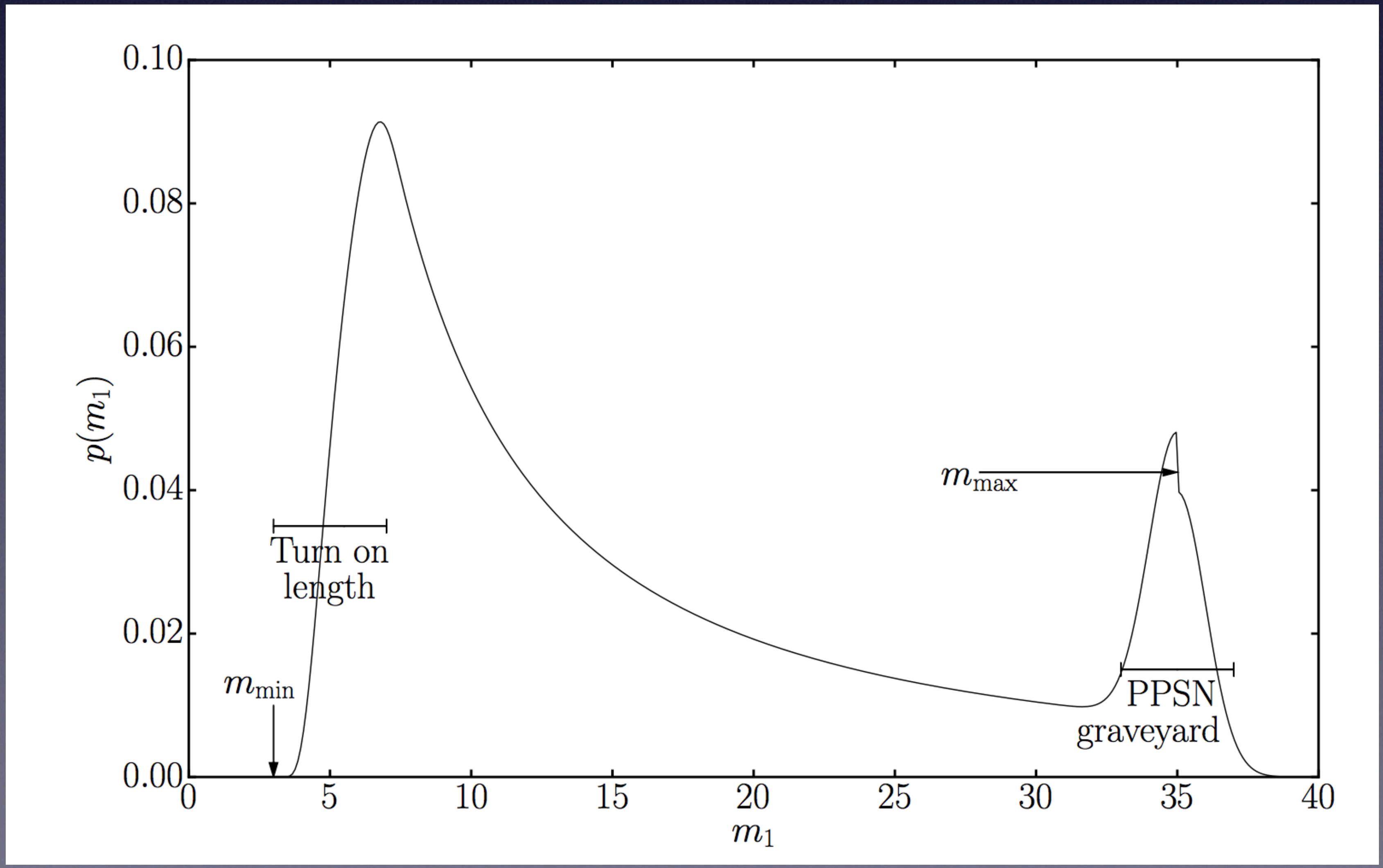

Talbot & Thrane 2018

Is there a pair instability gap?

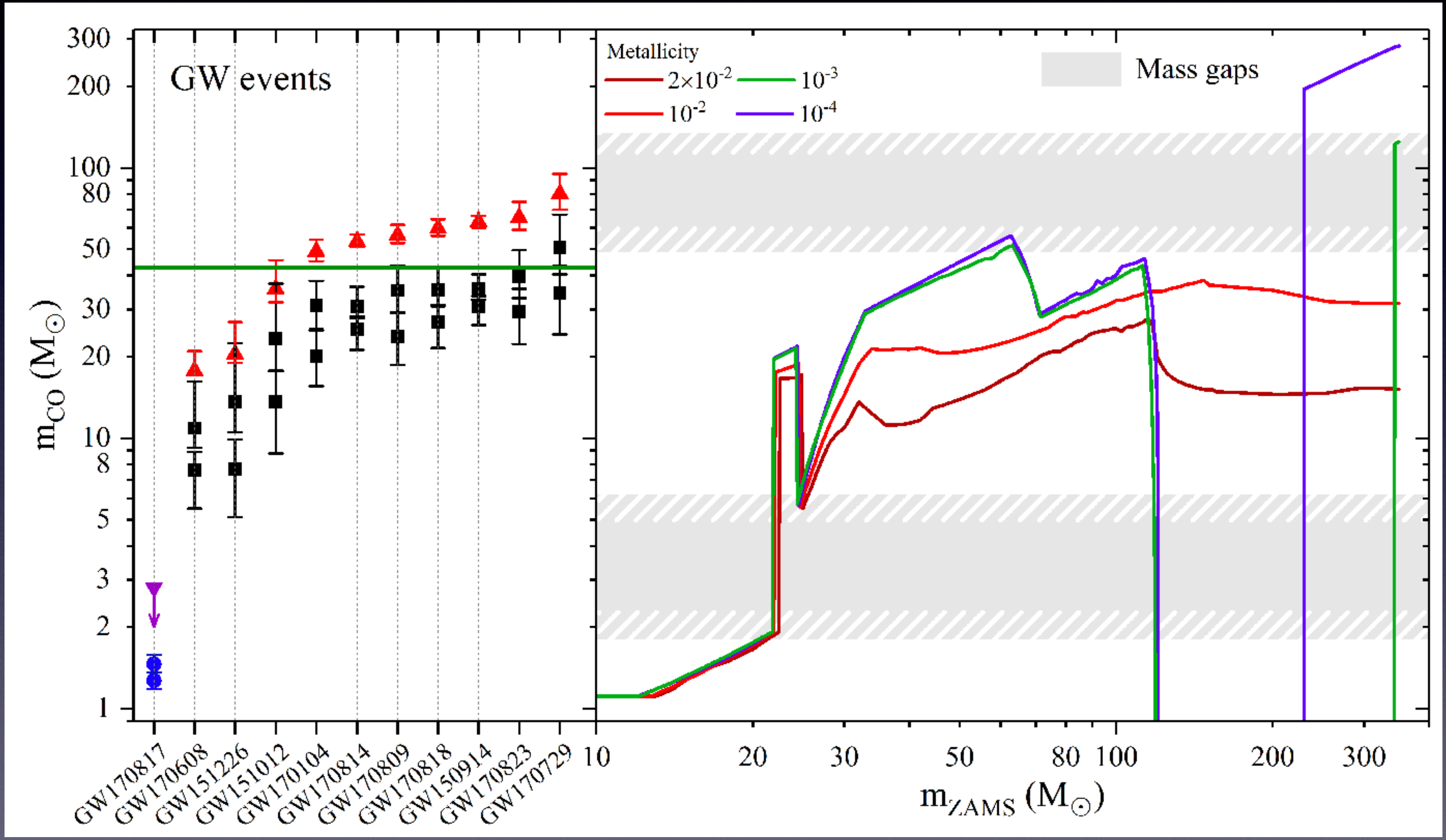

LSC 2018, O2

Is there a pair instability gap?

GW190521 has one component squarely inside mass gap

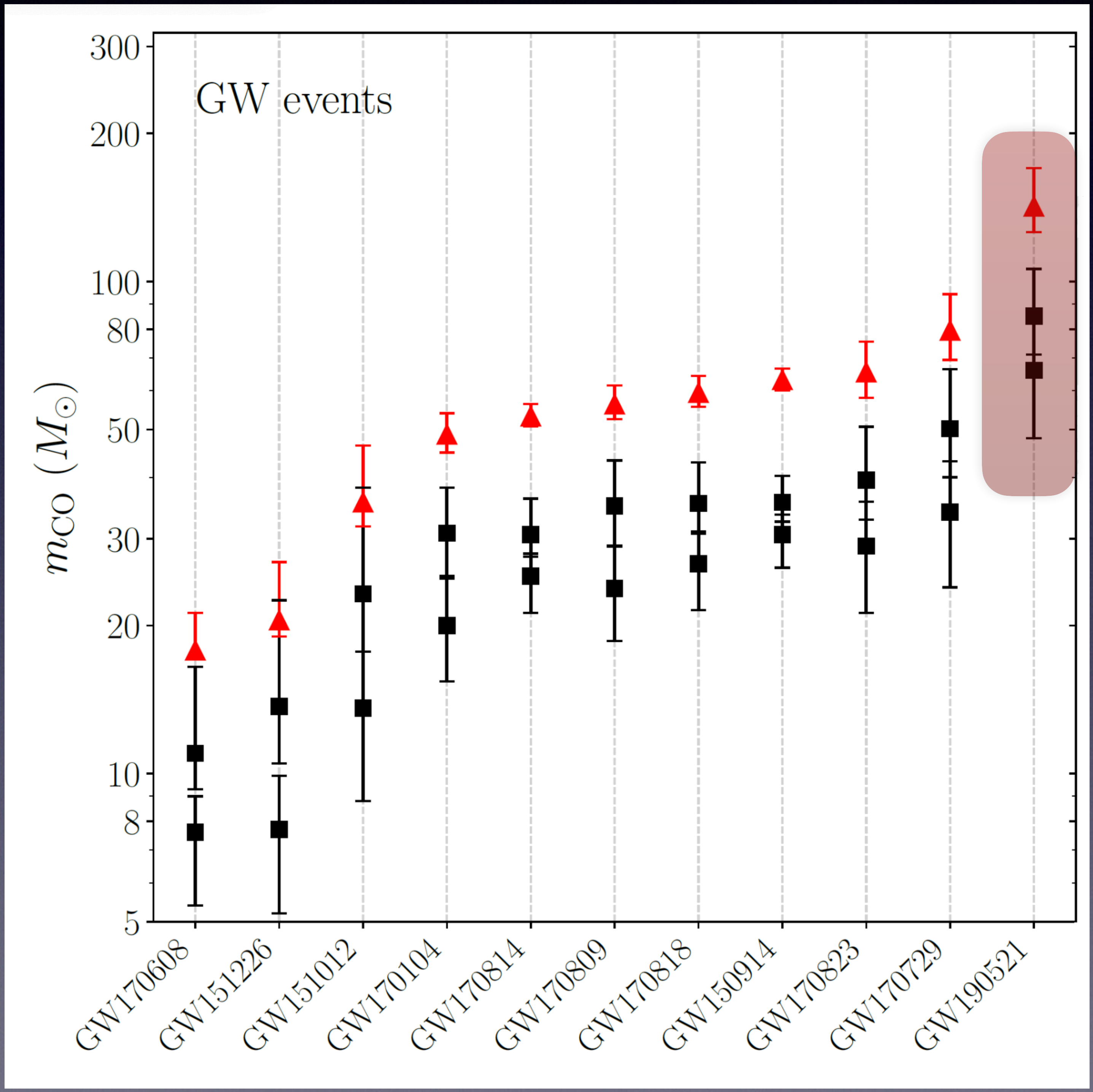

How do stellar-mass BH *binaries* form?

- In the field (plausible because ~70% of massive stars have companion, c.f. Sana et al 2012)

- In dense environments (globular clusters/nuclear star clusters) via dynamical mechanisms

- Primordial BHs? But problems with CMB/absence of enough MW candidates in radio/X-rays if one wants to explain all of Dark Matter. Formation mechanism also unclear (clustering vs lack of clustering), conflicting predictions for spins

How do stellar-mass BH *binaries* form?

- In the field (plausible because ~70% of massive stars have companion, c.f. Sana et al 2012)
- In dense environments (globular clusters/nuclear star clusters) via dynamical mechanisms
- ~~Primordial BHs? But problems with CMB/absence of enough MW candidates in radio/X-rays if one wants to explain all of Dark Matter. Formation mechanism also unclear (clustering vs lack of clustering), conflicting predictions for spins~~

Field BH binaries

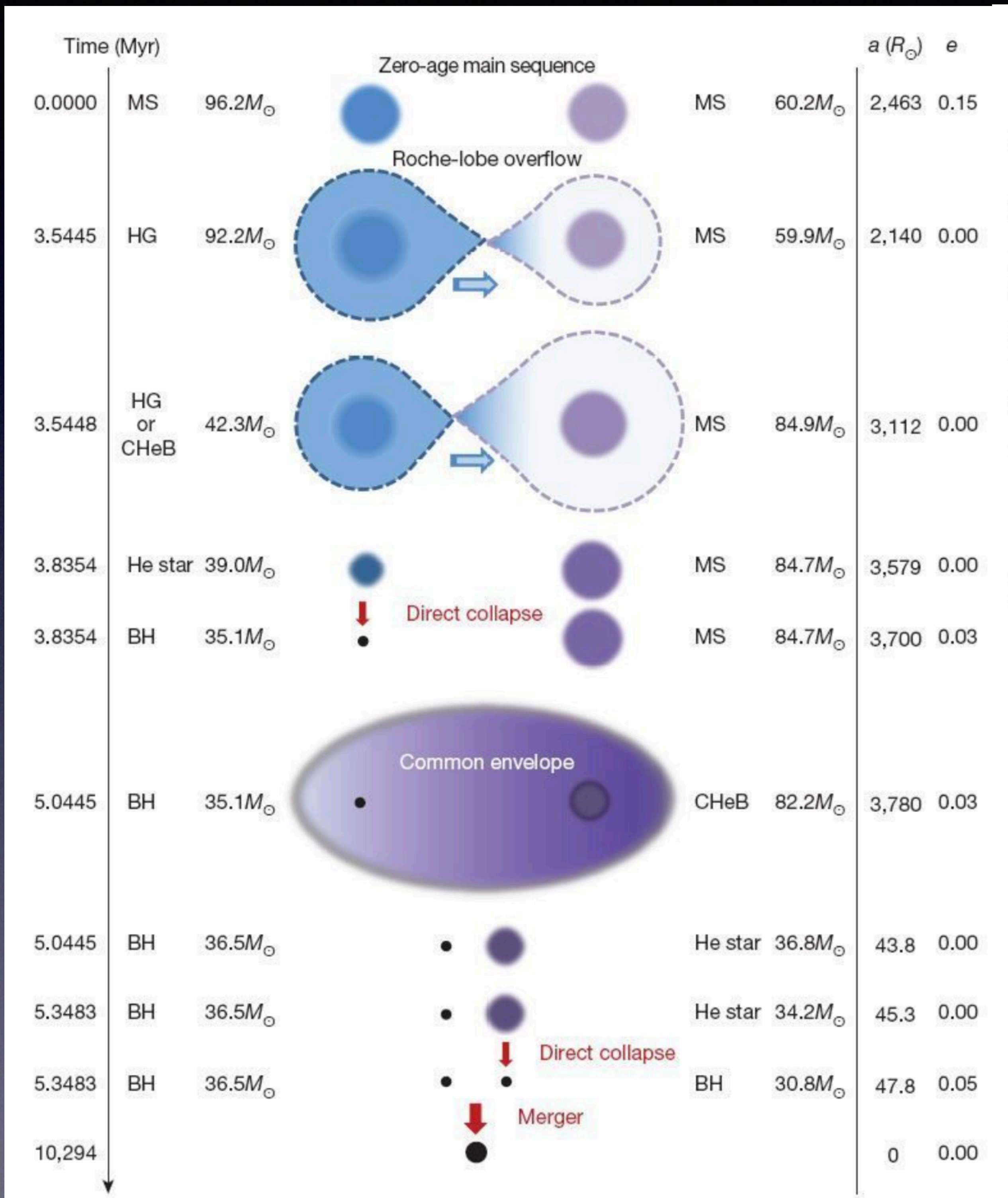

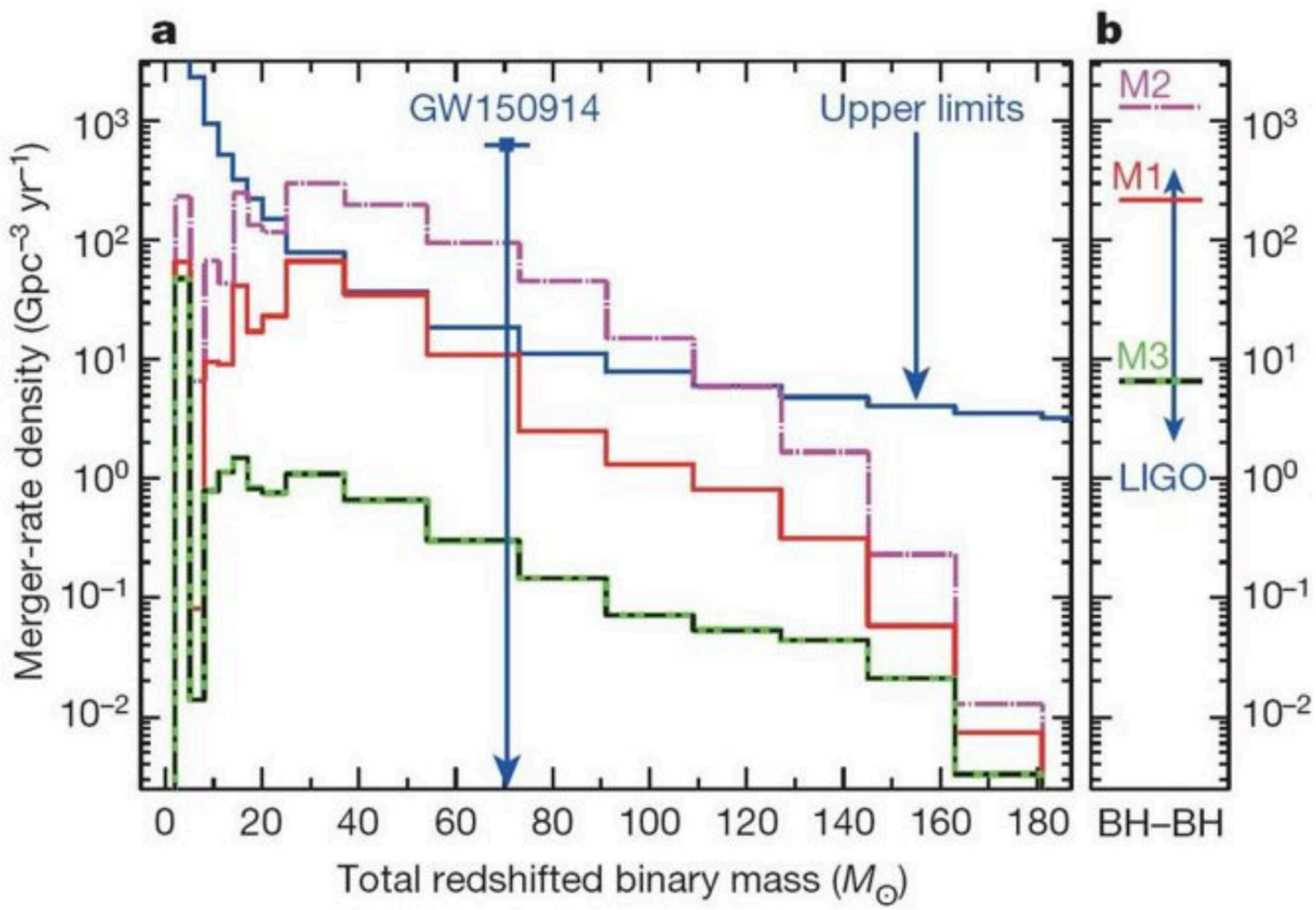

Merger rates for standard model (M1; red); optimistic common-envelope phase (M2; pink); and pessimistic large black-hole kicks (M3; green/black)

Belczynski et al 2016

Field BH binaries

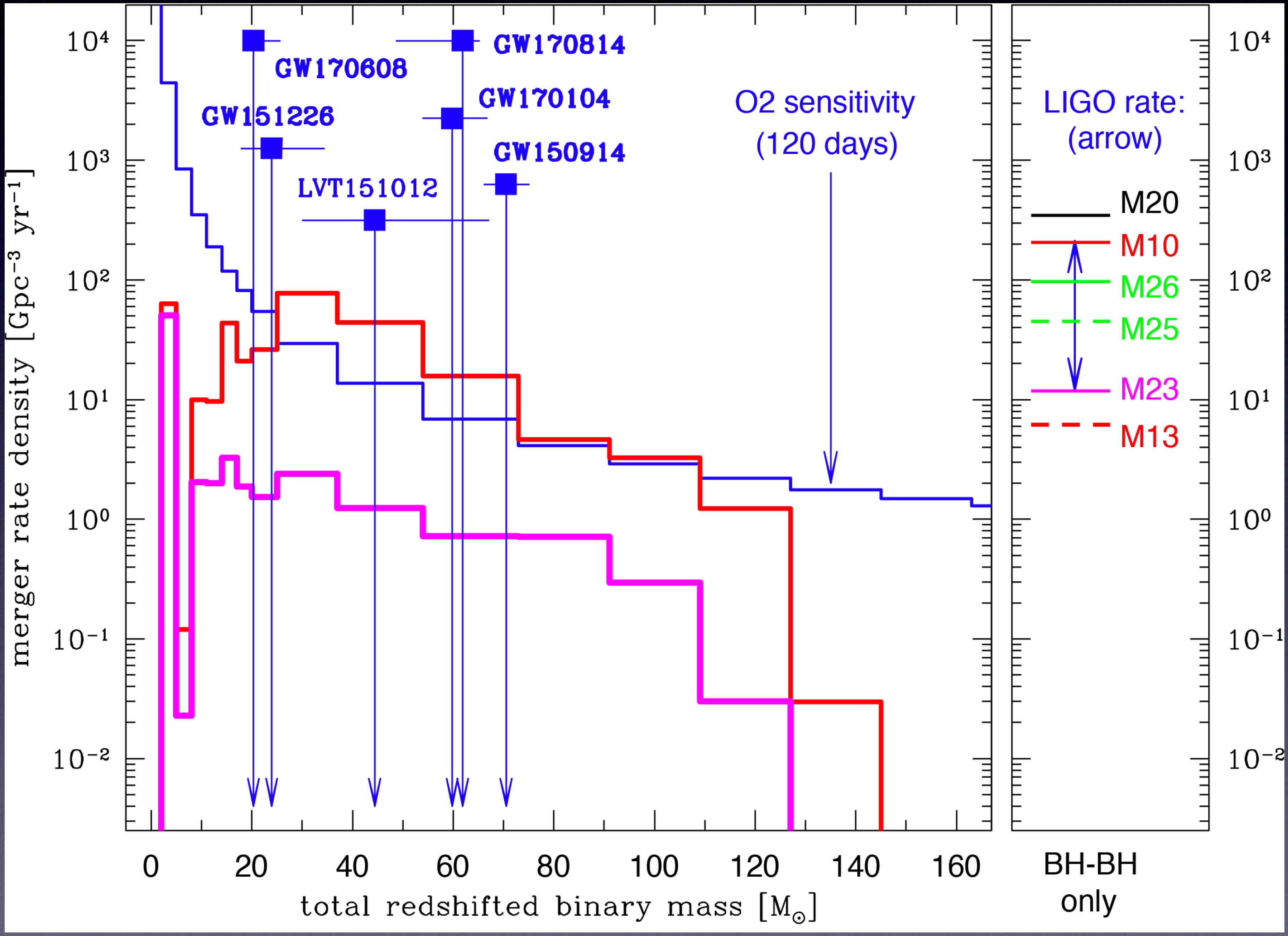

From www.syntheticuniverse.org

Dynamical channel

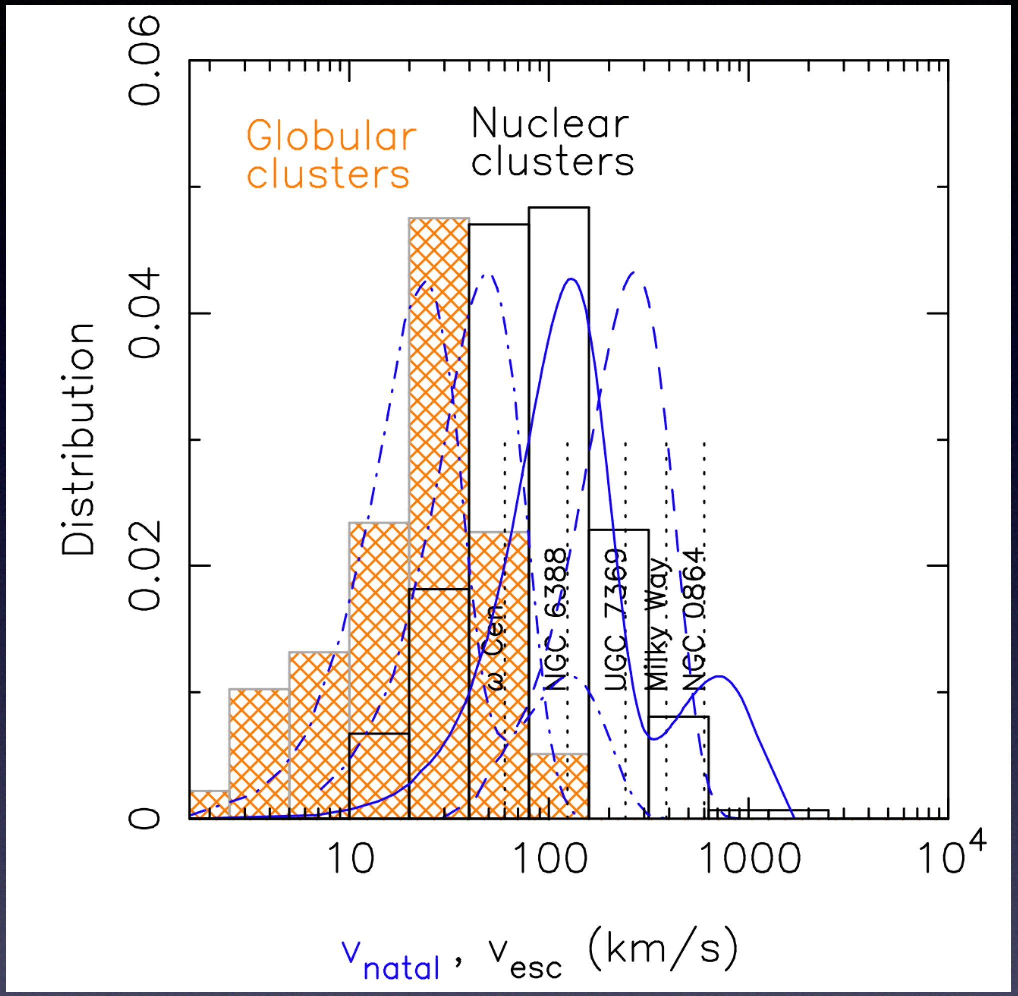

Antonini & Radio 2016

- Similar uncertainties (natal kicks)
- Possible in globular clusters and nuclear star clusters, or even in the field (field triples)
- May be as important as field channel

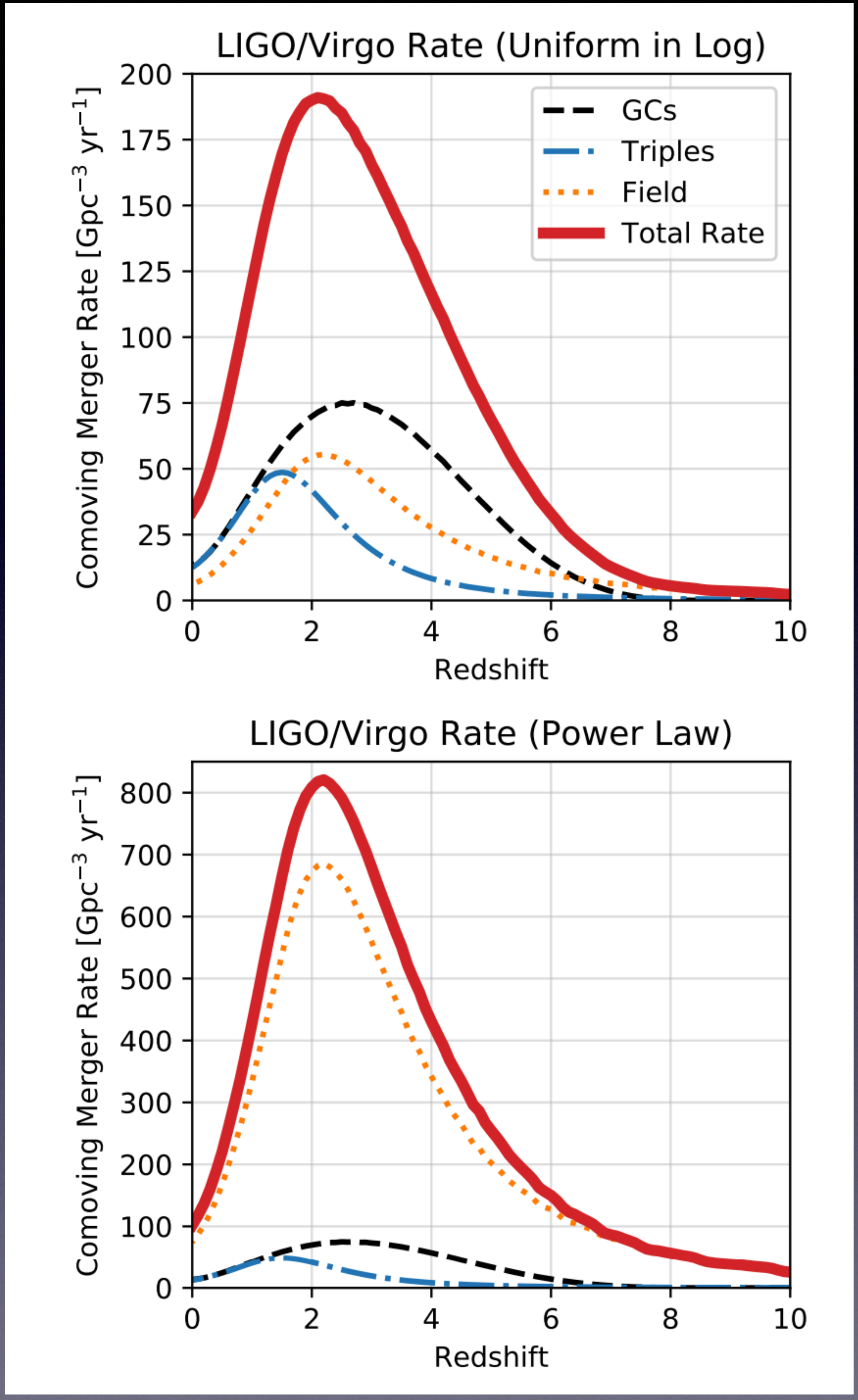

Rodriguez & Loeb 2018

Comparison to models

Misaligned spins possible in field channel if large kicks, natural in dynamical channel

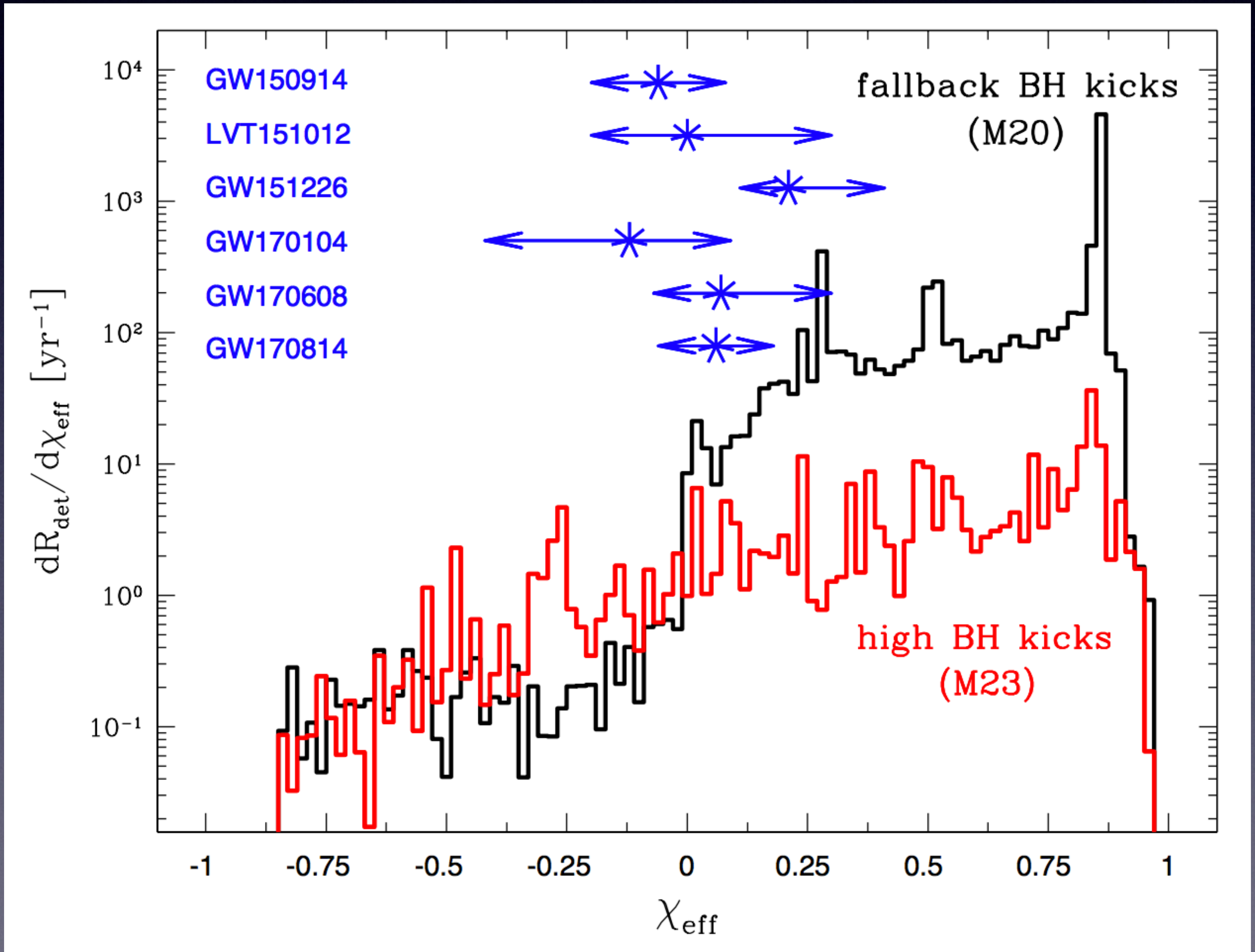

Figure from Belczynski et al 2017

Parametrized inspiral tests of GR

$$h_{ppE}(f) = h_{GR}(f)(1+\alpha u^a)e^{i\beta u^b}$$

$$u = (\pi \mathcal{M} f)^{1/3}$$

waveform regime	parameter	f−dependence
early-inspiral regime	$\delta\hat{\varphi}_0$	$f^{-5/3}$
	$\delta\hat{\varphi}_1$	$f^{-4/3}$
	$\delta\hat{\varphi}_2$	f^{-1}
	$\delta\hat{\varphi}_3$	$f^{-2/3}$
	$\delta\hat{\varphi}_4$	$f^{-1/3}$
	$\delta\hat{\varphi}_{5l}$	$\log(f)$
	$\delta\hat{\varphi}_6$	$f^{1/3}$
	$\delta\hat{\varphi}_{6l}$	$f^{1/3}\log(f)$
	$\delta\hat{\varphi}_7$	$f^{2/3}$

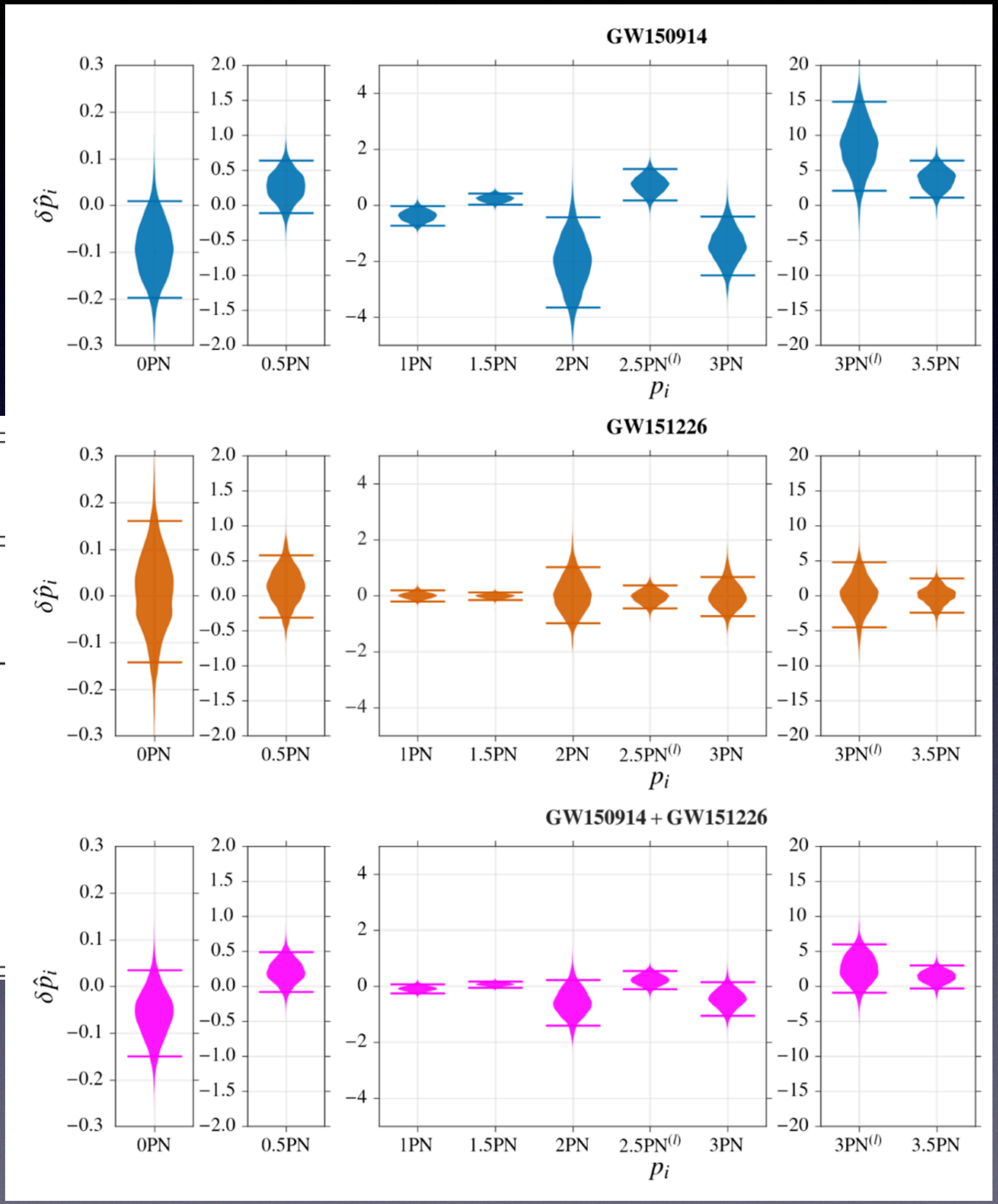

Caveat: ppE parameters may depend on sources (should be viewed as BH charges), so stacking may not be physically meaningful!

Parametrized inspiral tests of GR

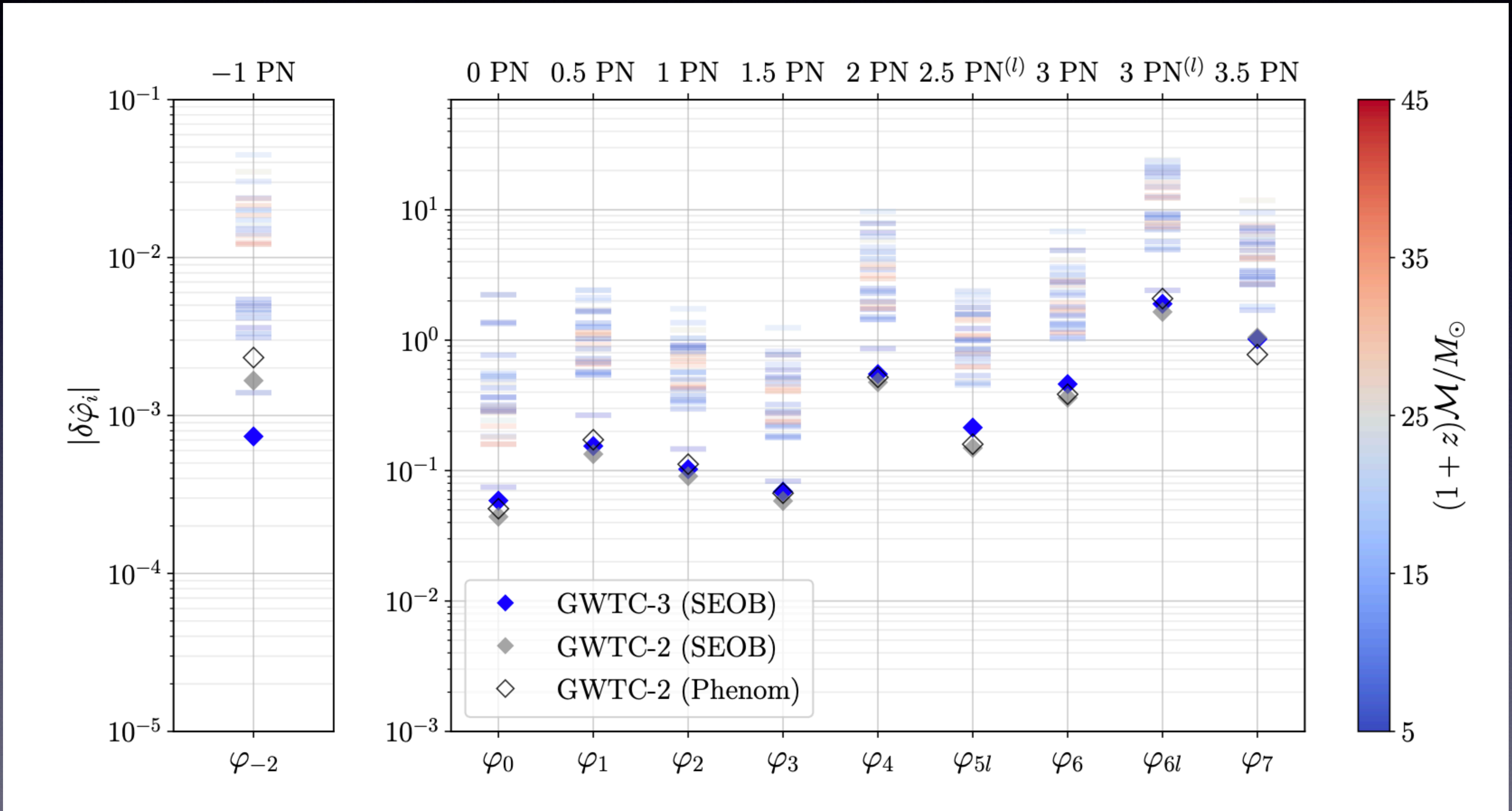

Absence of dipole emission in binary pulsars

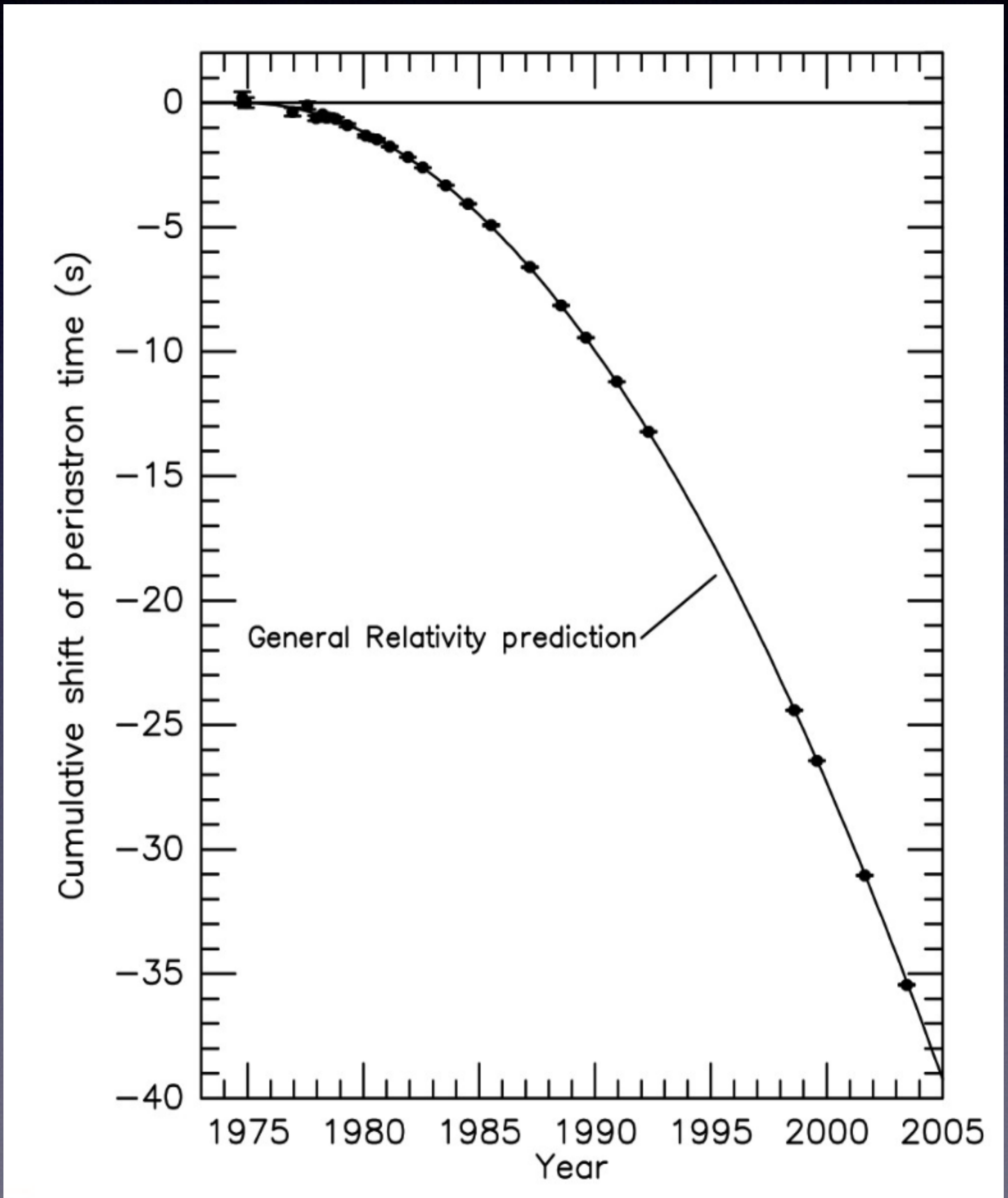

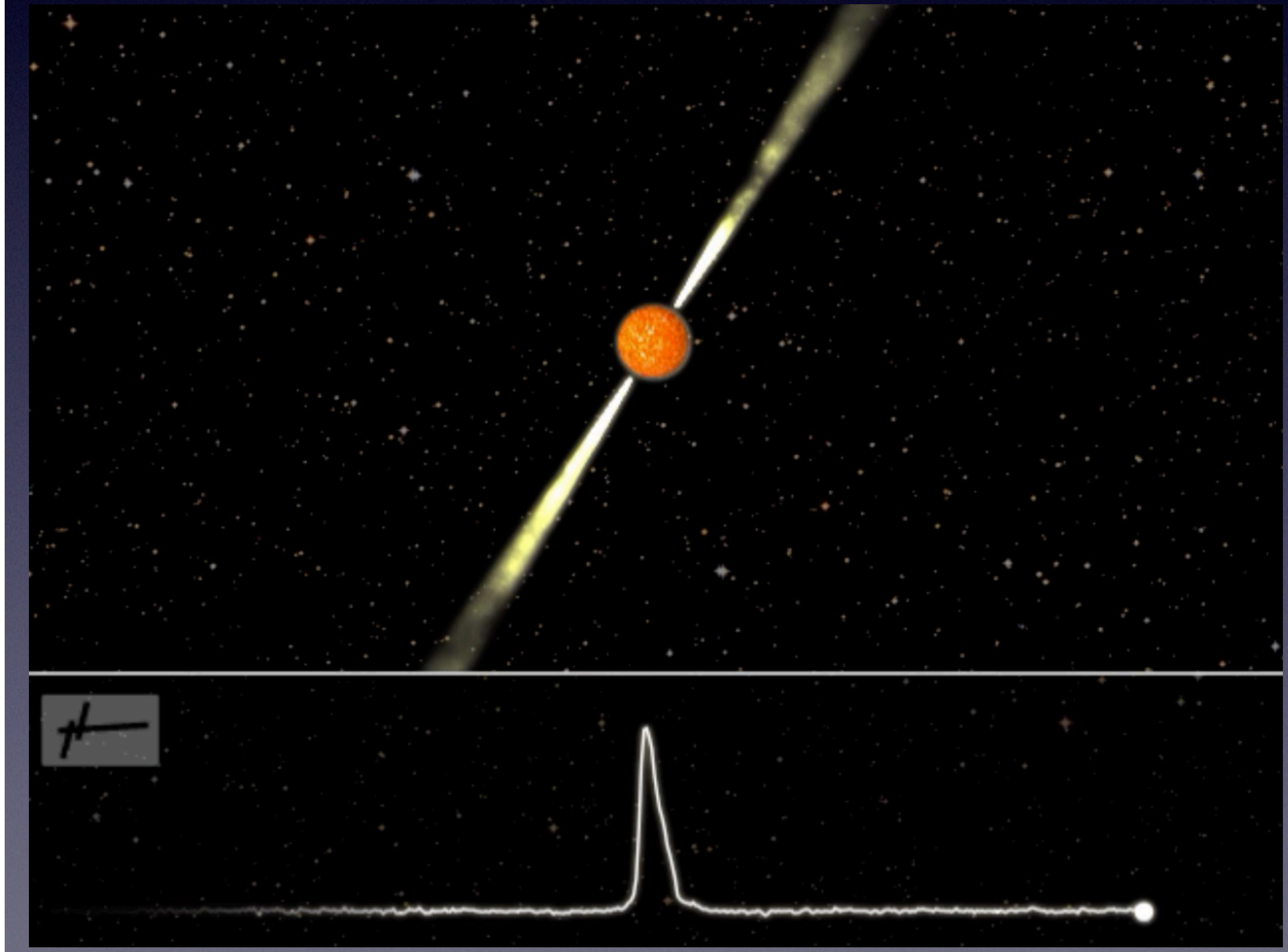

Absence of dipole emission in binary pulsars

An example: Lorentz-violating gravity (Horava)

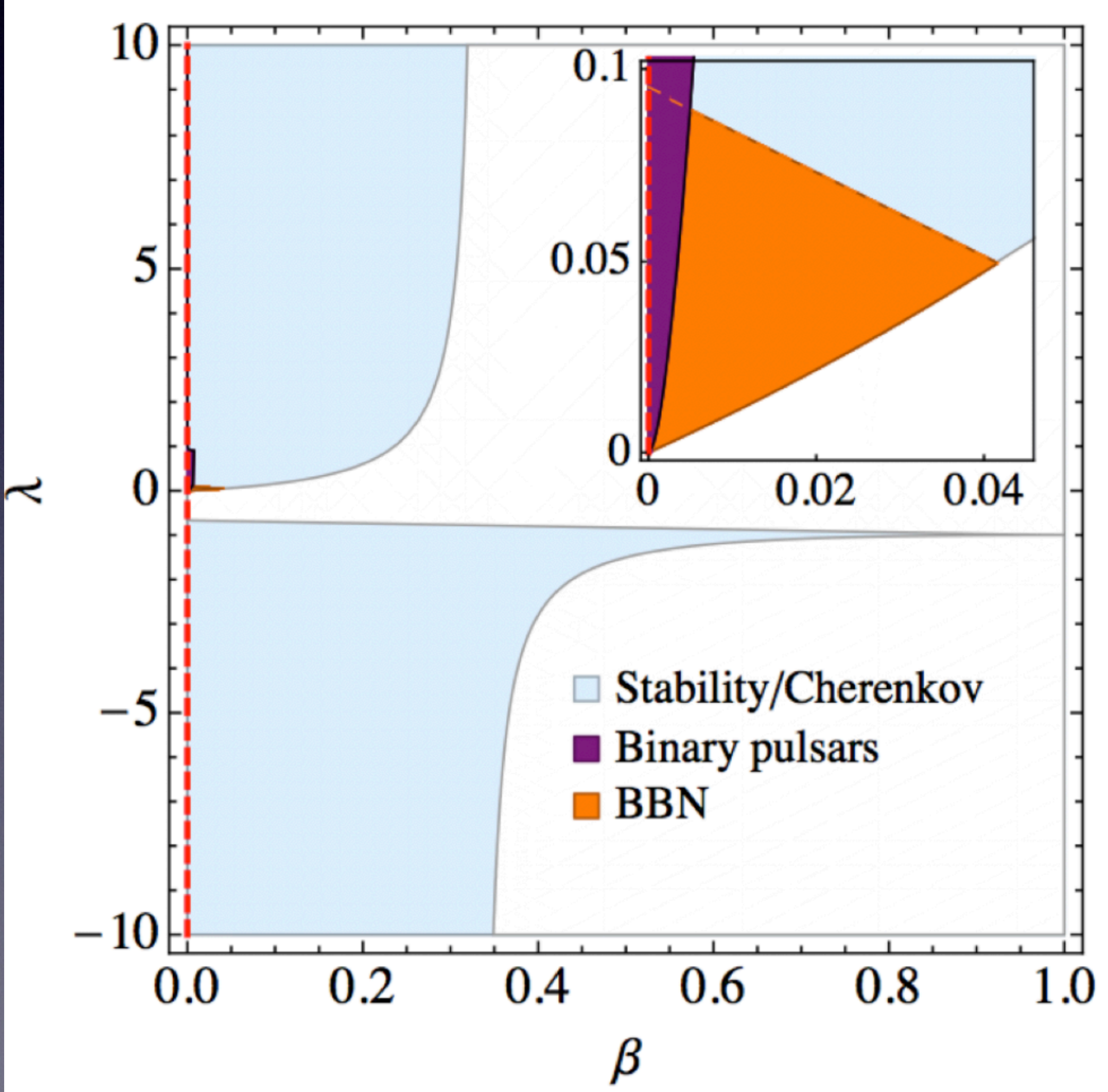

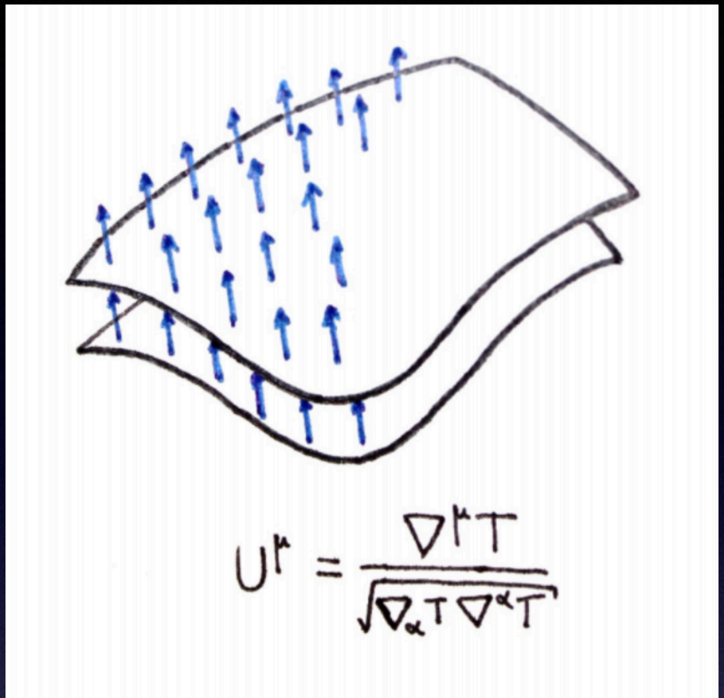

No ghosts+no gradient instabilities+solar system tests+absence of vacuum Cherenkov (to agree with cosmic rays)+BBN+pulsars +GW170817

Yagi, Blas, EB & Yunes 2014
Ramos & EB 2018, EB 2019,
Gupta+EB+2021

Stochastic background

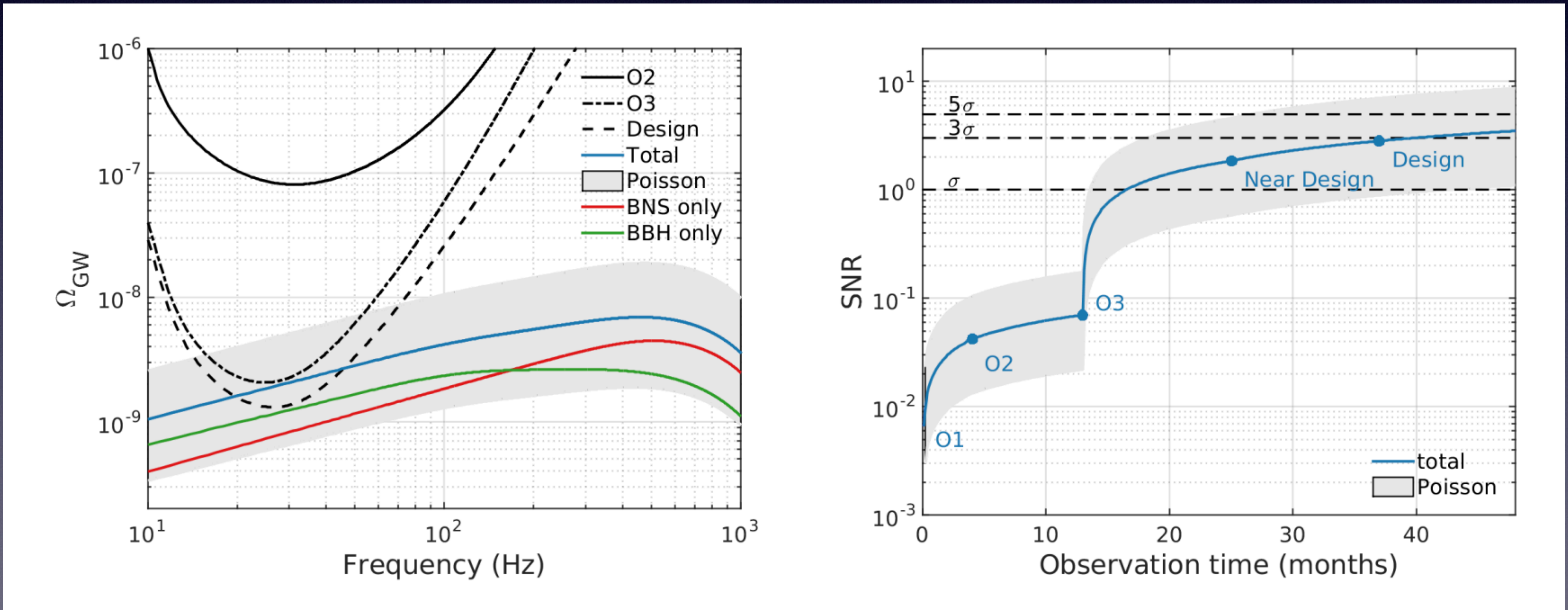

GWs from binary BHs

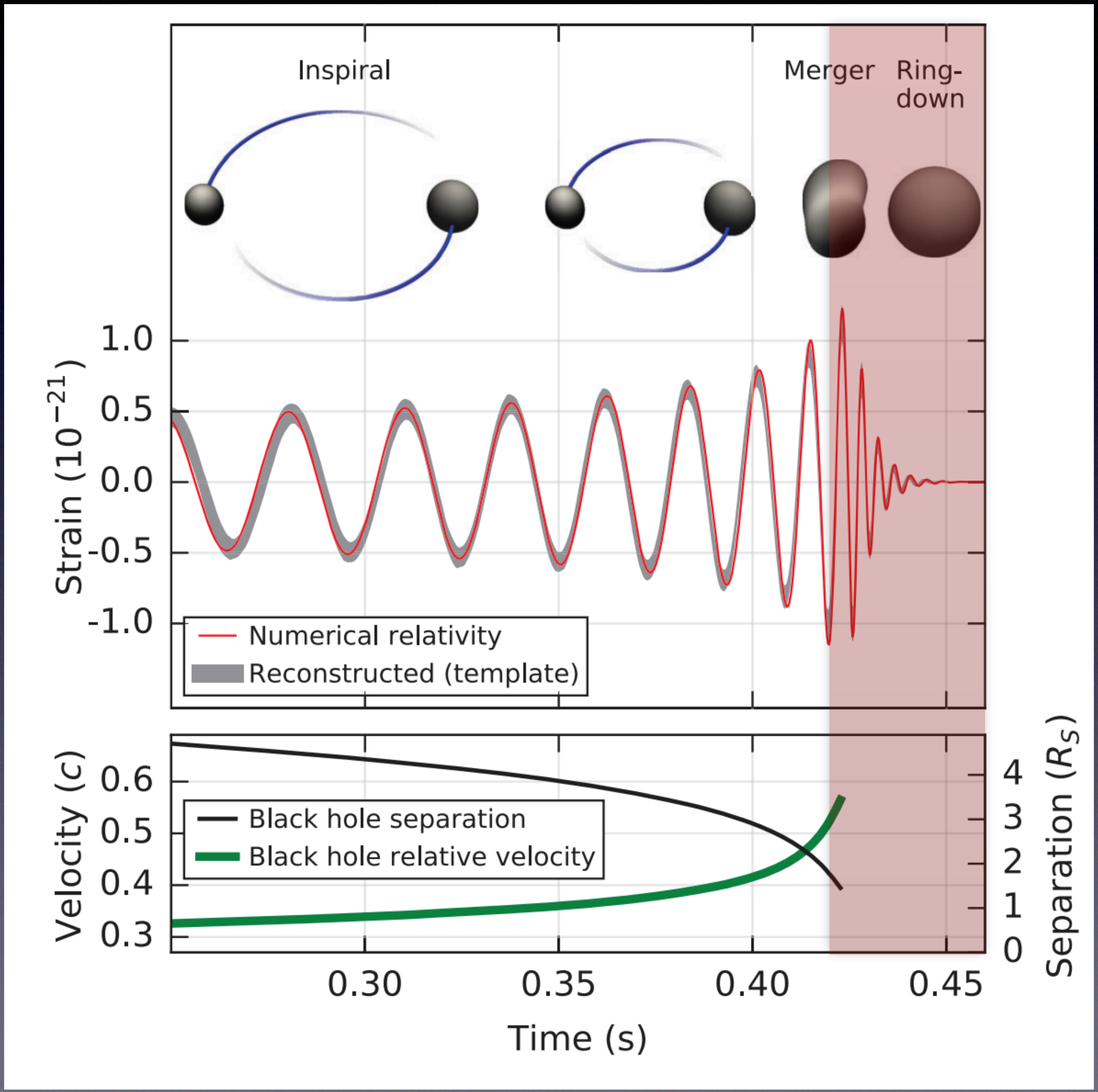

LSC collaboration 2015

Perturbations of non-spinning BHs

- Consider scalar field toy model first $$g^{\mu\nu}\nabla_\mu\nabla_\nu\varphi = 0$$

- On Schwarzschild, decompose in spherical harmonics

$$\varphi = \sum_{\ell,m} \frac{R_{\ell m}(r)}{r} Y_{\ell m}(\theta,\phi) e^{-i\omega t}$$

- Because of symmetry, equations “separate”:

$$\frac{\mathrm{d}^2 R}{\mathrm{d}r_*^2} + (\omega^2 - V)R = 0$$

$$r_* \equiv r + 2M \ln\left(\frac{r}{2M} - 1\right)$$

Tortoise coordinates ranging +/- ∞

$$V(r) \equiv \left(1 - \frac{2M}{r}\right)\left[\frac{l\,(l+1)}{r^2} + p\right]$$

$$p = 2M/r^3$$

Perturbations of non-spinning BHs

- Ingoing/Outgoing boundary conditions at event horizon/infinity
- Akin to solving Schrodinger equation in 1D in quantum mechanics 101
- Counting of degrees of freedom + continuity = discrete complex quasinormal mode frequencies
- Imaginary part of frequency shows linear stability
- Peak at ~ 3M as *l* diverges (because geometric optics limit of Klein-Gordon equation is geodesics equation)

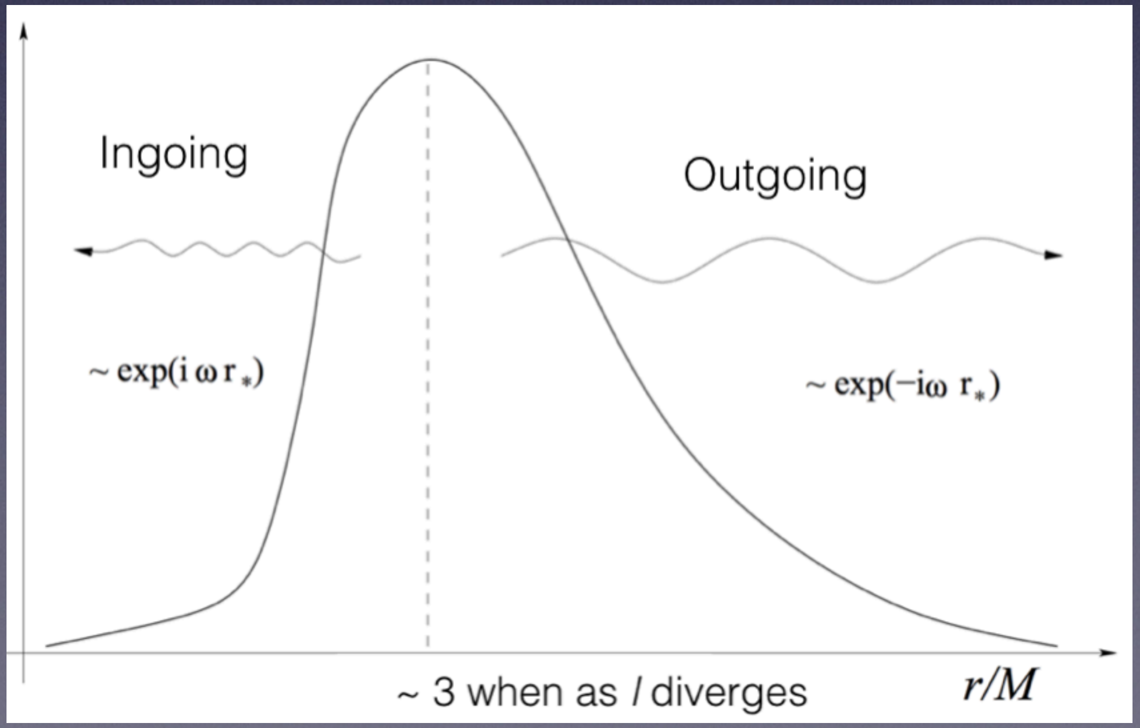

Perturbations of non-spinning BHs

- Separability on Schwarzschild extend to vector and tensor perturbations
- Expand in vector and tensor harmonics (of even/odd parity, c.f. E/B modes of CMB)

$$\psi_L{}^M{}_{,\mu} = \text{const}\frac{\partial}{\partial x^\mu} Y_L{}^M(x_2 x_3), \qquad \text{parity } (-)^L;$$

$$\phi_L{}^M{}_{,\mu} = \text{const}\,\epsilon_\mu{}^\nu \frac{\partial}{\partial x_\nu} Y_L{}^M(x_2 x_3), \quad \text{parity } (-)^{L+1}.$$

Basis for vectors on 2-sphere

$$\psi_L{}^M{}_{\mu\nu} = \text{const}\, Y_L{}^M{}_{;\mu\nu} (\text{covariant derivatives}), \qquad \text{parity } (-)^L;$$

$$\phi_L{}^M{}_{\mu\nu} = \text{const}\,\gamma_{\mu\nu} Y_L{}^M, \quad \text{parity } (-)^L;$$

$$\chi_L{}^M{}_{\mu\nu} = \tfrac{1}{2}\,\text{const}[\epsilon_\mu{}^\lambda \psi_L{}^M{}_{\lambda\nu} + \epsilon_\nu{}^\lambda \psi_L{}^M{}_{\lambda\mu}], \qquad \text{parity } (-)^{L+1}.$$

Basis for tensors on 2-sphere

Perturbations of non-spinning BHs

$$h_{\mu\nu}=\begin{vmatrix} 0 & 0 & -h_0(T,r)(\partial/\sin\theta\partial\varphi)Y_L{}^M & h_0(T,r)(\sin\theta\partial/\partial\theta)Y_L{}^M \\ 0 & 0 & -h_1(T,r)(\partial/\sin\theta\partial\varphi)Y_L{}^M & h_1(T,r)(\sin\theta\partial/\partial\theta)Y_L{}^M \\ \mathrm{Sym} & \mathrm{Sym} & h_2(T,r)(\partial^2/\sin\theta\partial\theta\partial\varphi-\cos\theta\partial/\sin^2\theta\partial\varphi)Y_L{}^M & \mathrm{Sym} \\ \mathrm{Sym} & \mathrm{Sym} & \frac{1}{2}h_2(T,r)(\partial^2/\sin\theta\partial\varphi\partial\varphi+\cos\theta\partial/\partial\theta-\sin\theta\partial^2/\partial\theta\partial\theta)Y_L{}^M & -h_2(T,r)(\sin\theta\partial^2/\partial\theta\partial\varphi-\cos\theta\partial/\partial\varphi)Y_L{}^M \end{vmatrix}$$

Odd-parity metric perturbations (Regge-Wheeler 1957)

$$h_{\mu\nu}=\begin{vmatrix} (1-2m^*/r)H_0(T,r)Y_L{}^M & H_1(T,r)Y_L{}^M & h_0(T,r)(\partial/\partial\theta)Y_L{}^M & h_0(T,r)(\partial/\partial\varphi)Y_L{}^M \\ H_1(T,r)Y_L{}^M & (1-2m^*/r)^{-1}H_2(T,r)Y_L{}^M & h_1(T,r)(\partial/\partial\theta)Y_L{}^M & h_1(T,r)(\partial/\partial\varphi)Y_L{}^M \\ \mathrm{Sym} & \mathrm{Sym} & \begin{array}{l} r^2[K(T,r) \\ \quad +G(T,r)(\partial^2/\partial\theta^2)]Y_L{}^M \end{array} & \mathrm{Sym} \\ \mathrm{Sym} & \mathrm{Sym} & \begin{array}{l} r^2G(T,r)(\partial^2/\partial\theta\partial\varphi \\ \quad -\cos\theta\partial/\sin\theta\partial\varphi)Y_L{}^M \end{array} & \begin{array}{l} r^2[K(T,r)\sin^2\theta \\ \quad +G(T,r)(\partial^2/\partial\varphi\partial\varphi \\ \quad +\sin\theta\cos\theta\partial/\partial\theta)]Y_L{}^M \end{array} \end{vmatrix}.$$

Even-parity metric perturbations (Zerilli 1970)

Perturbations of non-spinning BHs

$$h_{\mu\nu}=\begin{vmatrix} 0 & 0 & -h_0(T,r)(\partial/\sin\theta\,\partial\varphi)Y_L{}^M & h_0(T,r)(\sin\theta\,\partial/\partial\theta)Y_L{}^M \\ 0 & 0 & -h_1(T,r)(\partial/\sin\theta\,\partial\varphi)Y_L{}^M & h_1(T,r)(\sin\theta\,\partial/\partial\theta)Y_L{}^M \\ \mathrm{Sym} & \mathrm{Sym} & \cancel{h_2(T,r)(\partial^2/\sin\theta\,\partial\theta\,\partial\varphi-\cos\theta\,\partial/\sin^2\theta\,\partial\varphi)Y_L{}^M} & \cancel{\mathrm{Sym}} \\ \mathrm{Sym} & \mathrm{Sym} & \cancel{\tfrac{1}{2}h_2(T,r)(\partial^2/\sin\theta\,\partial\varphi\,\partial\varphi+\cos\theta\,\partial/\partial\theta-\sin\theta\,\partial^2/\partial\theta\,\partial\theta)Y_L{}^M} & \cancel{-h_2(T,r)(\sin\theta\,\partial^2/\partial\theta\,\partial\varphi-\cos\theta\,\partial/\partial\varphi)Y_L{}^M} \end{vmatrix}$$

Odd-parity metric perturbations (Regge-Wheeler 1957):
2 free radial functions

$$h_{\mu\nu}=\begin{vmatrix} (1-2m^*/r)H_0(T,r)Y_L{}^M & H_1(T,r)Y_L{}^M & \cancel{h_0(T,r)(\partial/\partial\theta)Y_L{}^M} & \cancel{h_0(T,r)(\partial/\partial\varphi)Y_L{}^M} \\ H_1(T,r)Y_L{}^M & (1-2m^*/r)^{-1}H_2(T,r)Y_L{}^M & \cancel{h_1(T,r)(\partial/\partial\theta)Y_L{}^M} & \cancel{h_1(T,r)(\partial/\partial\varphi)Y_L{}^M} \\ \cancel{\mathrm{Sym}} & \cancel{\mathrm{Sym}} & r^2[K(T,r)\ \cancel{+G(T,r)(\partial^2/\partial\theta^2)}]Y_L{}^M & \cancel{\mathrm{Sym}} \\ \cancel{\mathrm{Sym}} & \cancel{\mathrm{Sym}} & r^2\cancel{G(T,r)(\partial^2/\partial\theta\,\partial\varphi-\cos\theta\,\partial/\sin\theta\,\partial\varphi)Y_L{}^M} & r^2[K(T,r)\sin^2\theta + \cancel{G(T,r)(\partial^2/\partial\varphi\,\partial\varphi} + \cancel{\sin\theta\cos\theta\,\partial/\partial\theta)}]Y_L{}^M \end{vmatrix}.$$

Even-parity metric perturbations (Regge-Wheeler 1957, Zerilli 1970):
4 free radial functions, but 2 algebraic relations from Einstein eqs

Perturbations of non-spinning BHs

Construct complex variables out of each pair of free radial functions

$$\frac{d^2\Psi_s}{dr_*^2} + \left(\omega^2 - V_s\right)\Psi_s = 0\,.$$

$$V^-_{s=2} = f(r)\left[\frac{l(l+1)}{r^2} - \frac{6M}{r^3}\right]$$

Odd-parity

$$V^+_{s=2} = \frac{2f(r)}{r^3}\frac{9M^3 + 3\lambda^2 M r^2 + \lambda^2(1+\lambda)r^3 + 9M^2\lambda r}{(3M+\lambda r)^2}$$

Even-parity

$\lambda \equiv (l-1)(l+2)/2$ $\quad$ $f(r) = 1 - 2M/r$

Effective potentials peak at r=3M in the large *l* limit
(i.e. in the geodesics limit)

Perturbations of spinning BHs

- Separability of equations not at all obvious in Kerr, but possible due to "hidden symmetry" (c.f. Carter's constant)

- Use Newman-Penrose scalars (projections of Weyl curvature on null tetrad) to get Teukolsky equation

$$\Psi_0 = -C_{1313} = -C_{\mu\nu\lambda\sigma} l^\mu m^\nu l^\lambda m^\sigma\,,$$
$$\Psi_4 = -C_{2424} = -C_{\mu\nu\lambda\sigma} n^\mu m^{*\nu} n^\lambda m^{*\sigma}$$

$$\psi(t, r, \theta, \phi) = \frac{1}{2\pi}\int e^{-i\omega t} \sum_{l=|s|}^{\infty} \sum_{m=-l}^{l} e^{im\phi}\, {}_sS_{lm}(\theta) R_{lm}(r) d\omega$$

$$\left[\frac{\partial}{\partial u}(1-u^2)\frac{\partial}{\partial u}\right] {}_sS_{lm}$$ Spin-weighted spheroidal harmonics

$$+\left[a^2\omega^2u^2 - 2a\omega s u + s + {}_sA_{lm} - \frac{(m+su)^2}{1-u^2}\right] {}_sS_{lm} = 0$$

$$\Delta\partial_r^2 R_{lm} + (s+1)(2r-2M)\partial_r R_{lm} + V R_{lm} = 0\,.$$

s	$(+2, -2)$
ψ	$(\Psi_0, \rho^{-4}\Psi_4)$

$$V = 2is\omega r - a^2\omega^2 - {}_sA_{lm} + \frac{1}{\Delta}\left[(r^2+a^2)^2\omega^2 - 4Mam\omega r + a^2m^2 + is\left(am(2r-2M) - 2M\omega(r^2-a^2)\right)\right]$$

$u \equiv \cos\theta,\ \Delta = (r - r_-)(r - r_+)$

${}_sA_{lm}(a=0) = l(l+1) - s(s+1)$ Separation constant

Perturbations of spinning BHs

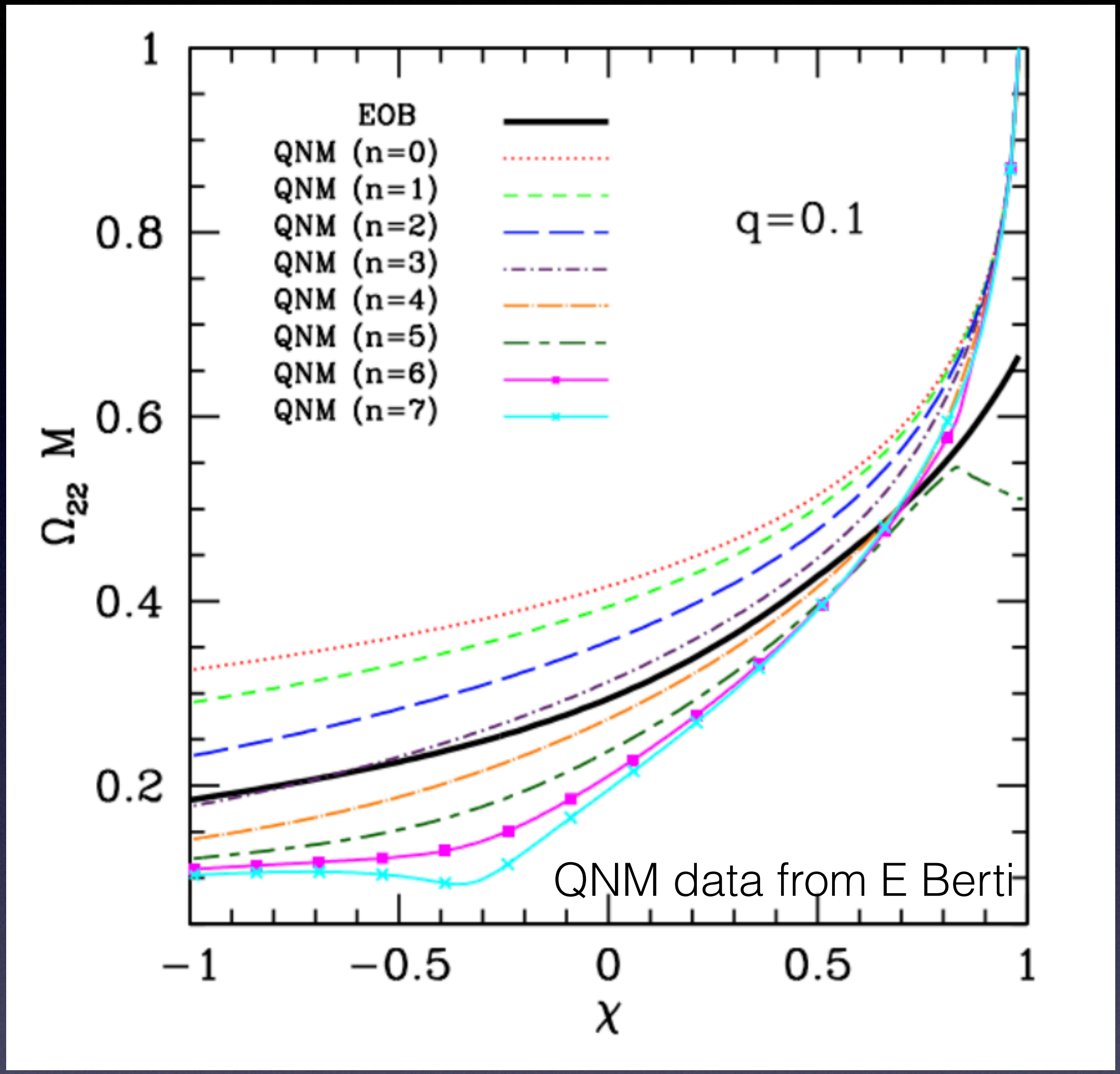

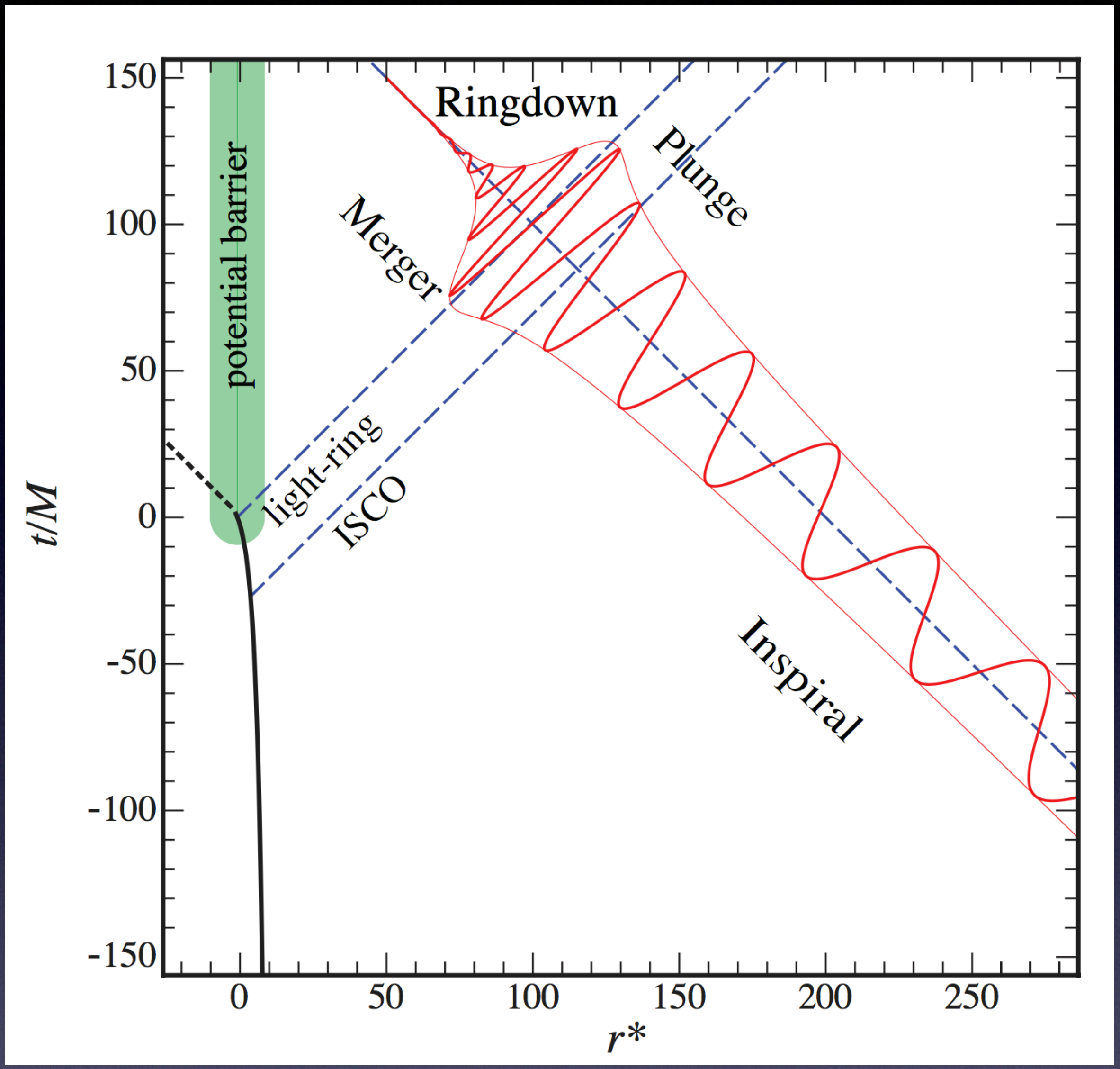

- Connection to circular photon orbit frequency ω and Lyapunov coefficient λ (i.e. curvature of geodesics effective potential) in geometric optics limit!

$$\omega_{ln}^{m=l} \approx l\omega_{+} - i\lambda_{+}(n+1/2)$$

- Amplitude of modes depends on merger physics/initial conditions; set by "continuity" near circular photon orbit in phenomenological waveform models (e.g. EOB)

Ringdown tests of the no-hair theorem

$$\omega_{\ell m} = \omega_{\ell m}^{GR}(M, J)(1 + \delta\omega_{\ell m}) \quad \tau_{\ell m} = \tau_{\ell m}^{GR}(M, J)(1 + \delta\tau_{\ell m})$$

- Difficult with 2nd generation detectors because little SNR in ringdown

- Can perform consistency tests between merger/ringdown

- Overtones of 22 mode may help (Giesler+2019)

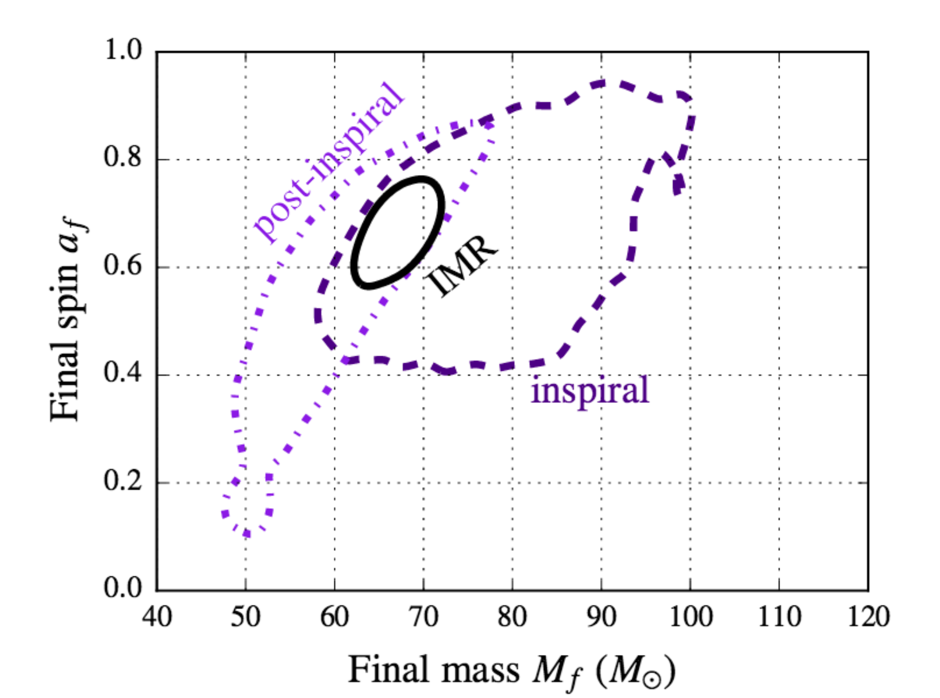

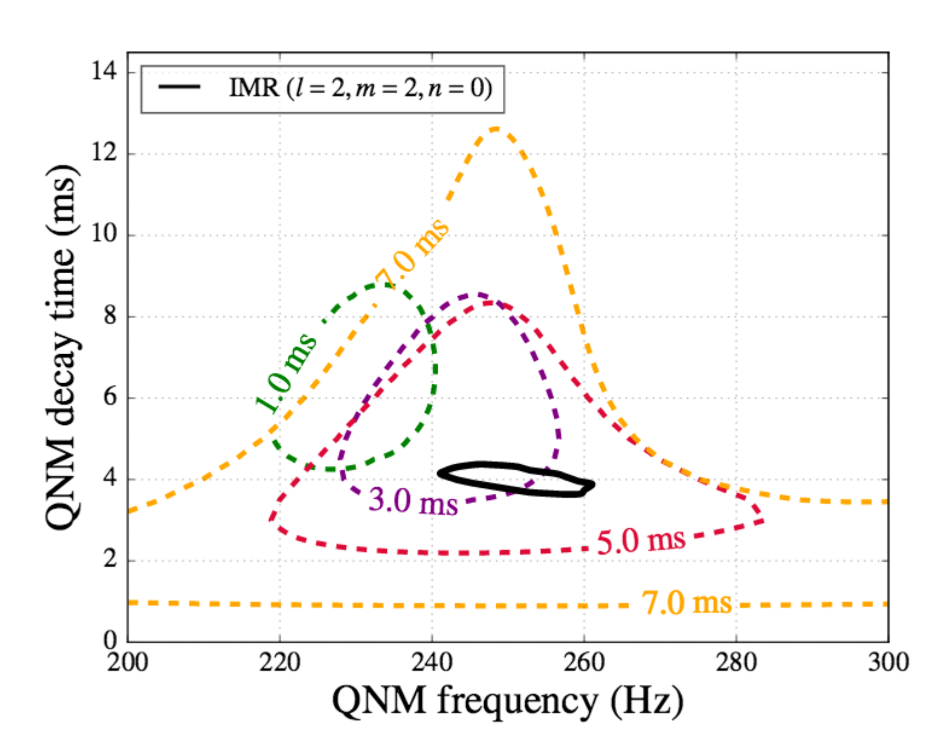

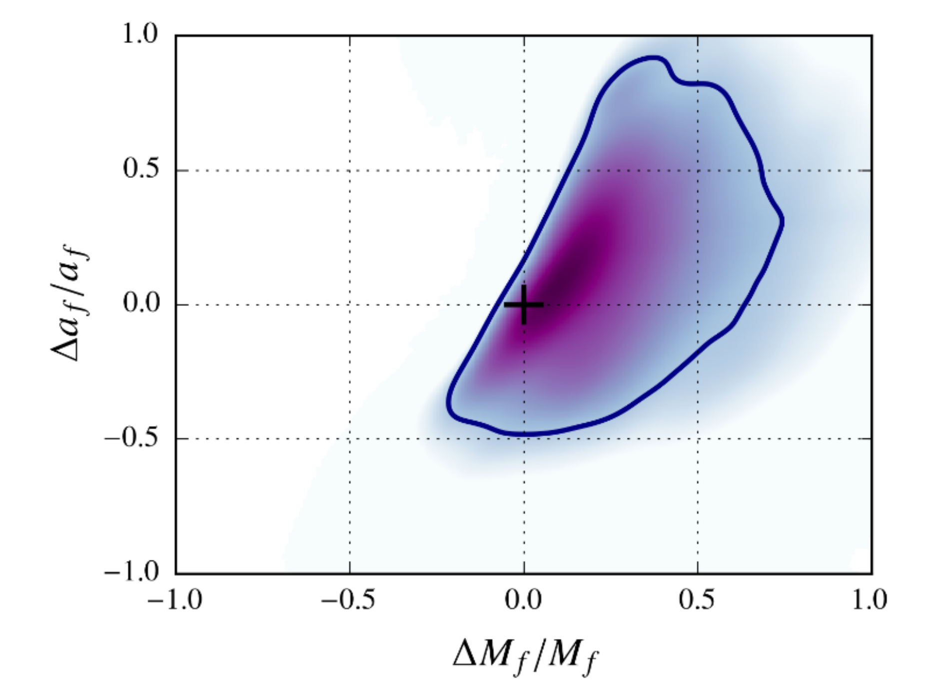

From the LSC paper on tests of GR

LVKC BHs not the biggest in the Universe!

A monster of 4.5 million solar masses in the centre of our Galaxy!

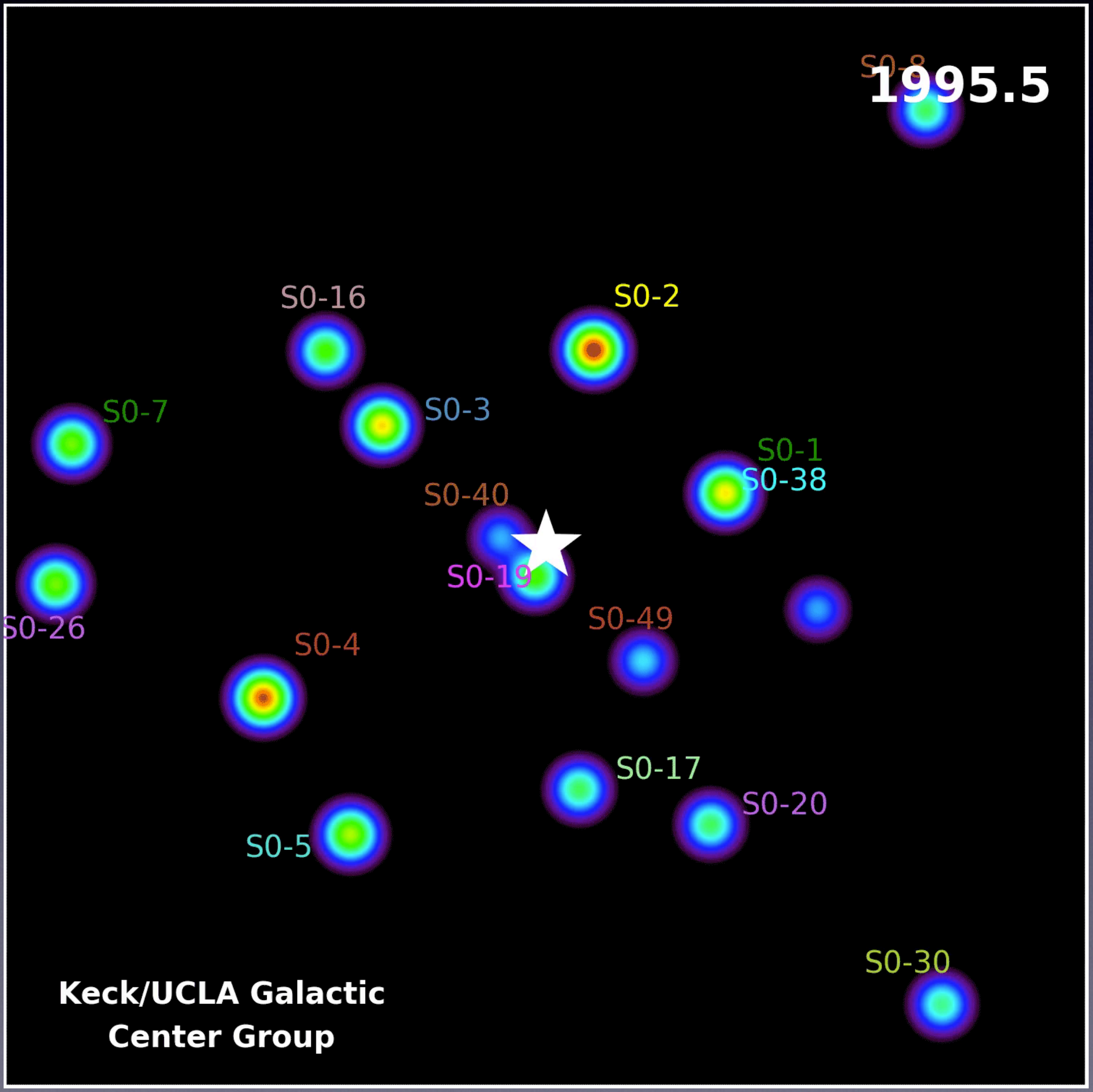

Galaxies merge…

… so massive BHs must merge too!

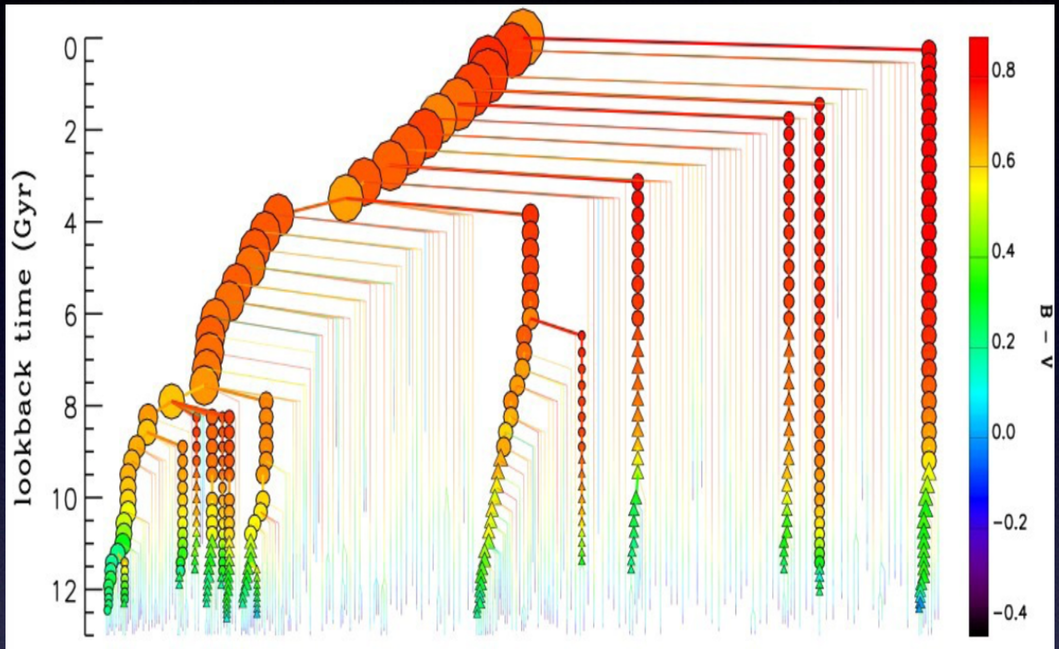

Figure from De Lucia & Blaizot 2007

+

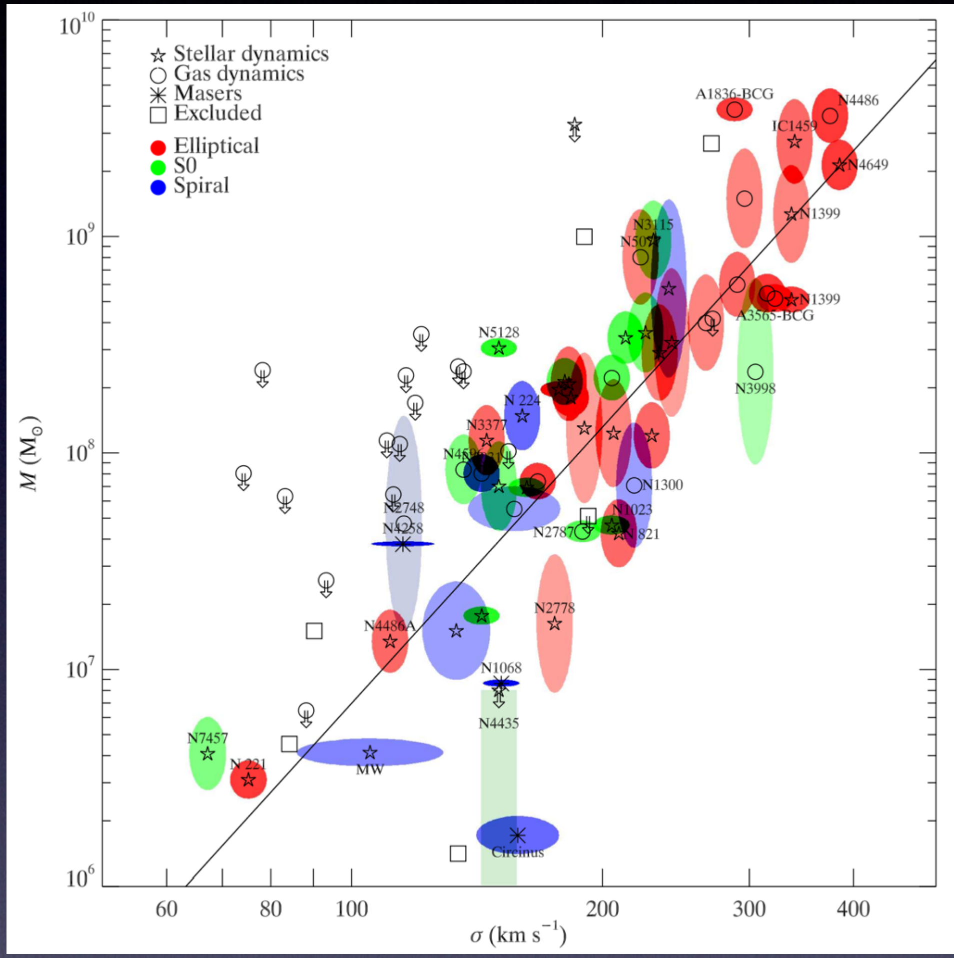

Ferrarese & Merritt 2000
Gebhardt et al. 2000,
Gültekin et al (2009)

=

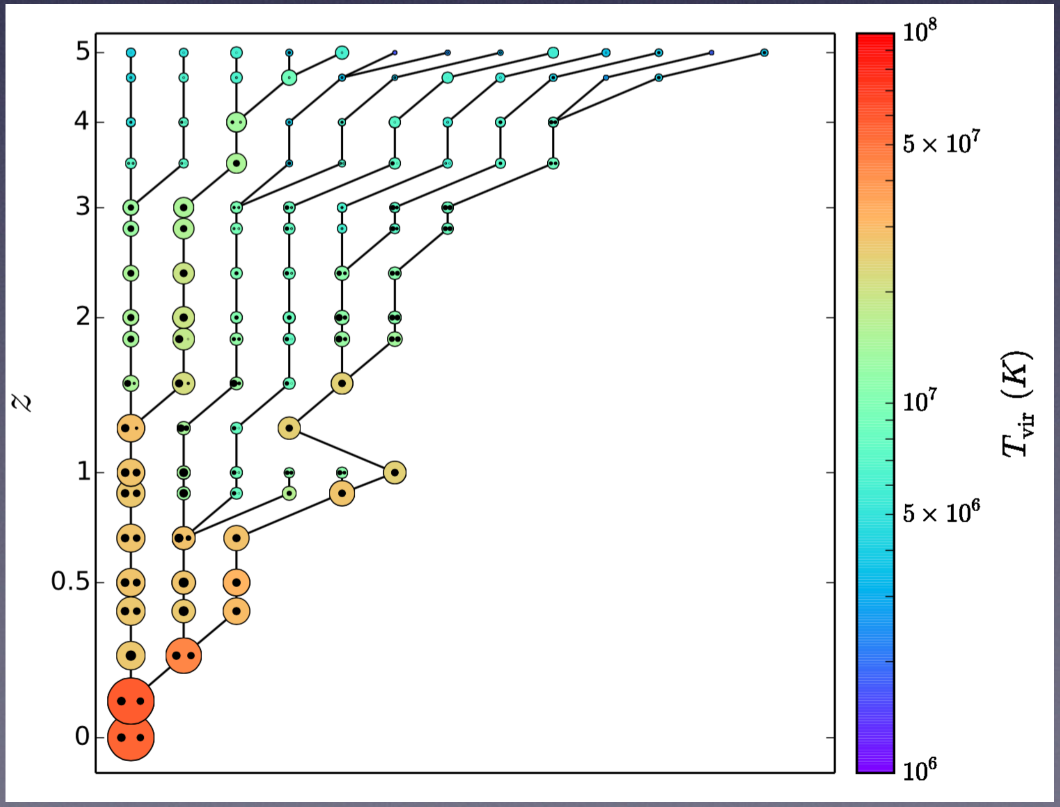

EB 2012
Figure credits: Lucy Ward

What links large and small scale?

- Small to large: BH jets or disk winds transfer kinetic energy to the galaxy and keep it “hot”, quenching star formation (”AGN feedback”). Needed to reconcile ΛCDM bottom-up structure formation with observed “downsizing” of cosmic galaxies

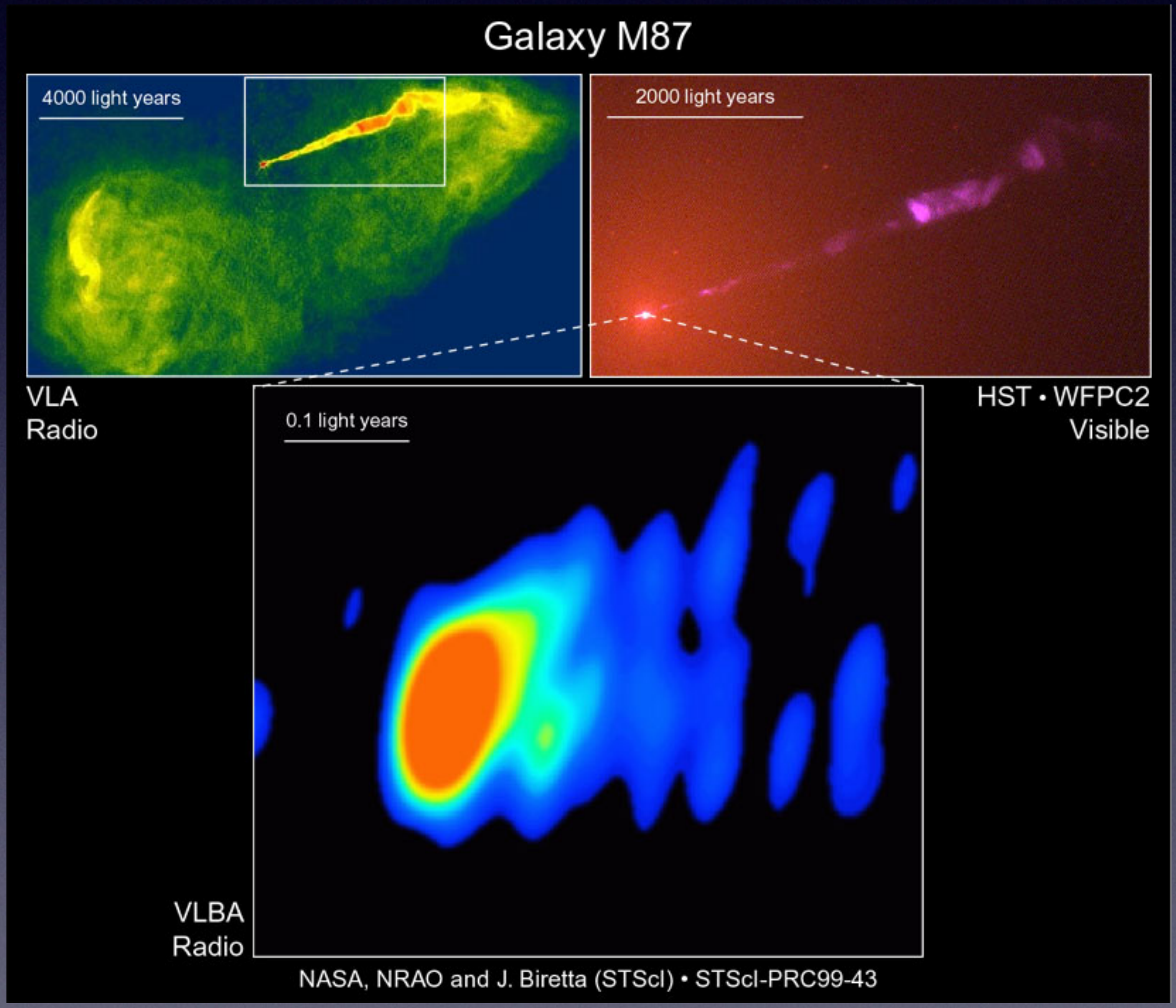

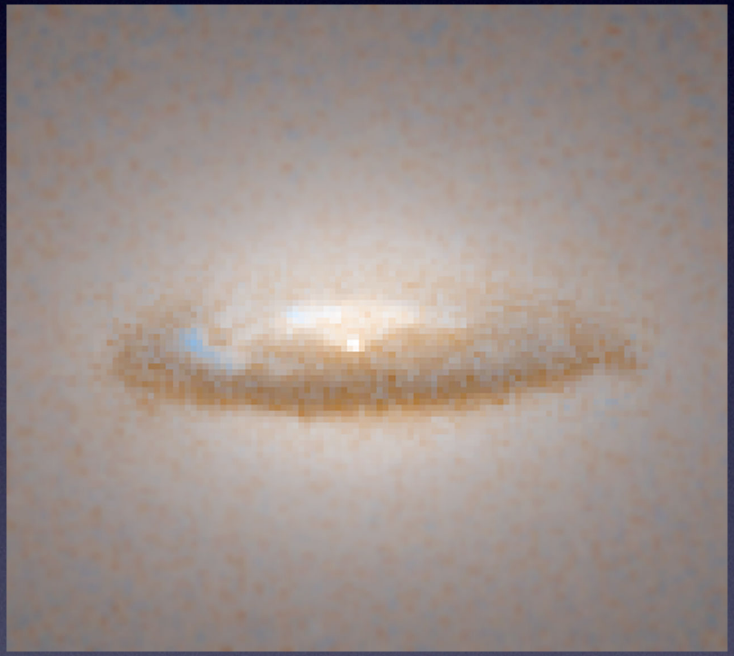

Disk of dust and gas around the massive BH in NGC 7052

- Large to small: galaxies provide fuel to BHs to grow (”accretion”)

Fossil evidence for massive BH mergers

- Nuclear Star Clusters: masses up to ~10^7 M_{sun}, r ~ pc
- BH binaries eject stars by slingshot effect and through remnant's recoil ("erosion")
- Erosion by BH binaries crucial to reproduce NSC scaling relations

$$M_{\rm ej} \approx 0.7 q^{0.2} M_{\rm bin} + 0.5 M_{\rm bin} \ln\left(\frac{a_{\rm h}}{a_{\rm gr}}\right) + 5 M_{\rm bin}\left(V_{\rm kick}/V_{\rm esc}\right)^{1.75} ,$$

Antonini, EB and Silk 2015a,b

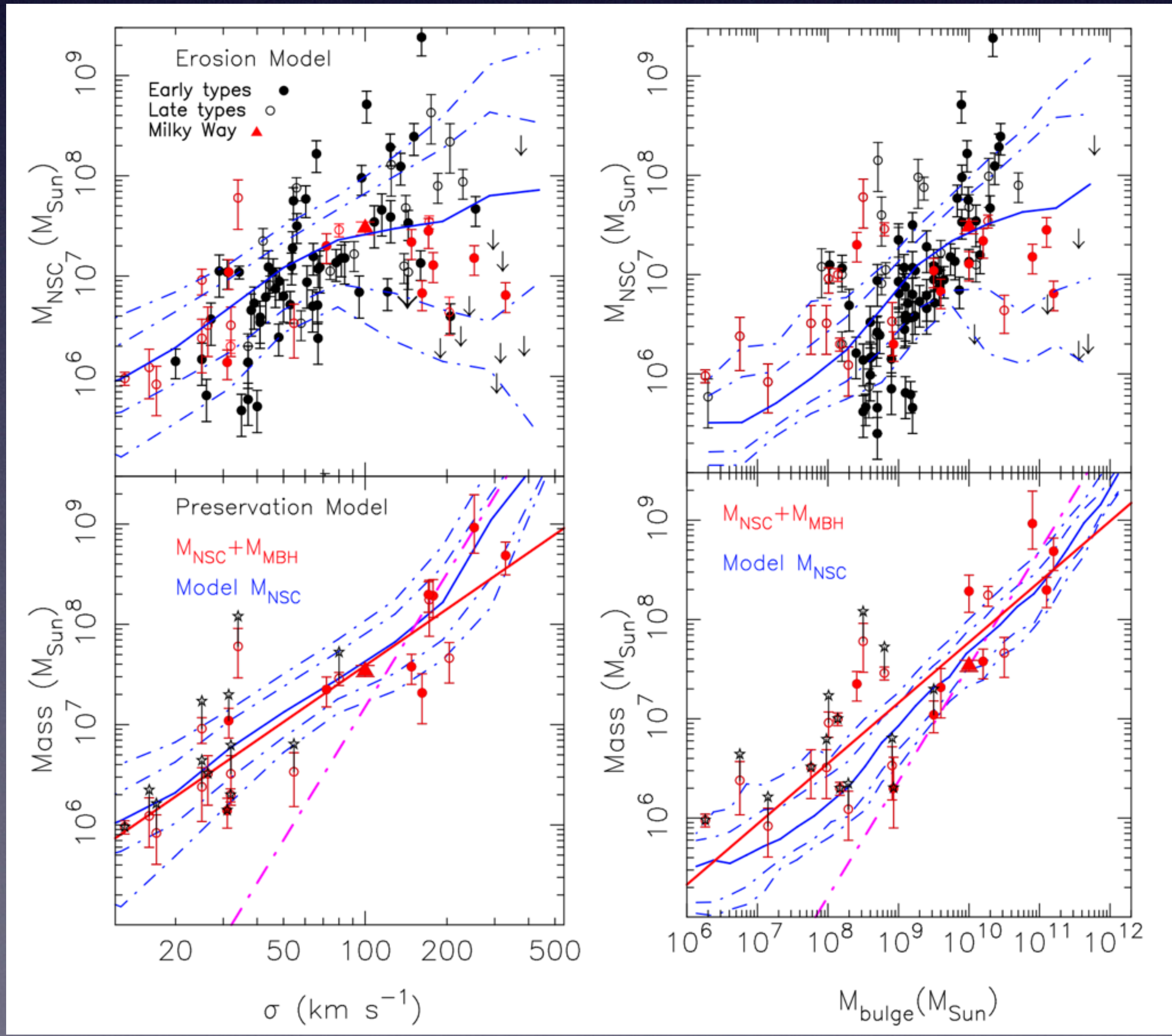

GWs from massive BHs

$$f_{\rm GW} = \frac{6 \times 10^4}{\tilde{m}\tilde{R}^{3/2}}\,{\rm Hz} \qquad \tilde{R} = R/(Gm/c^2)$$
$$\tilde{m} = m/M_\odot$$

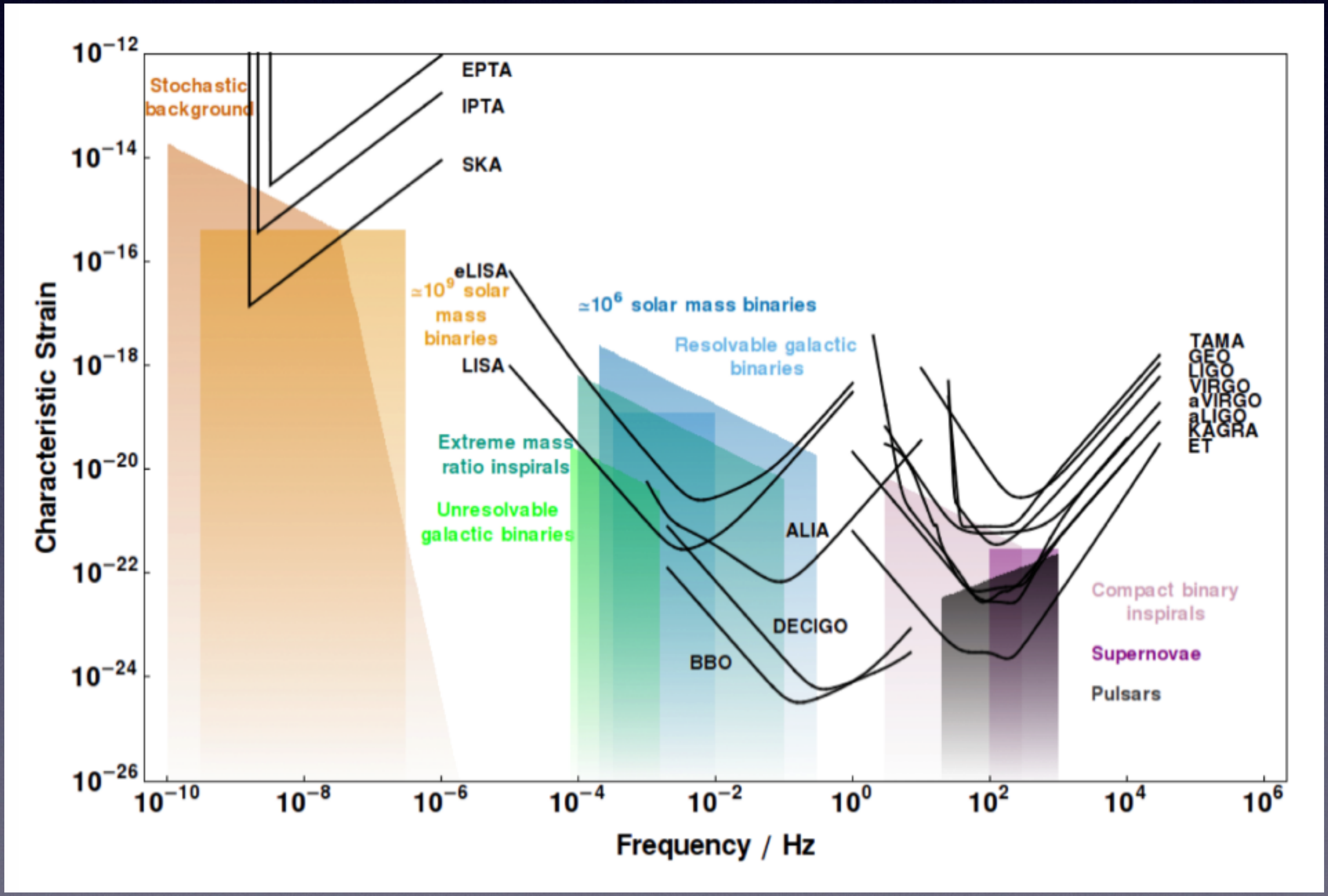

Problem: terrestrial detectors blind at f ≲ 1-10 Hz (seismic noise)

The space race!

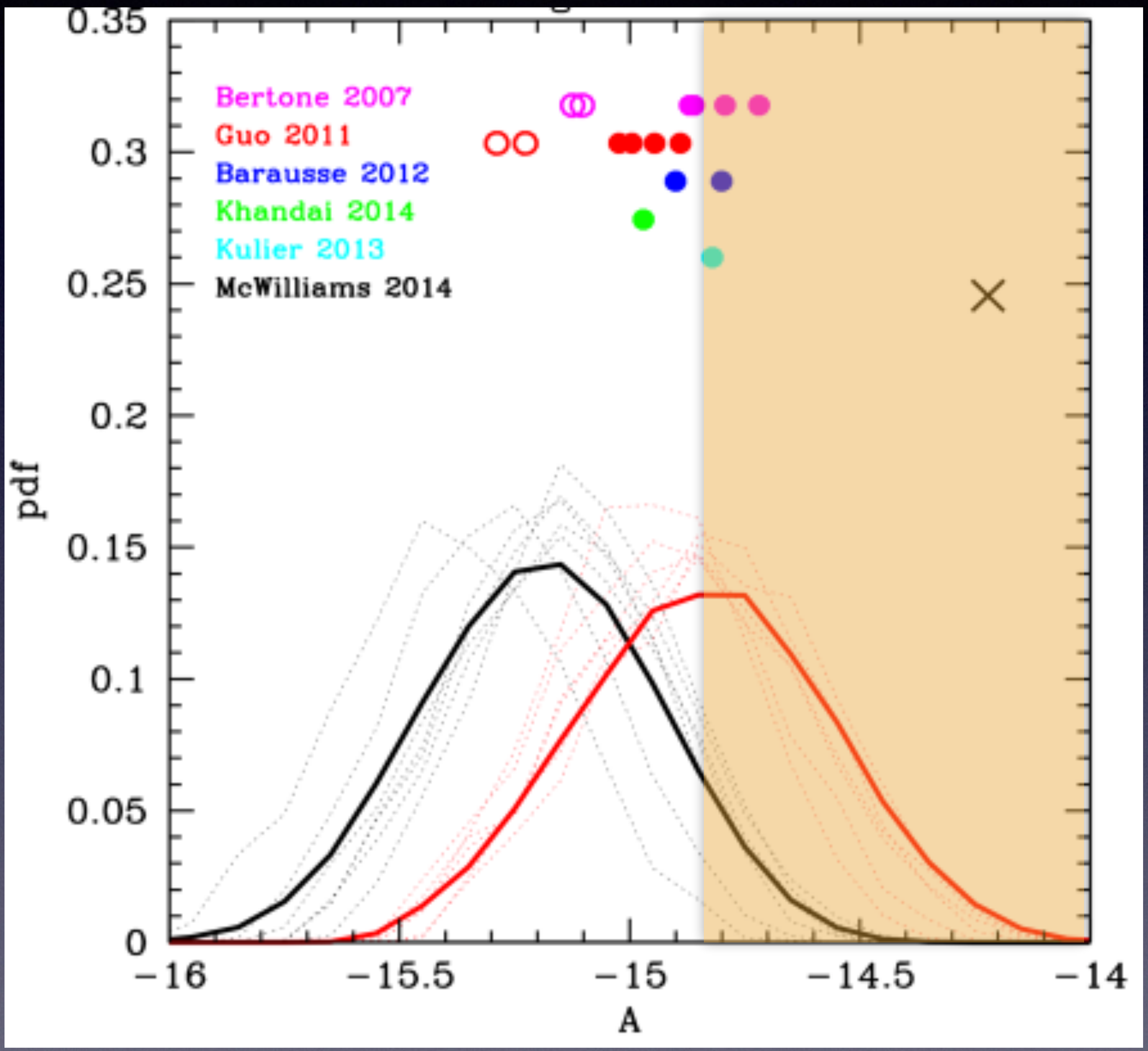

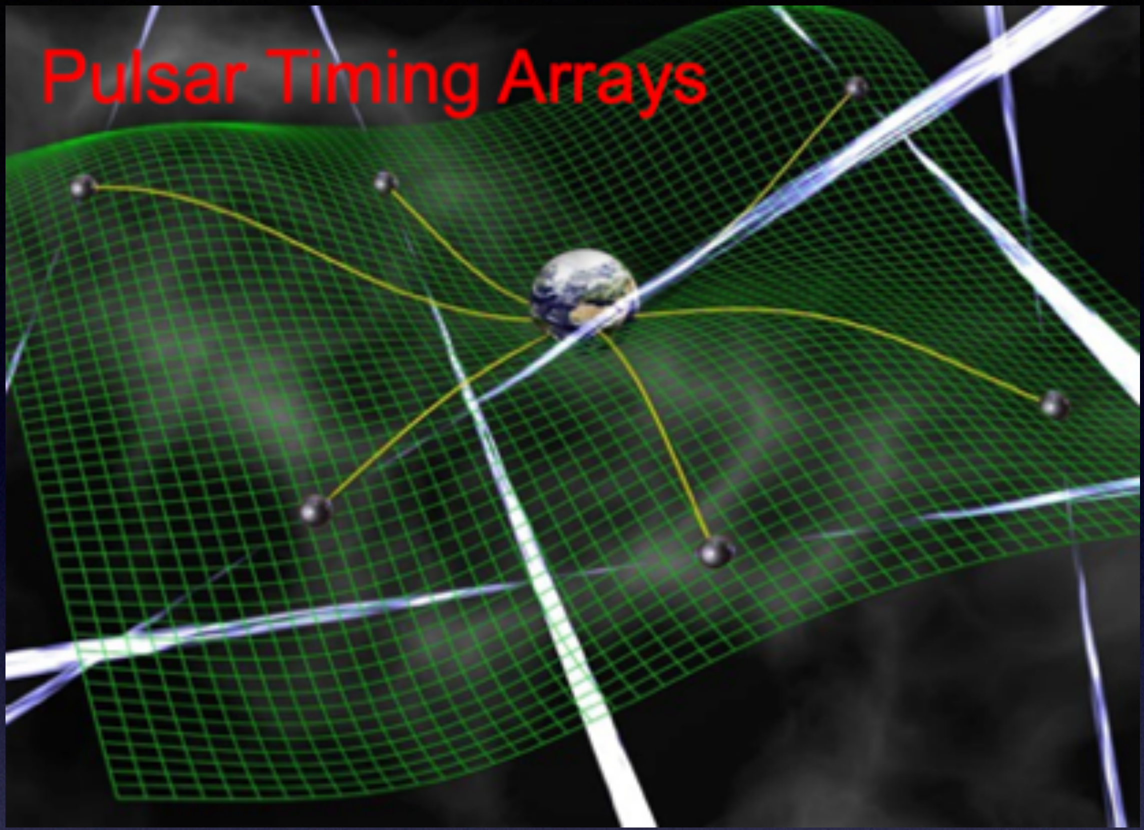

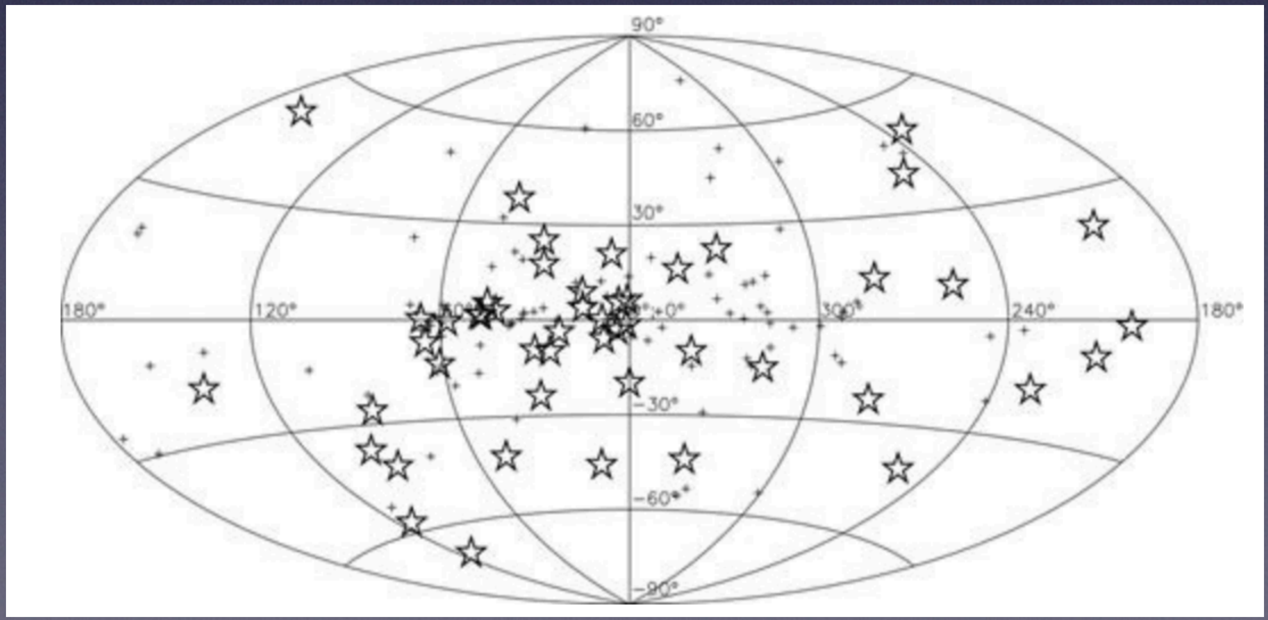

Background characteristic strain at f=1/yr is $A<1.45 \times 10^{-15}$ (Nanograv 2018)

Laser Interferometer Space Antenna (LISA)

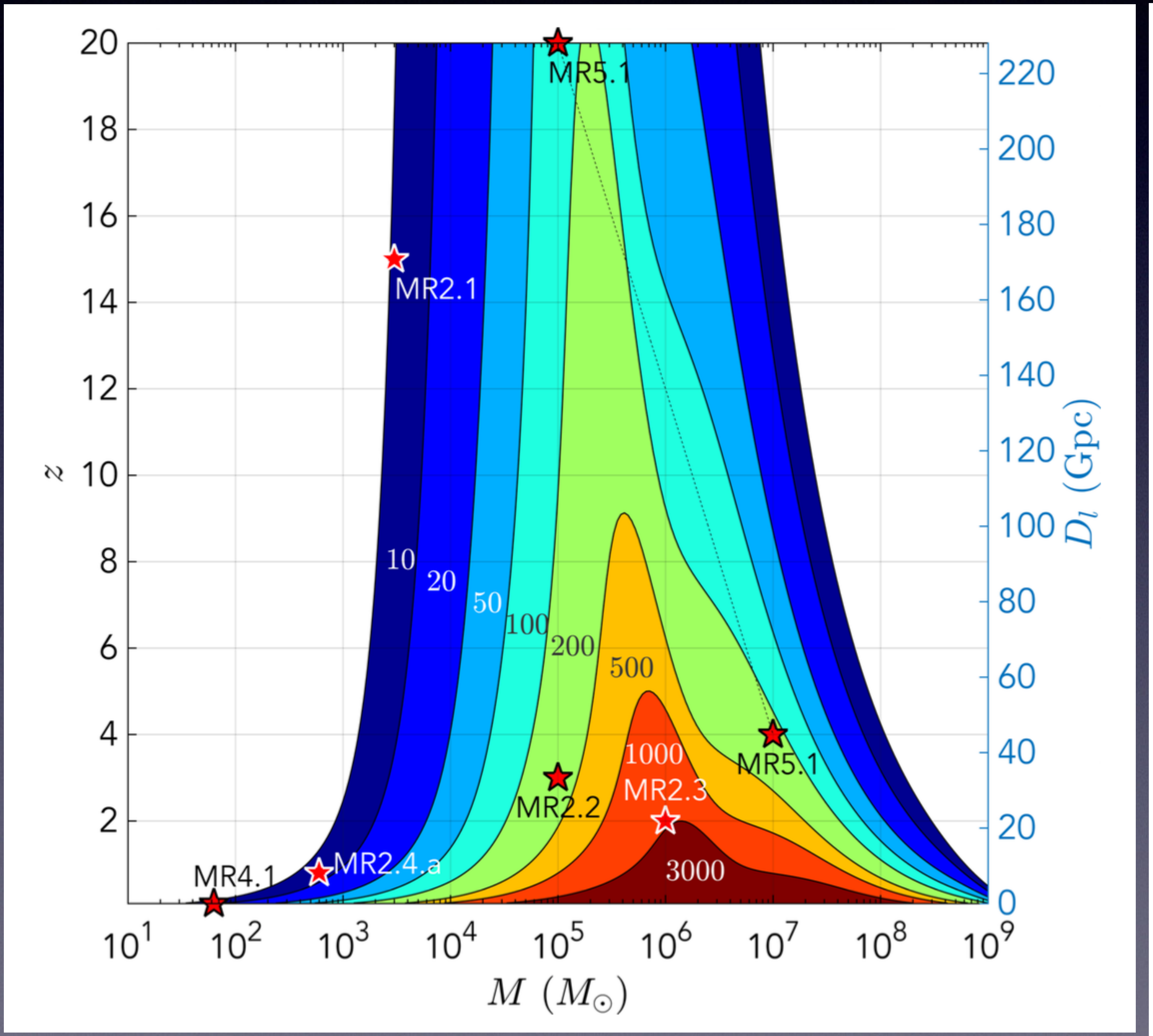

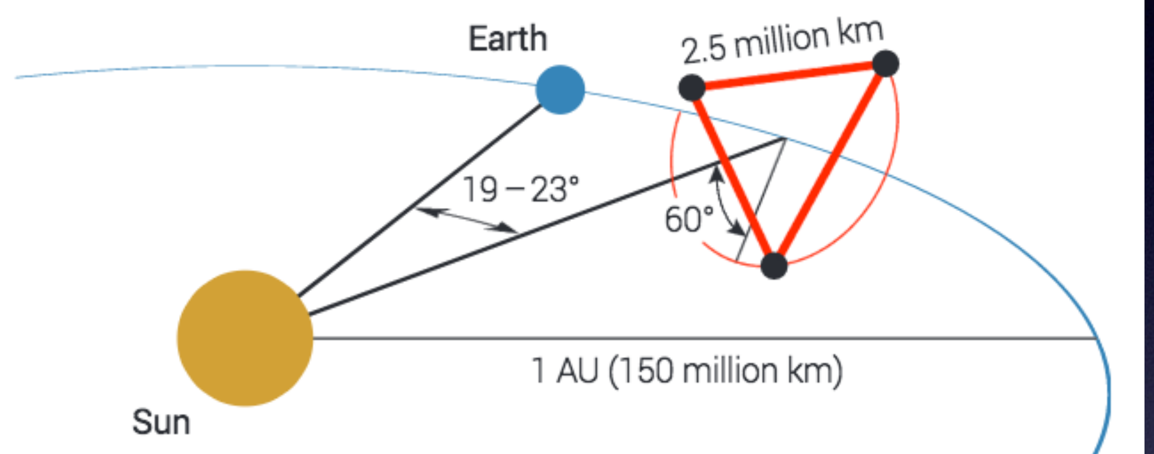

launch ~ 2032

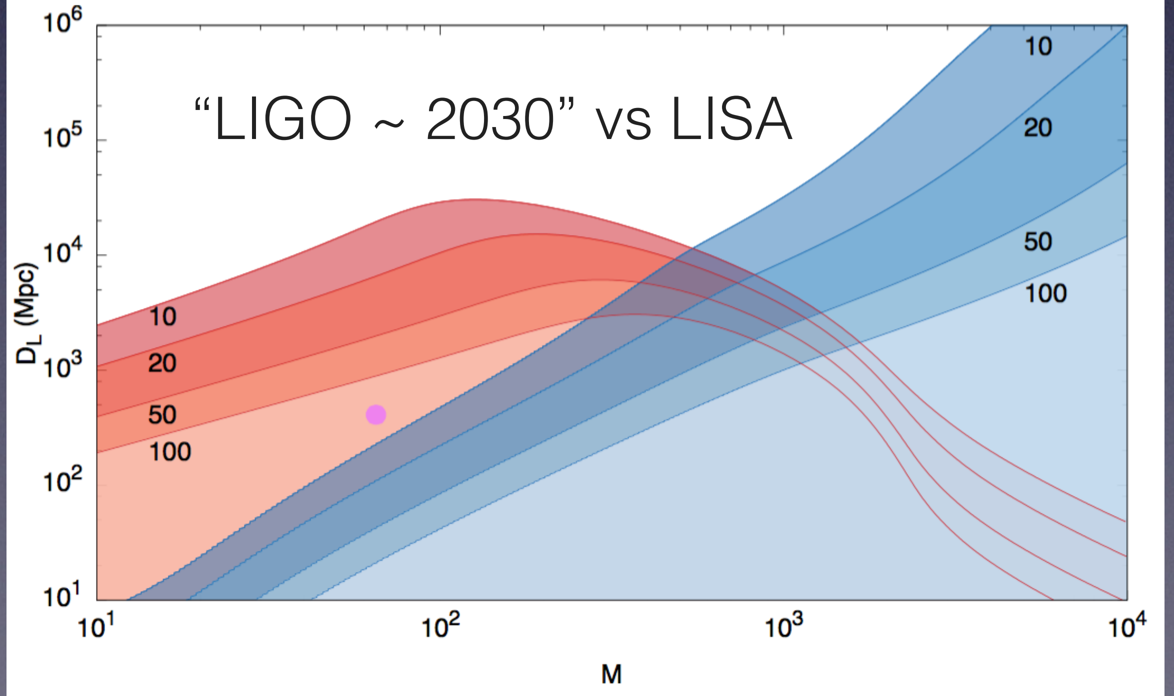

Galaxy/BH co-evolution

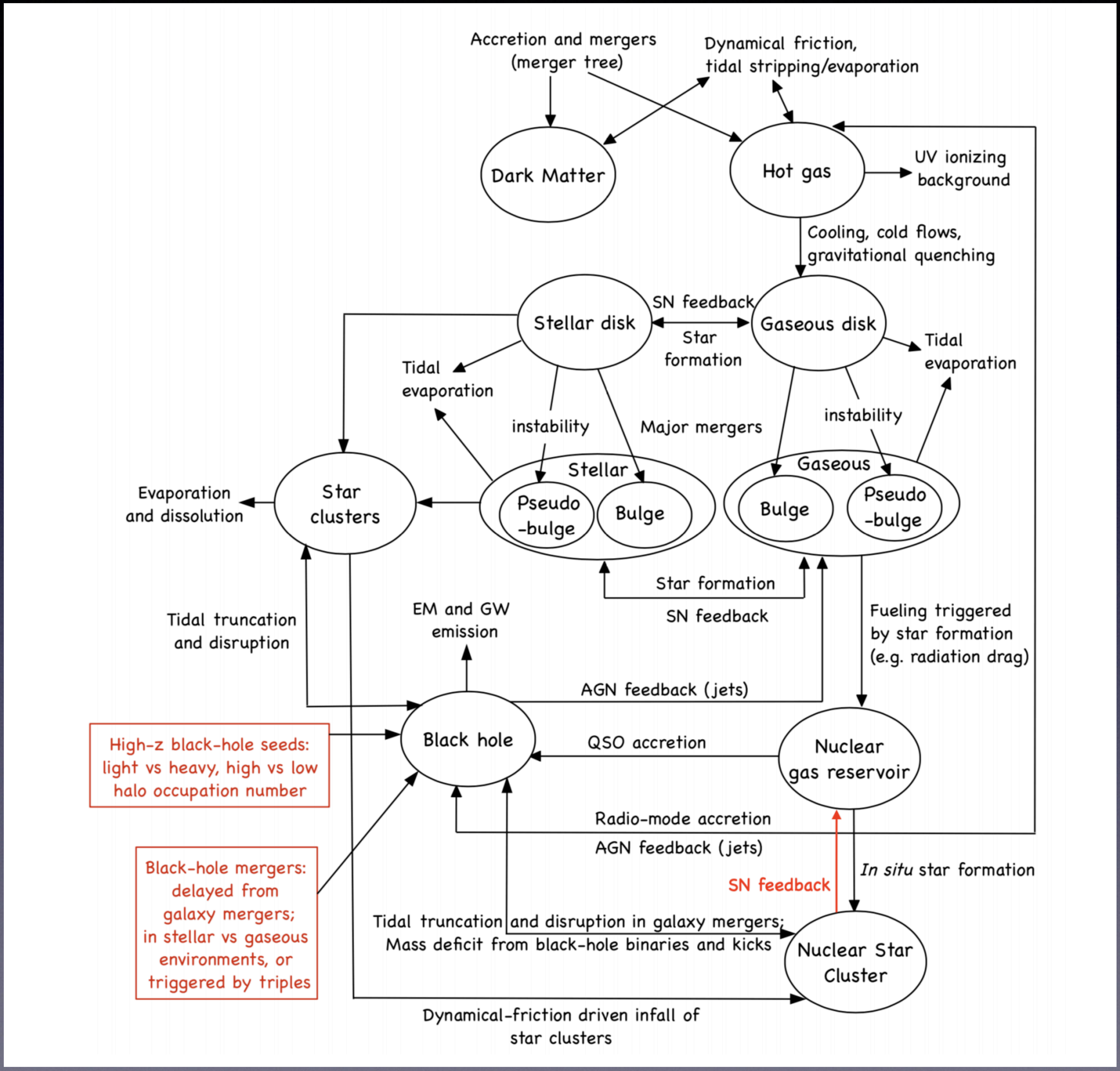

EB 2012, 2020

How big are baby black holes?

vs

Light seeds from PopIII stars (~100 M_{sun})

vs

Heavy seeds from instabilities of protogalactic disks (~10^5 M_{sun})

The "final pc problem"

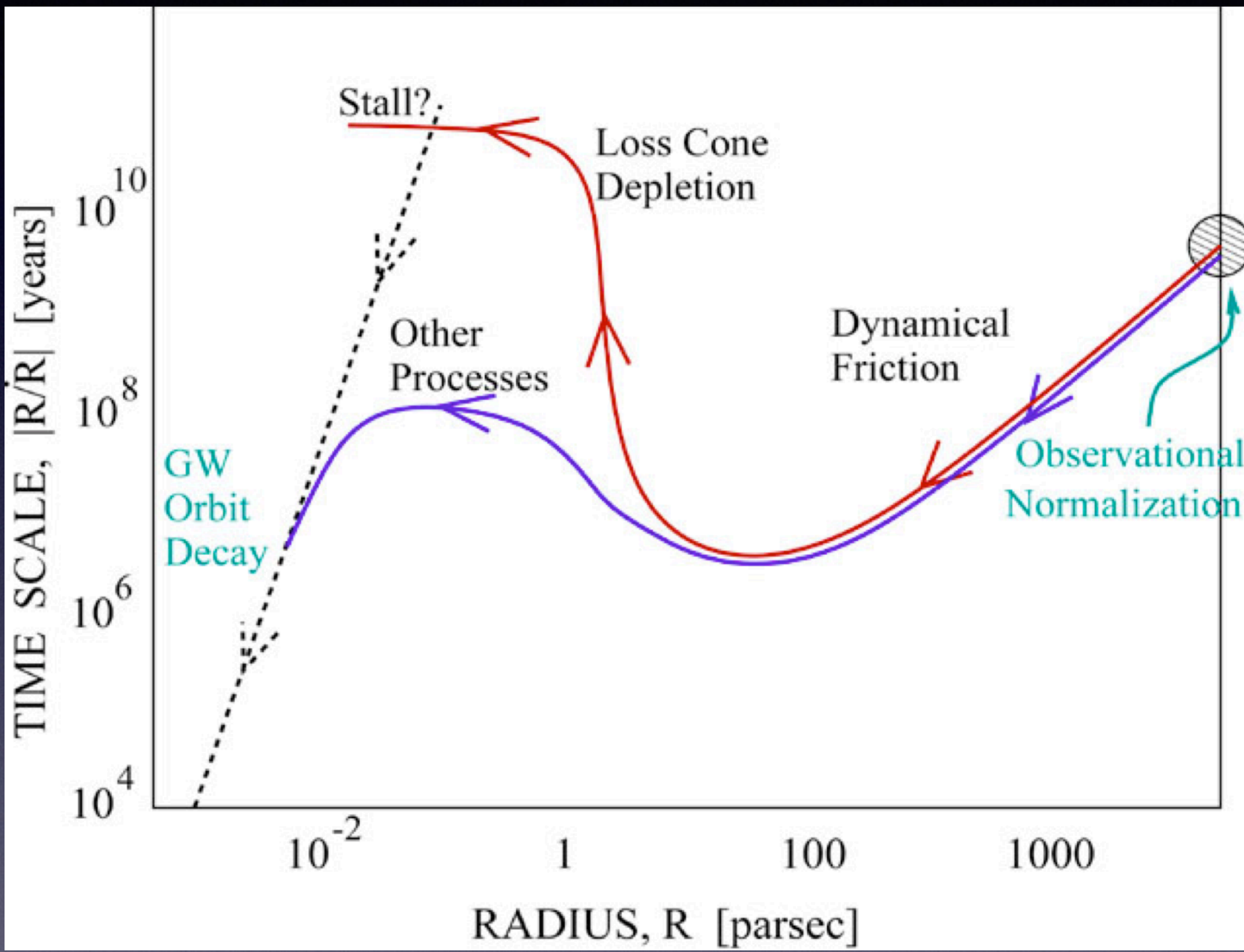

Begelman, Blandford & Rees 1980

Delays between halo and BH mergers

- Halo-halo dynamical friction+tidal disruption/evaporation
- From kpc to tens of pc: galaxy-galaxy dynamical friction/tidal disruption; BH-galaxy dynamical friction
- 3-body interactions with stars on timescales of 1-10 Gyr
- Gas-driven planetary-like migration on timescales ≳ 10 Myr
- Triple massive BH systems on timescales of 0.1-1 Gyr

Detection rates

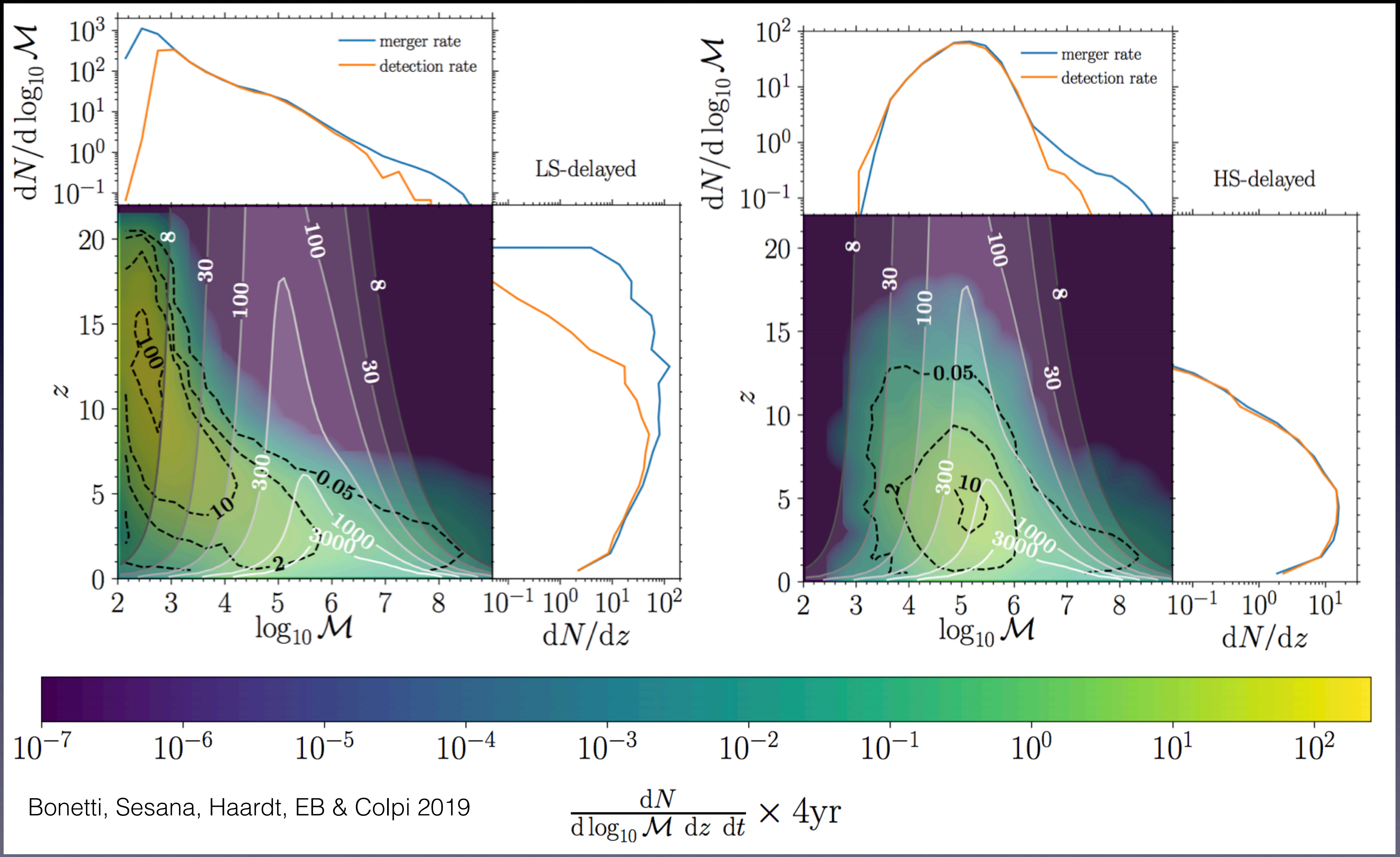

“short delays” (no kpc-to-100 pc delays), no SN winds

Detection rates

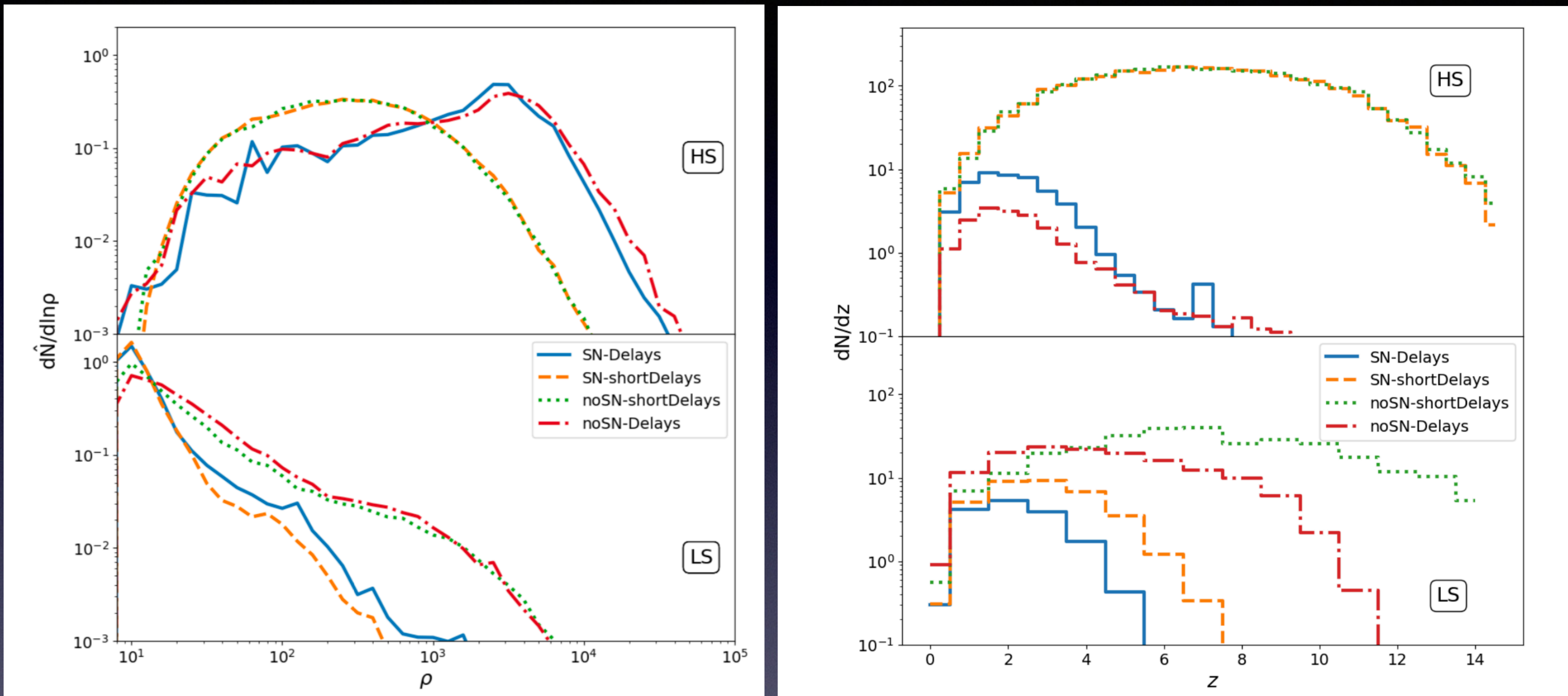

Model	LS		HS	
	Total	Detected	Total	Detected
SN feedback				
SN-Delays	48	16	25	25
SN-shortDelays	178	36	1269	1269
No SN feedback				
noSN-Delays	192	146	10	10
noSN-shortDelays	1159	307	1288	1288

EB+2020

Can we learn something from PTA limits?

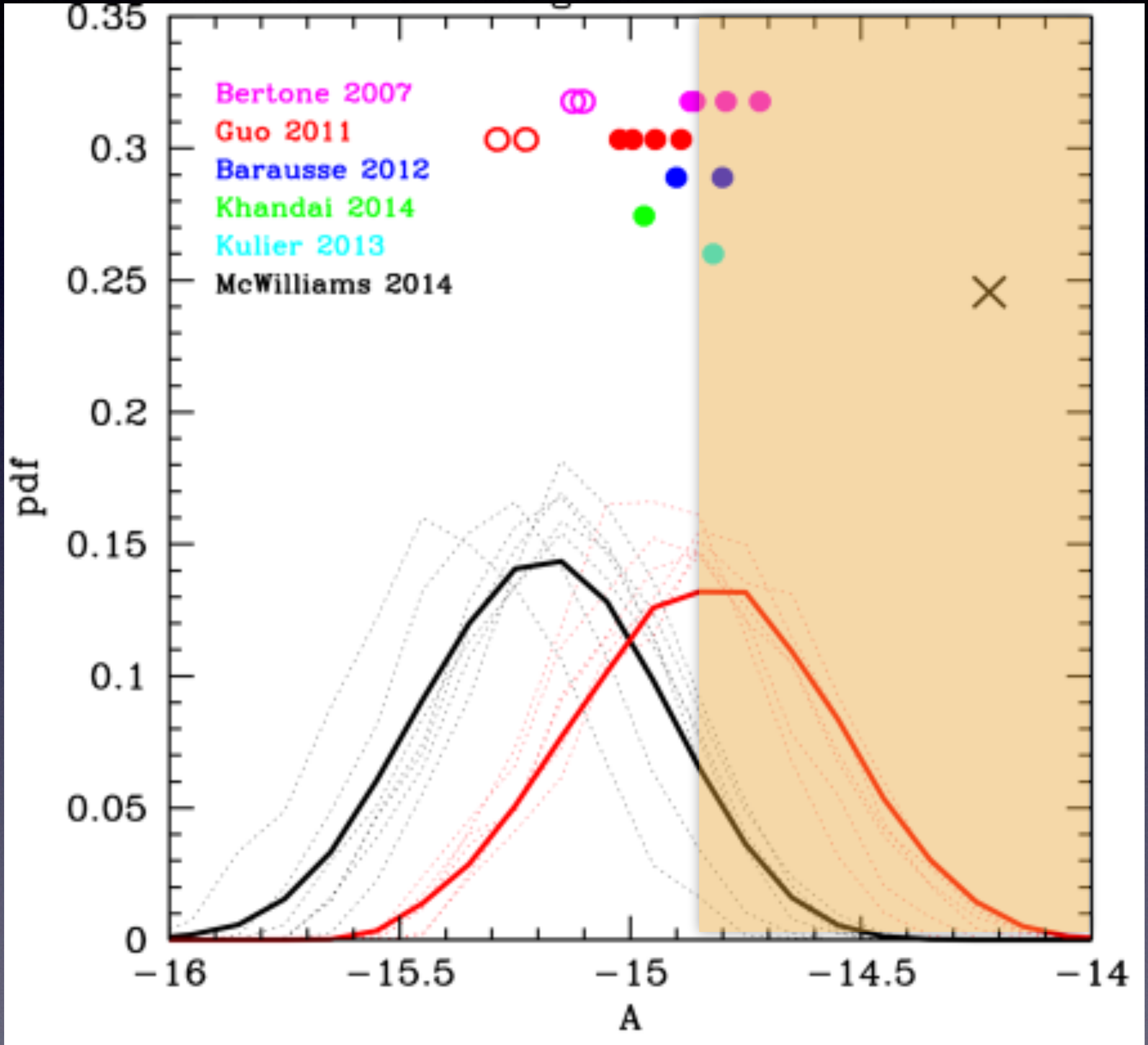

Background characteristic strain at f=1/yr is $A<1.45 \times 10^{-15}$ (Nanograv 2018)

A possible detection?

arXiv.org > astro-ph > arXiv:2009.04496

Search...

Help | Advanced

Astrophysics > High Energy Astrophysical Phenomena

[Submitted on 9 Sep 2020 (v1), last revised 8 Jan 2021 (this version, v2)]

The NANOGrav 12.5-year Data Set: Search For An Isotropic Stochastic Gravitational-Wave Background

Zaven Arzoumanian, Paul T. Baker, Harsha Blumer, Bence Becsy, Adam Brazier, Paul R. Brook, Sarah Burke-Spolaor, Shami Chatterjee, Siyuan Chen, James M. Cordes, Neil J. Cornish, Fronefield Crawford, H. Thankful Cromartie, Megan E. DeCesar, Paul B. Demorest, Timothy Dolch, Justin A. Ellis, Elizabeth C. Ferrara, William Fiore, Emmanuel Fonseca, Nathan Garver-Daniels, Peter A. Gentile, Deborah C. Good, Jeffrey S. Hazboun, A. Miguel Holgado, Kristina Islo, Ross J. Jennings, Megan L. Jones, Andrew R. Kaiser, David L. Kaplan, Luke Zoltan Kelley, Joey Shapiro Key, Nima Laal, Michael T. Lam, T. Joseph W. Lazio, Duncan R. Lorimer, Jing Luo, Ryan S. Lynch, Dustin R. Madison, Maura A. McLaughlin, Chiara M. F. Mingarelli, Cherry Ng, David J. Nice, Timothy T. Pennucci, Nihan S. Pol, Scott M. Ransom, Paul S. Ray, Brent J. Shapiro-Albert, Xavier Siemens, Joseph Simon, Renee Spiewak, Ingrid H. Stairs, Daniel R. Stinebring, Kevin Stovall, Jerry P. Sun, Joseph K. Swiggum, Stephen R. Taylor, Jacob E. Turner, Michele Vallisneri, Sarah J. Vigeland, Caitlin A. Witt (for the NANOGrav Collaboration)

We search for an isotropic stochastic gravitational-wave background (GWB) in the 12.5-year pulsar timing data set collected by the North American Nanohertz Observatory for Gravitational Waves. Our analysis finds strong evidence of a stochastic process, modeled as a power-law, with common amplitude and spectral slope across pulsars. The Bayesian posterior of the amplitude for an $f^{-2/3}$ power-law spectrum, expressed as the characteristic GW strain, has median 1.92×10^{-15} and 5%--95% quantiles of 1.37--2.67×10^{-15} at a reference frequency of $f_{\rm yr} = 1$ yr^{-1}. The Bayes factor in favor of the common-spectrum process versus independent red-noise processes in each pulsar exceeds $10,000$. However, we find no statistically significant evidence that this process has quadrupolar spatial correlations, which we would consider necessary to claim a GWB detection consistent with general relativity. We find that the process has neither monopolar nor dipolar correlations, which may arise from, for example, reference clock or solar system ephemeris systematics, respectively. The amplitude posterior has significant support above previously reported upper limits; we explain this in terms of the Bayesian priors assumed for intrinsic pulsar red noise. We examine potential implications for the supermassive black hole binary population under the hypothesis that the signal is indeed astrophysical in nature.

Tension with upper limit due to priors?

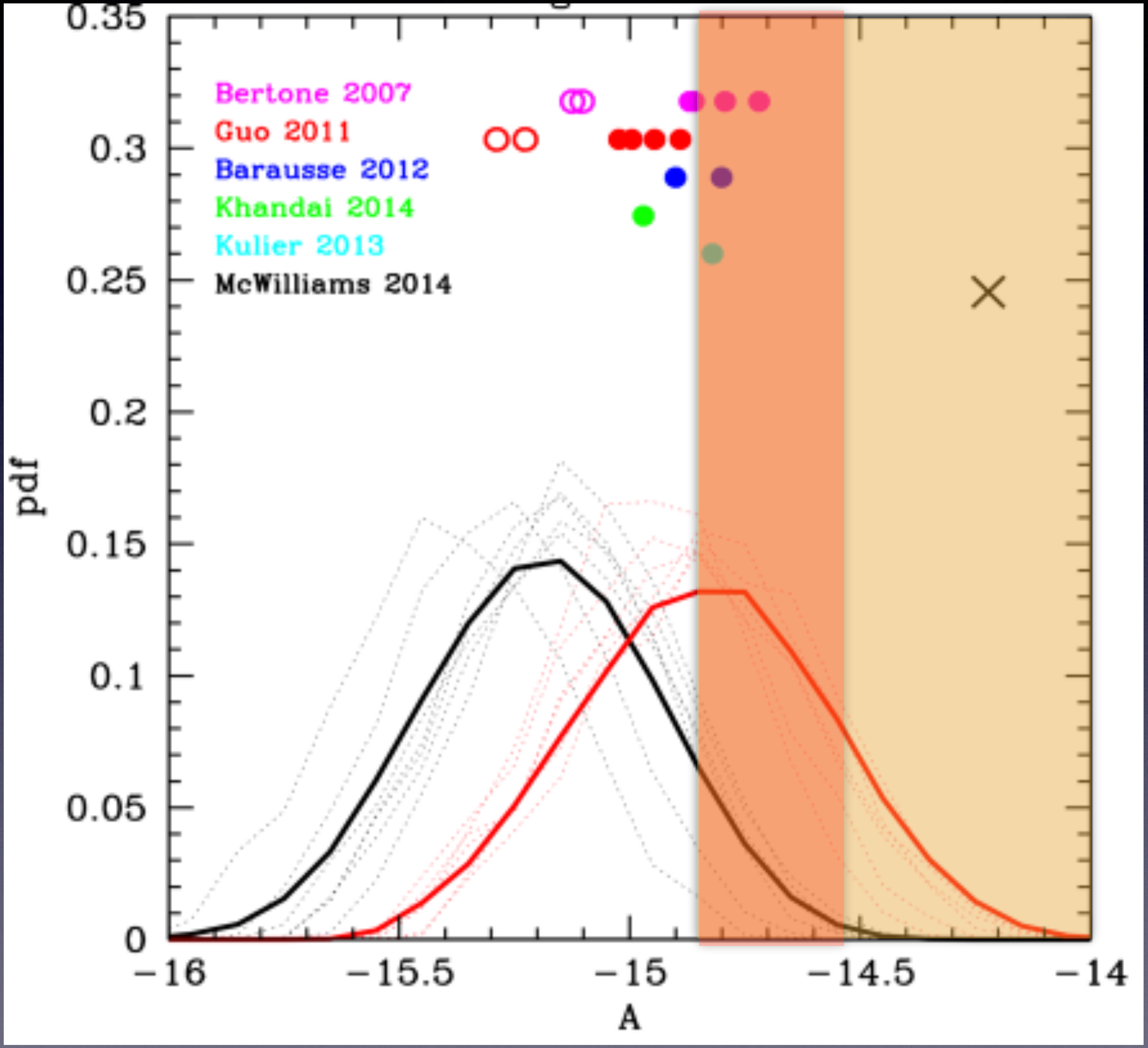

Multi-band gravitational-wave astronomy

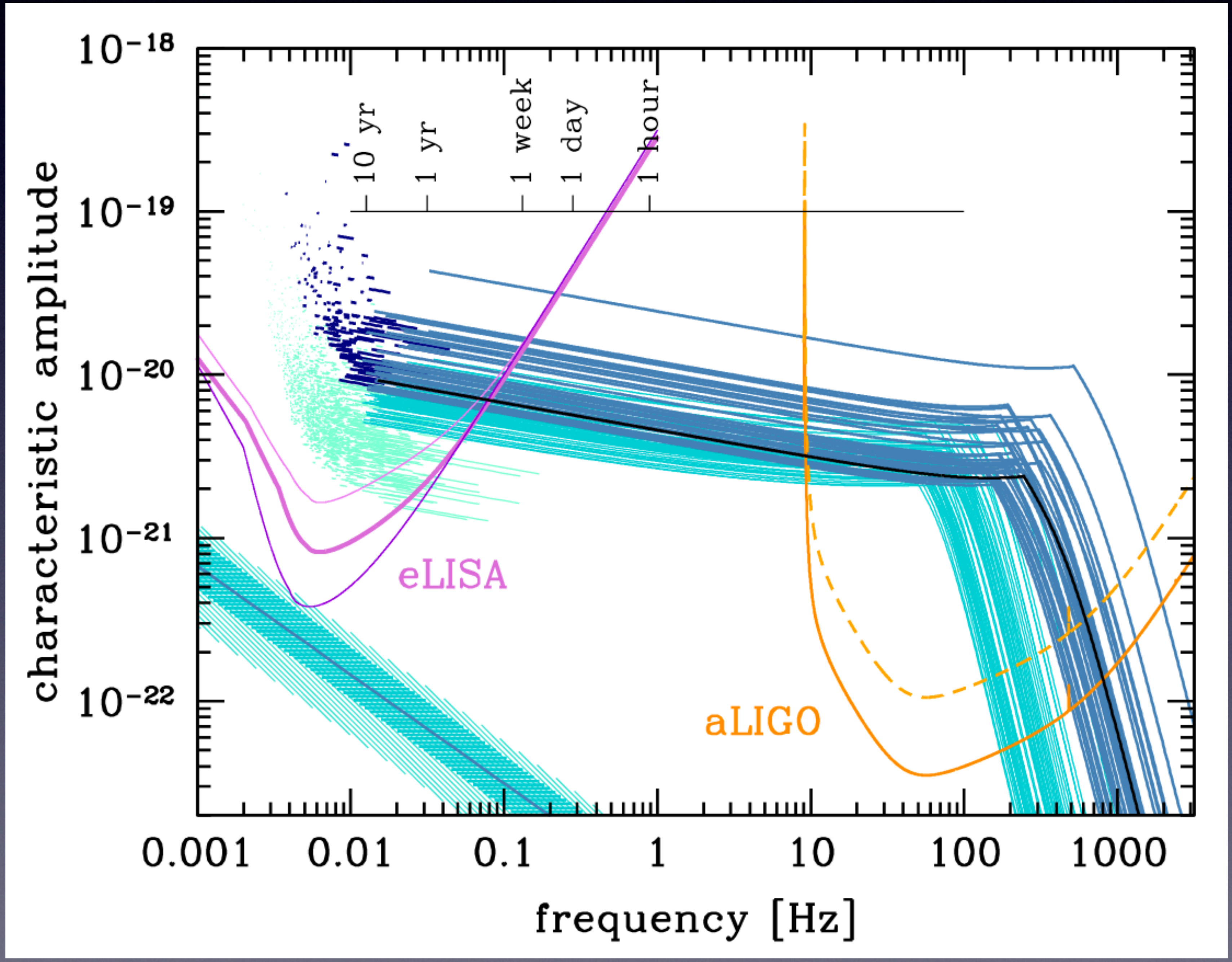

Sesana 2016

Multi-band gravitational-wave astronomy

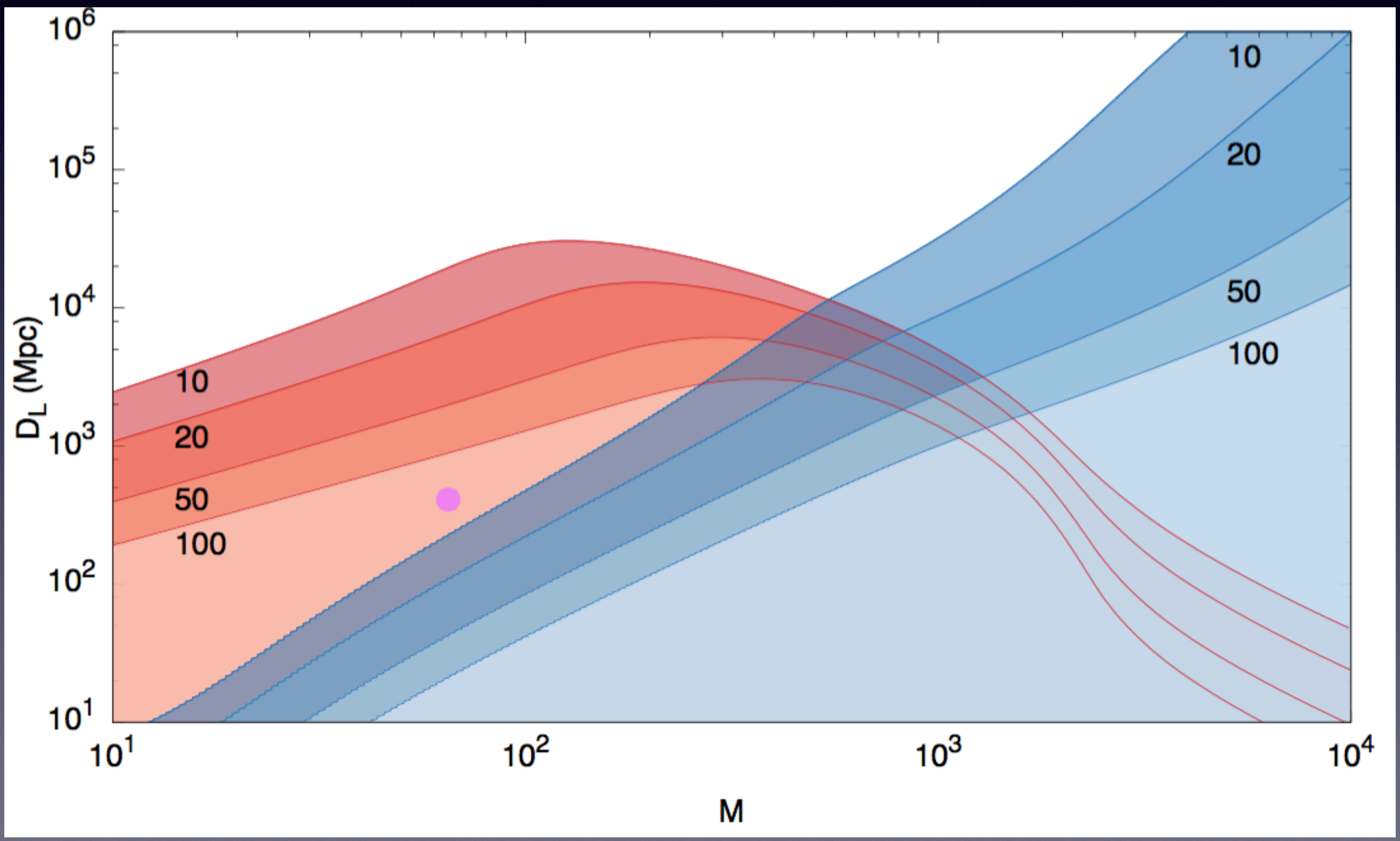

Tests of the equivalence principle with multi-band observations

- Smoking-gun sign of deviation from GR/BH "hairs" would be BH-BH dipole emission (-1PN term in phase/flux)

$$\dot{E}_{\rm GW} = \dot{E}_{\rm GR}\left[1 + B\left(\frac{Gm}{r_{12}c^2}\right)^{-1}\right]$$

- Pulsar constrain |B| ≲ 10^{-7}, GW150914-like systems + LISA will constrain same dipole term in BH-BH systems to comparable accuracy

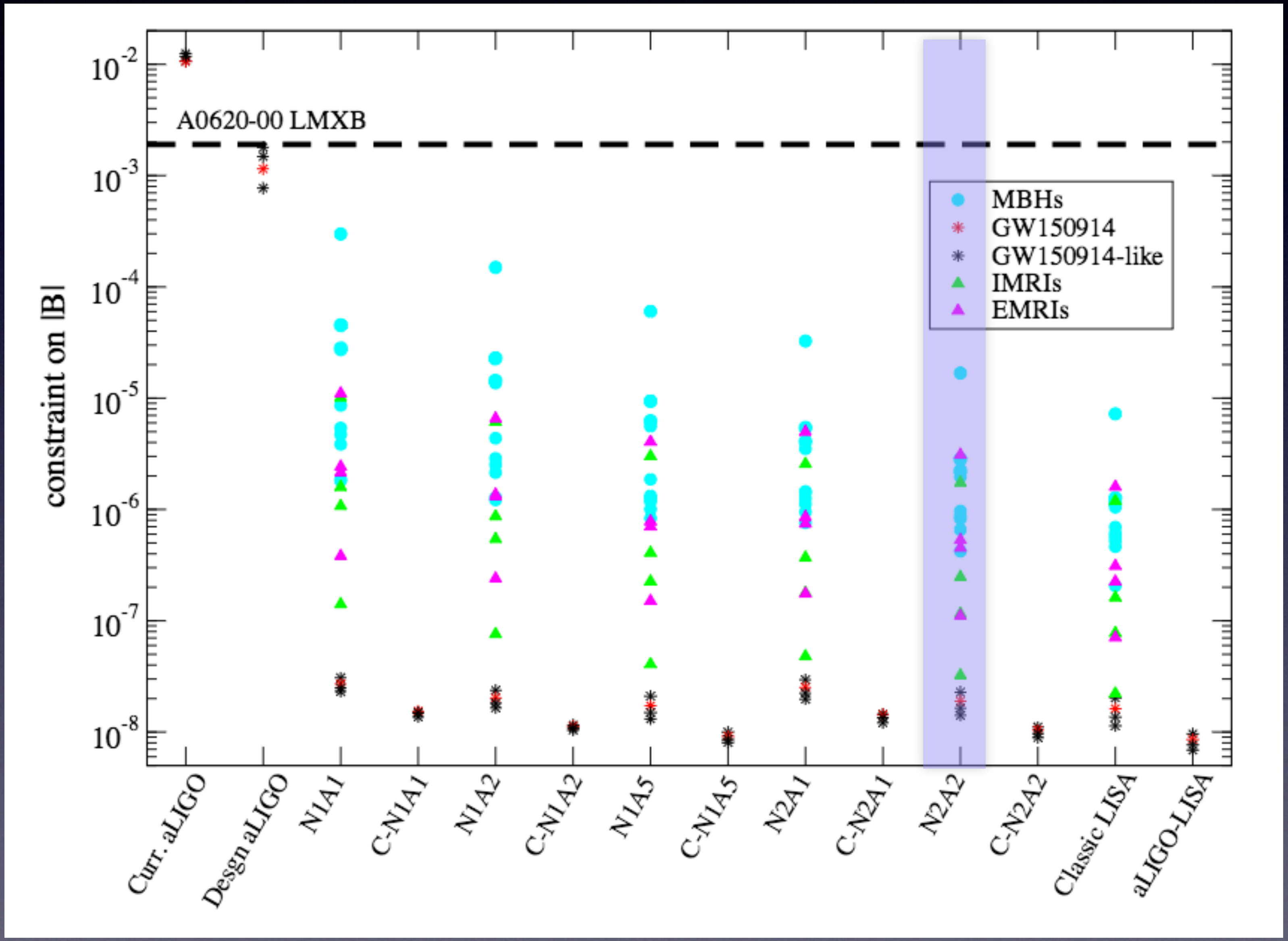

From EB, Yunes & Chamberlain 2016

Ringdown tests

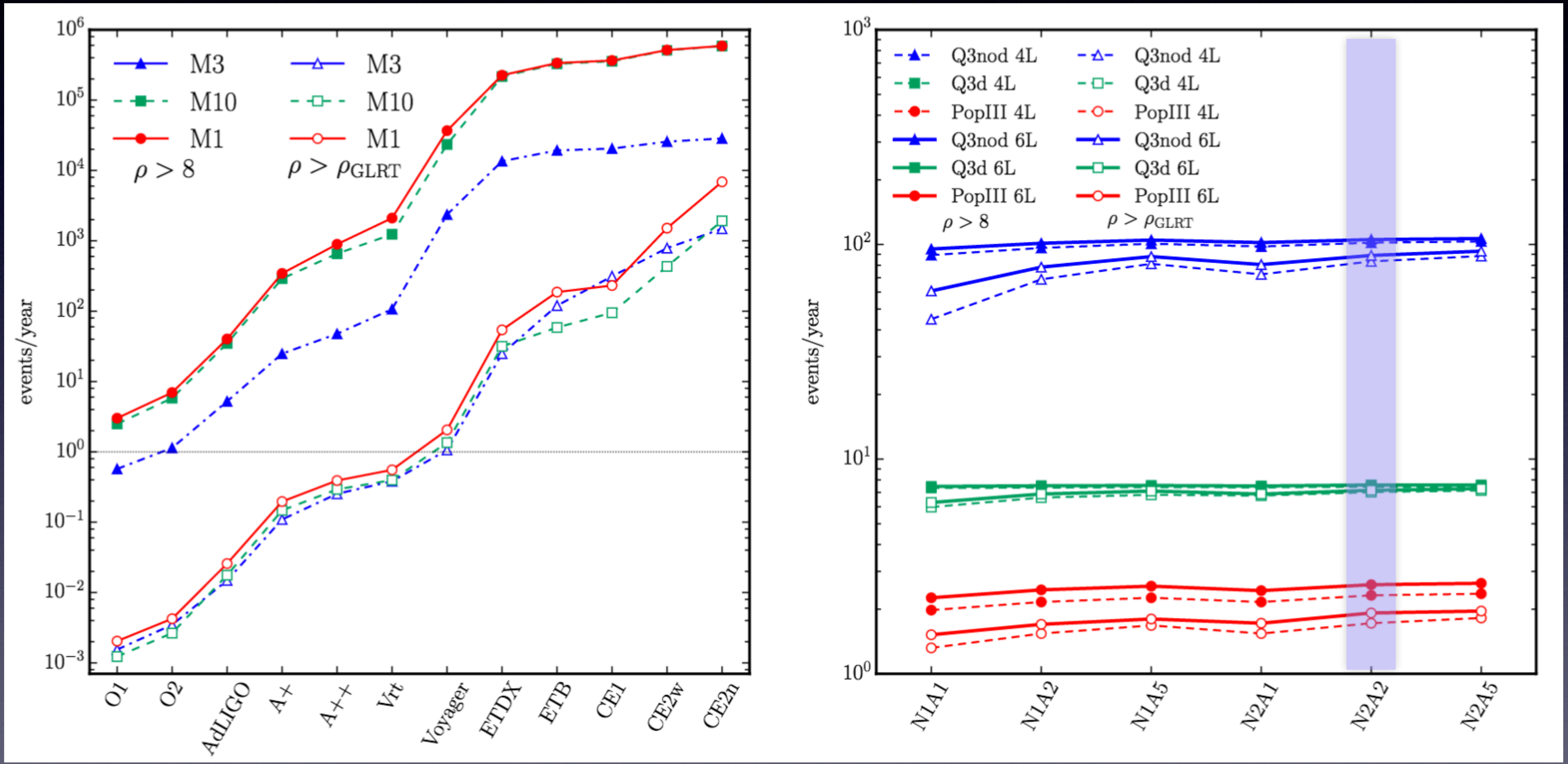

$$\rho_{\mathrm{GLRT}} \equiv \min(\rho^{2,3}_{\mathrm{GLRT}}, \rho^{2,4}_{\mathrm{GLRT}})$$

Berti, Sesana, EB, Cardoso, Belczynski, 2016

But overtones of 22 mode may help (Giesler+2019)

More science with LISA…

- Galactic white-dwarf binaries
- Extreme mass ratio inspirals: star or "LIGO" BH + massive BH:

- Will test the "no hair" theorem

- Akin to mapping Earth's gravitational field with artificial satellites

- Stochastic backgrounds from inflation/phase transitions in the early universe

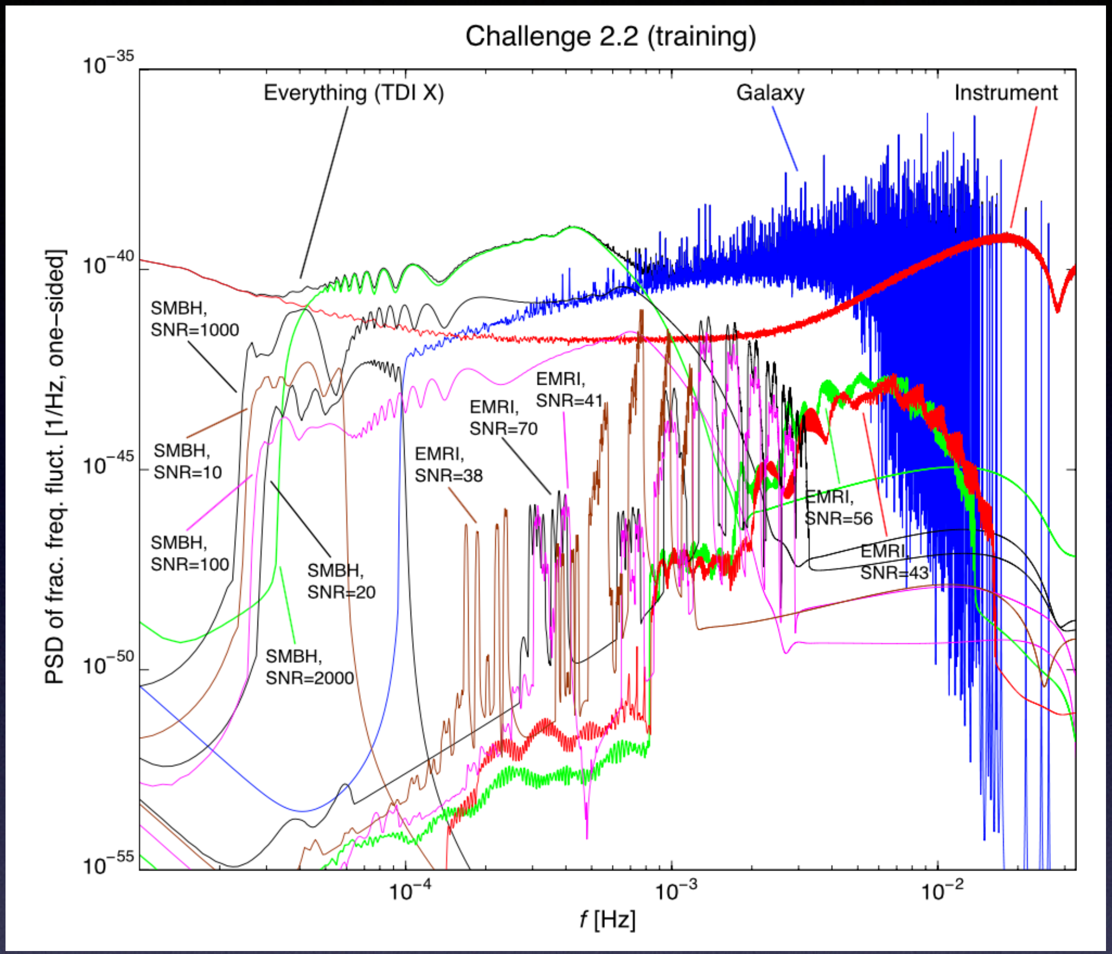

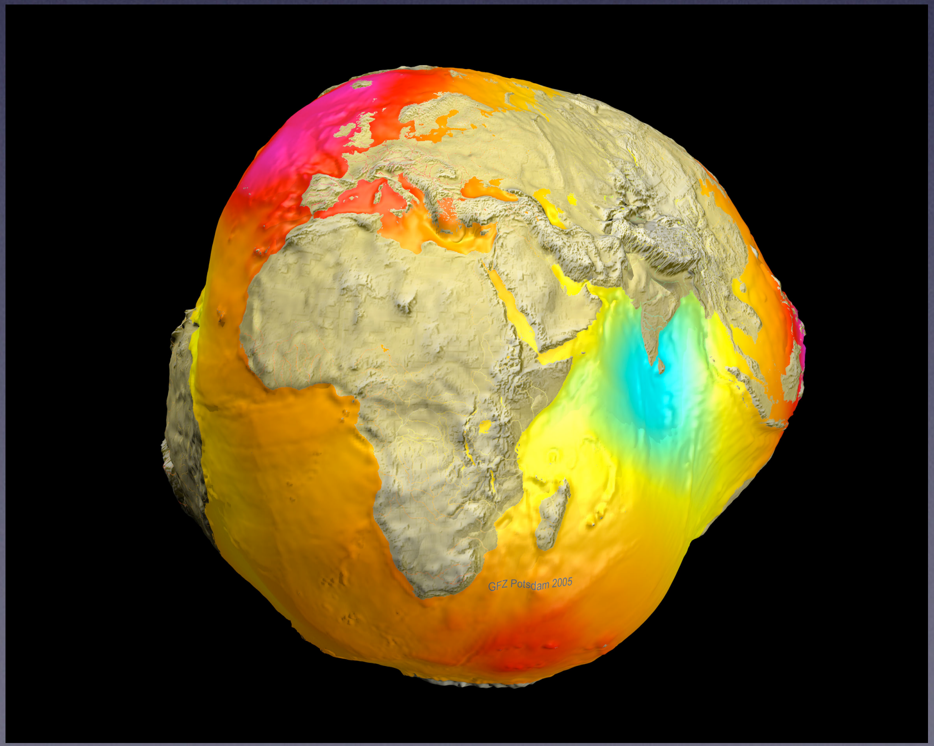

Light bosons and GWs

- Scalars ubiquitous in string theory, inflation, dark matter models (e.g. fuzzy/axionic dark matter)
- Useful as toy models for unknown phenomena/ interactions (e.g. modifications of GR)
- “Light” means <~ 1.e-10 eV
- Effect of mass term expected to be qualitatively similar for all boson degrees of freedom
- Can form condensates around rotating BHs if Compton wavelength ~ BH size

Self-gravitating scalar configurations

- Scalars can form self-gravitating configurations, especially if complex, massive (to avoid dispersion to infinity) and time dependent (to provide pressure): boson stars, oscillatons

- Around BHs, massive real (complex) scalars can form quasi-stationary (stationary) configurations: boson clouds or condensates, hairy BHs

BH-boson condensates

- Formation linked to superradiant instabilities/Penrose process (amplification of scattered waves with $\omega < m\Omega_H$)
- BH with high enough spin and “mirror” are superradiance unstable (BH bomb; Zeldovich 71, Press & Teukolsky 72, Cardoso et al 04)
- In ergoregion, negative energy modes can be produced but are confined (only positive energy modes can travel to infinity)
- By energy conservation, more and more negative energy modes can be produced, which may cause instability according to boundary conditions (at horizon and spatial infinity)

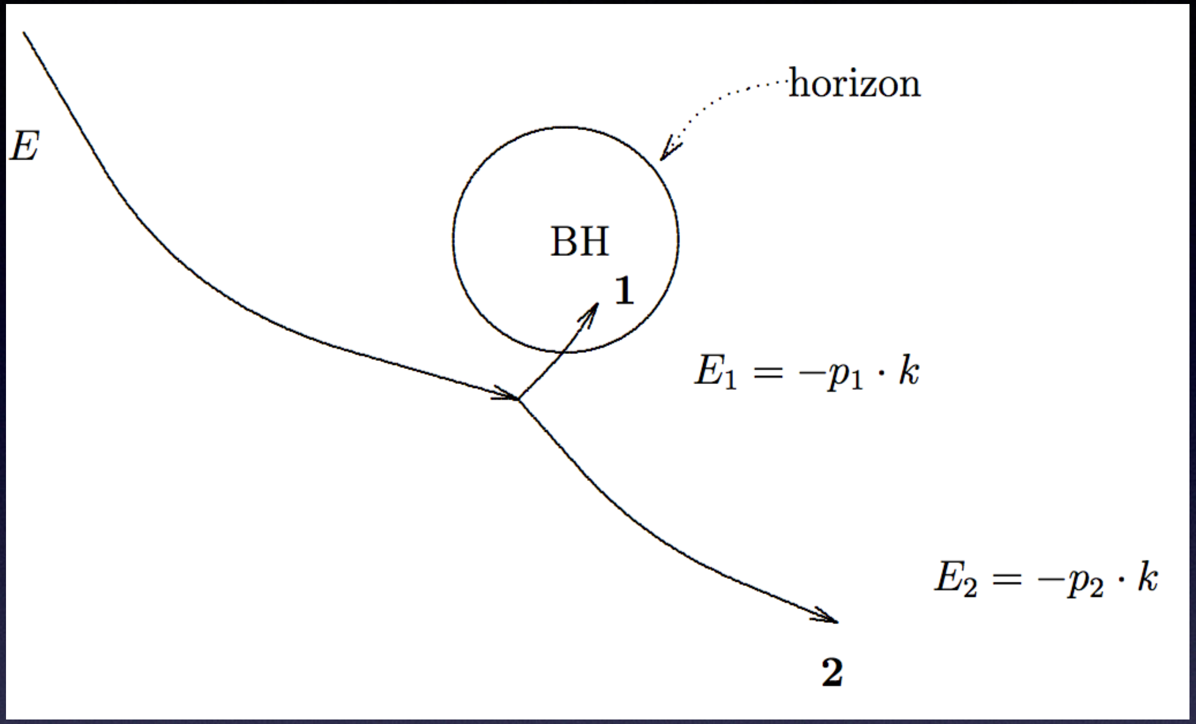

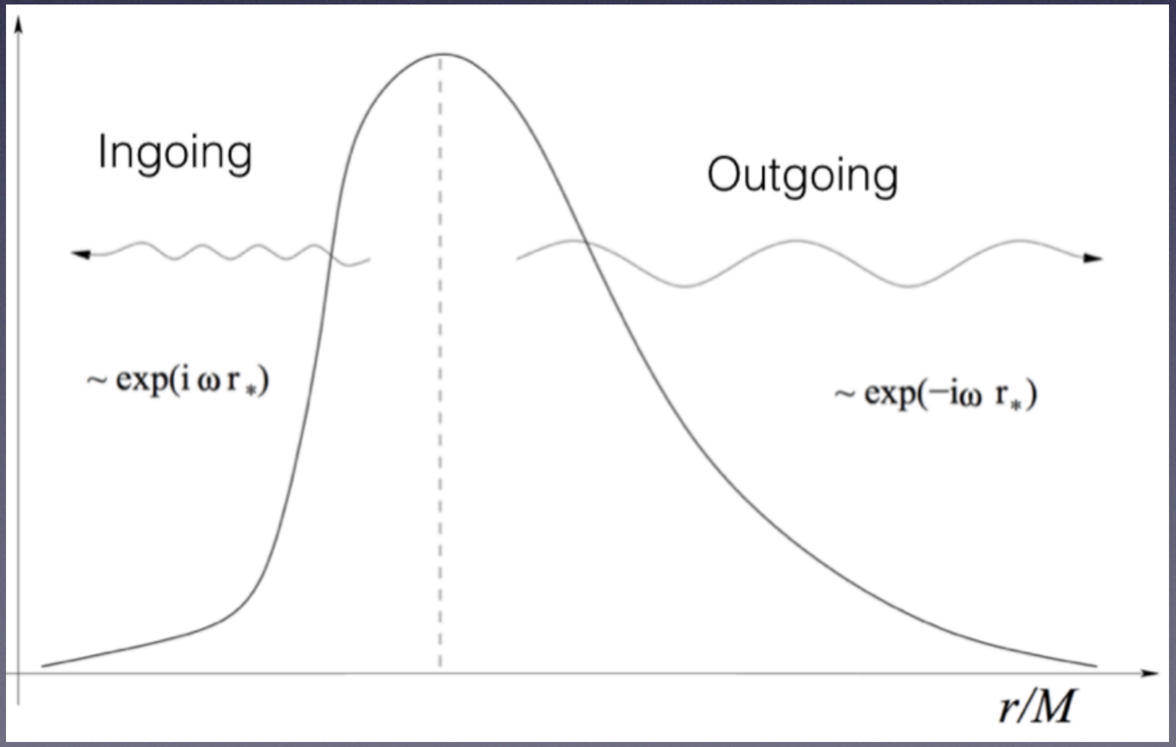

BH-boson condensates

- Formation linked to superradiant instabilities/Penrose process (amplification of scattered waves with $\omega < m\Omega_H$)
- BH with high enough spin and “mirror” are superradiance unstable (BH bomb; Zeldovich 71, Press & Teukolsky 72, Cardoso et al 04)
- In ergoregion, negative energy modes can be produced but are confined (only positive energy modes can travel to infinity)
- By energy conservation, more and more negative energy modes can be produced, which may cause instability according to boundary conditions (at horizon and spatial infinity)

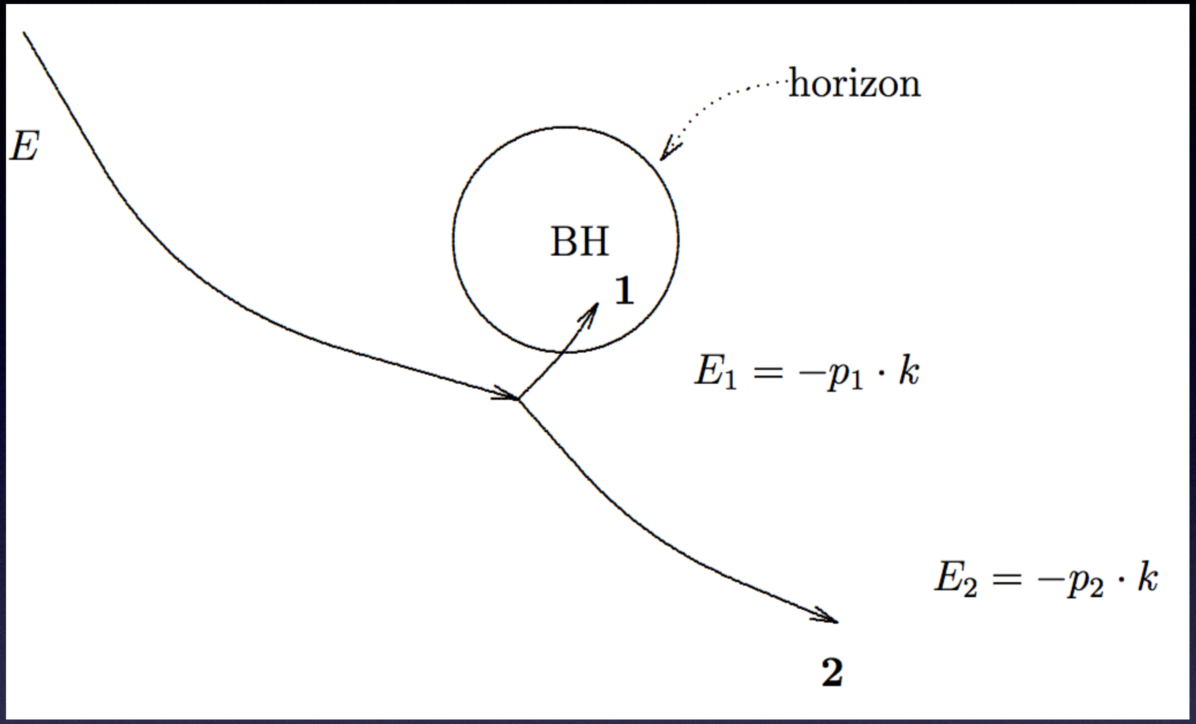

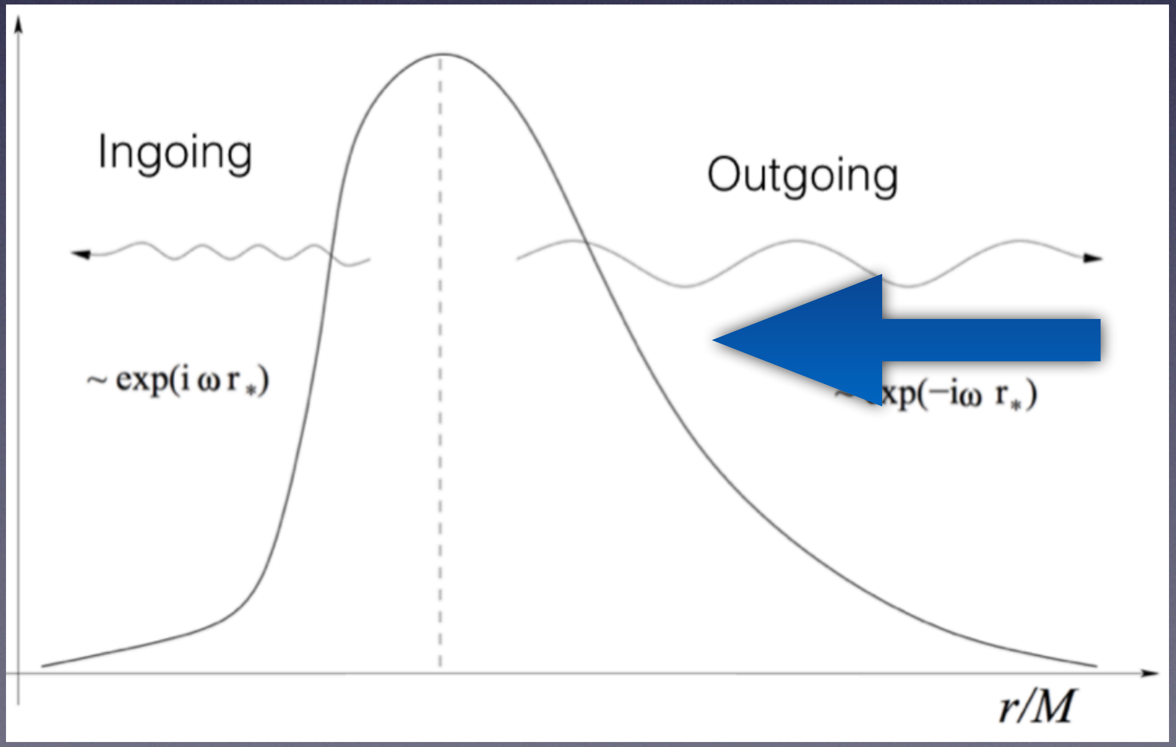

Superradiance from near horizon physics

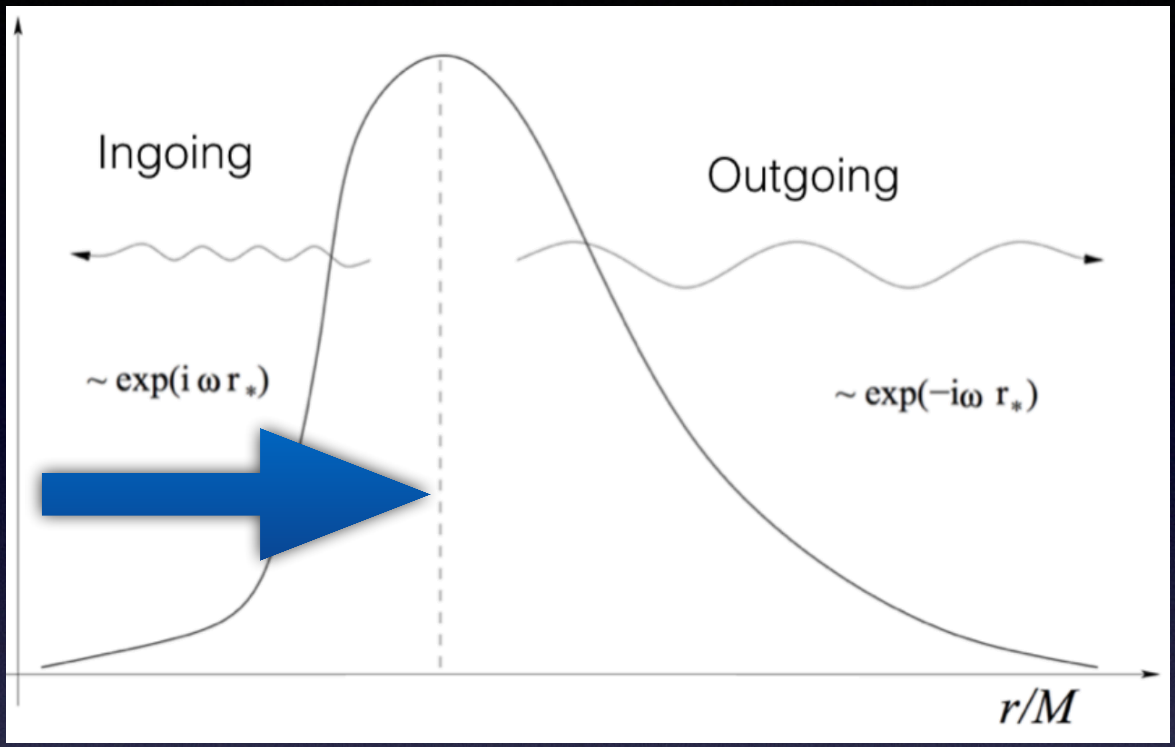

- Deviations away from Kerr geometry near horizon (e.g. firewalls, gravastars, wormholes, Lorentz violations, etc) can produce significant changes in QNM spectrum
- Delays $\Delta t \sim \log[r_0/(2M) - 1]$

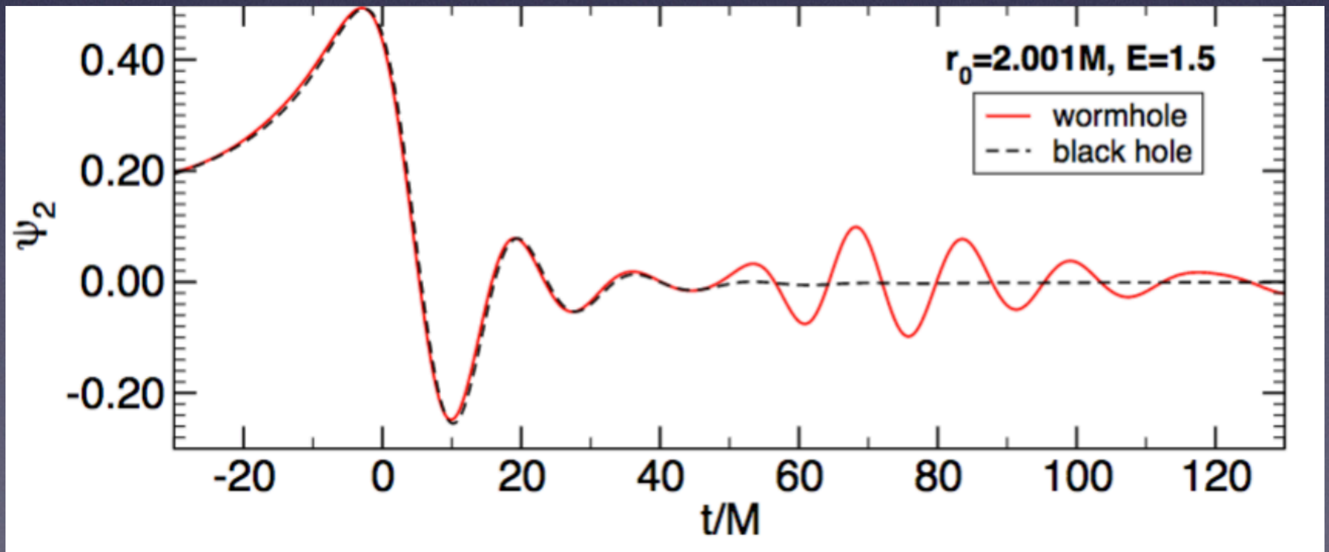

Cardoso, Franzin & Pani 2016

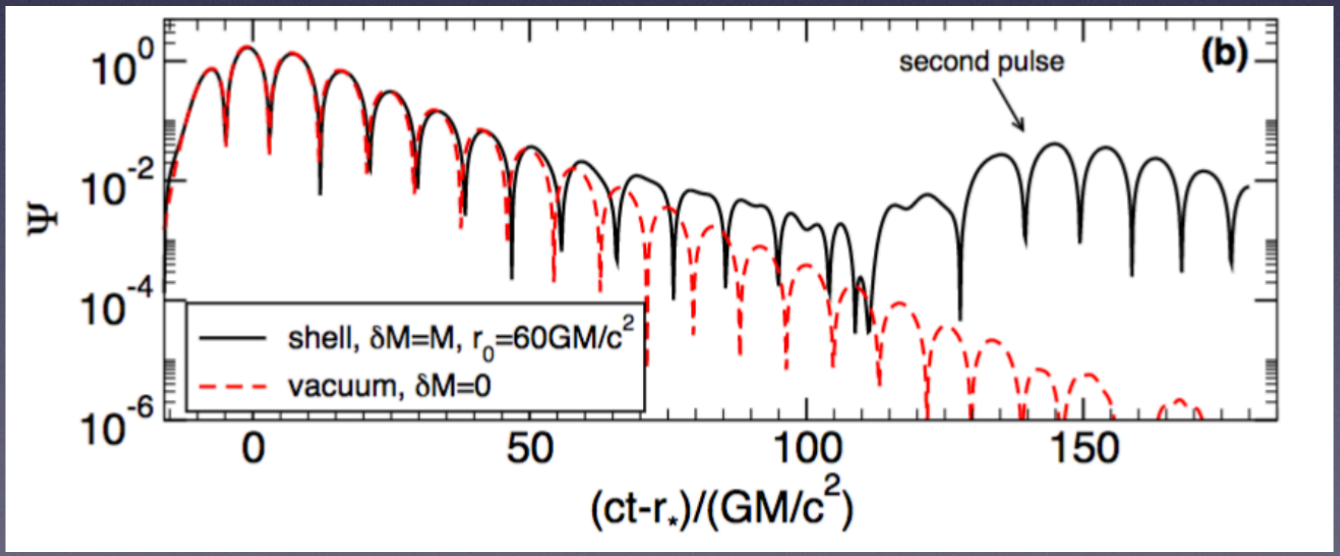

EB, Cardoso & Pani 2014

BH-boson condensates

- Same instability of spinning BH + massive boson (mass acts as "mirror" and allows for bound states), but NOT for fermions. Cf Damour, Deruelle & Ruffini 76

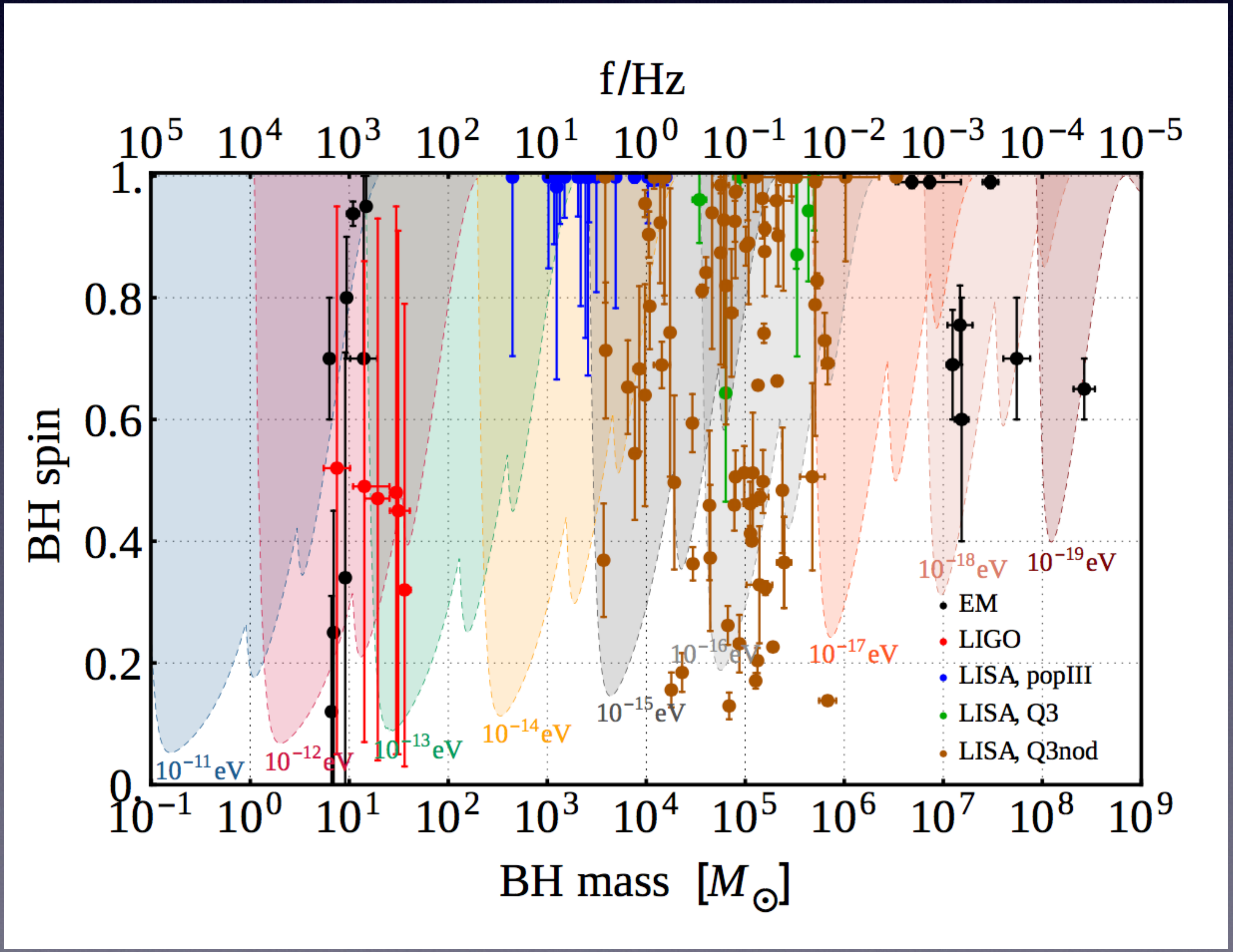

Instability end point

- BH sheds excess spin (and to a lesser degree mass) into a mostly dipolar rotating boson cloud …

$$m_s \equiv \mu\hbar,$$

$$\omega_R \sim \mu - \frac{M^2\mu^3}{8}$$

$$\Phi = A_0 g(r)\cos(m_\phi\phi - \omega_R t)\sin\theta\,,$$

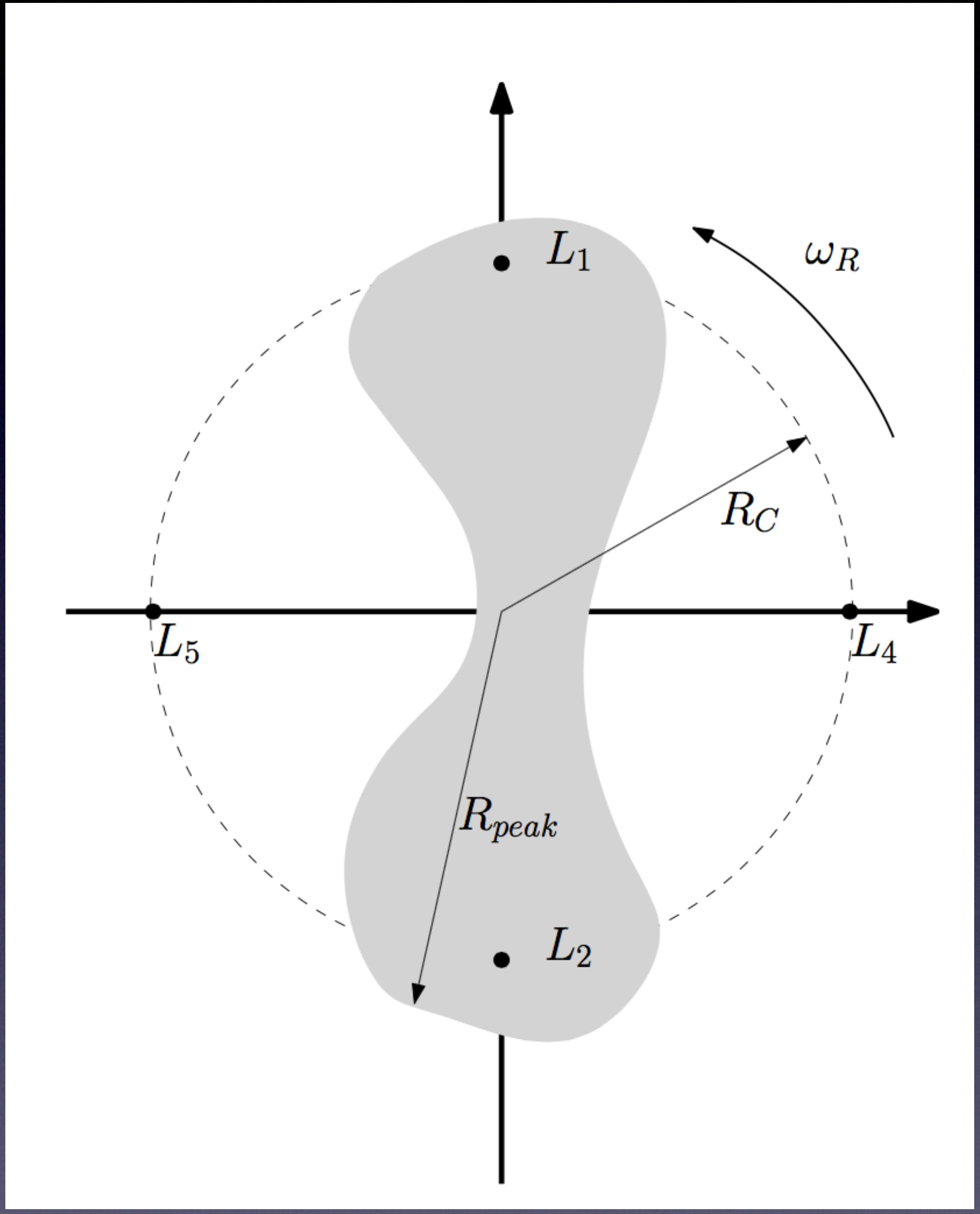

- … till instability saturates

$$\mu \sim m\Omega_{\rm H}$$

$$\tau_{\rm inst} \sim 0.07\,\chi^{-1}\left(\frac{M}{10\,M_\odot}\right)\left(\frac{0.1}{M\mu}\right)^9 \mathrm{yr}\,,$$

(for Mμ<<1 and χ<<1; max instability for Mμ=0.42)

GW emission

- Long-lived rotating scalar dipole produces almost monochromatic GWs via quadrupole formula on timescale

$$\tau_{\rm GW} \sim 6 \times 10^4 \, \chi^{-1} \left(\frac{M}{10\, M_\odot}\right) \left(\frac{0.1}{M\mu}\right)^{15} \, \mathrm{yr}$$

$$h = \sqrt{\frac{2}{5\pi}} \frac{GM}{c^2 r} \left(\frac{M_S}{M}\right) A(\chi, f_s M) \, ,$$ rms strain amplitude

$$\omega \sim \mu$$ frequency

Background from isolated spinning BHs

energy emission efficiency

$$f_{\rm ax} \sim \mathcal{O}(1\%)$$

monochromatic GW in source frame

$$\Delta \ln f \;\sim\; 1$$

LISA band

massive BHs ~ 10^4-10^7 M_{sun}, m_s~10^{-16} - 10^{-18} eV

$$\rho_{\rm BH} \;\sim\; \mathcal{O}(10^4) M_\odot/{\rm Mpc}^3$$

$$\Omega_{\rm GW,\,ax} = (1/\rho_{\rm c})(d\rho_{\rm GW}/d\ln f) \sim f_{\rm ax}\rho_{\rm BH}/\rho_{\rm c}$$

$$\Omega^{\rm LISA}_{\rm GW,\,ax} \;\sim\; 10^{-9}$$

Background from isolated spinning BHs

energy emission efficiency

$$f_{\rm ax} \sim \mathcal{O}(1\%)$$

monochromatic GW in source frame

$$\Delta \ln f \sim 1$$

LIGO/Virgo band

stellar-mass BHs ~ 10-50 M_{sun}, $m_s \sim 10^{-13}$ - 10^{-12} eV

$$\Omega_{\rm GW,\,bin} \sim f_{\rm GW} f_{\rm m} \rho_{\rm BH}/\rho_c$$

$$f_{\rm GW} \sim \mathcal{O}(1\%) \qquad f_{\rm m} \sim \mathcal{O}(1\%)$$

$$\Omega_{\rm GW,\,ax}/\Omega_{\rm GW,\,bin} \sim f_{\rm ax}/(f_{\rm GW} f_{\rm m}) \sim 10^2$$

$$\Omega_{\rm GW,\,bin} \sim 10^{-9} - 10^{-8} \qquad \Omega^{\rm LIGO}_{\rm GW,\,ax} \sim 10^{-7} - 10^{-6}$$

Background from isolated spinning BHs

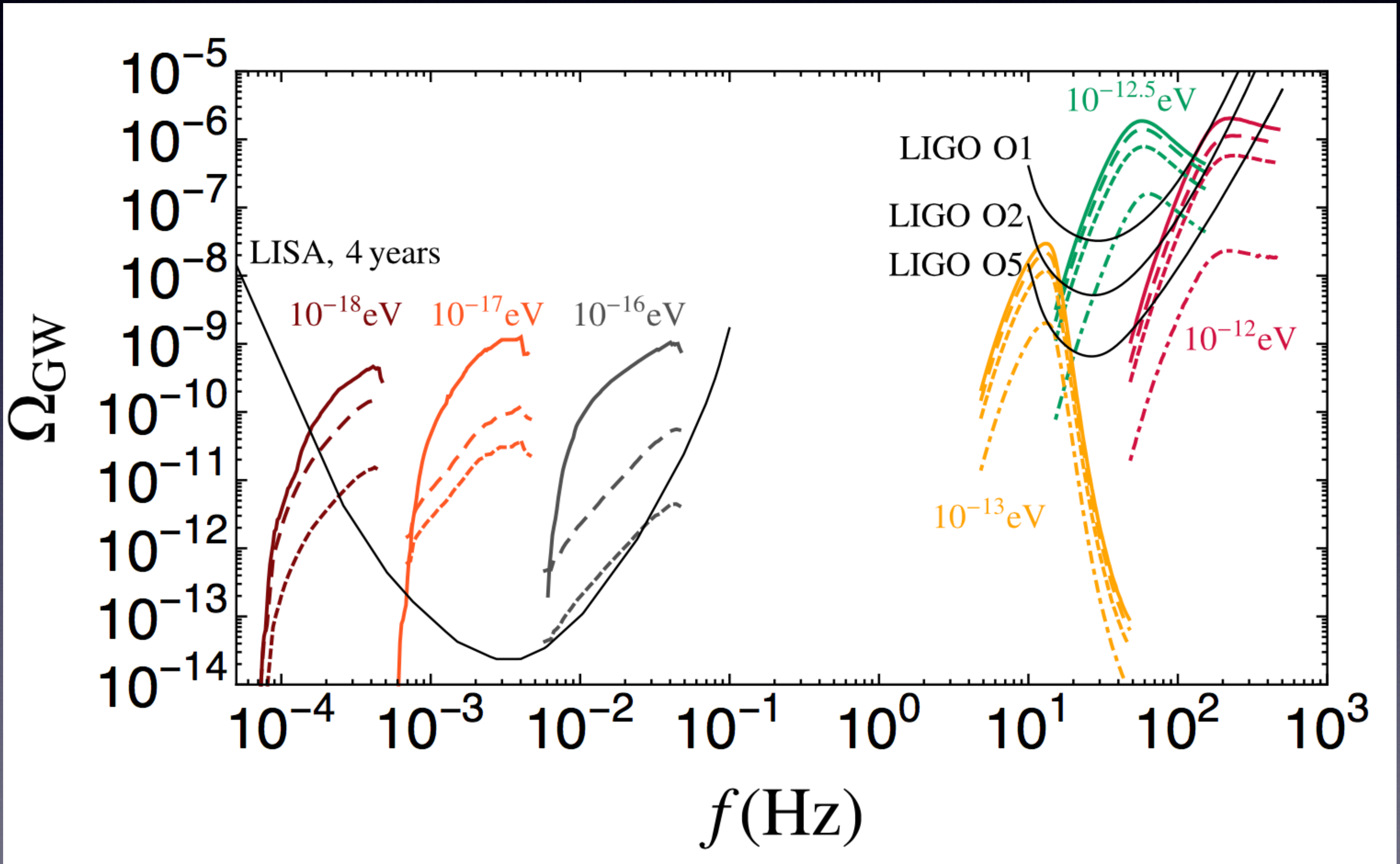

Brito EB, et al 2017

Bounds on BH mimickers

BH mimickers with no horizon are unstable to superradiance

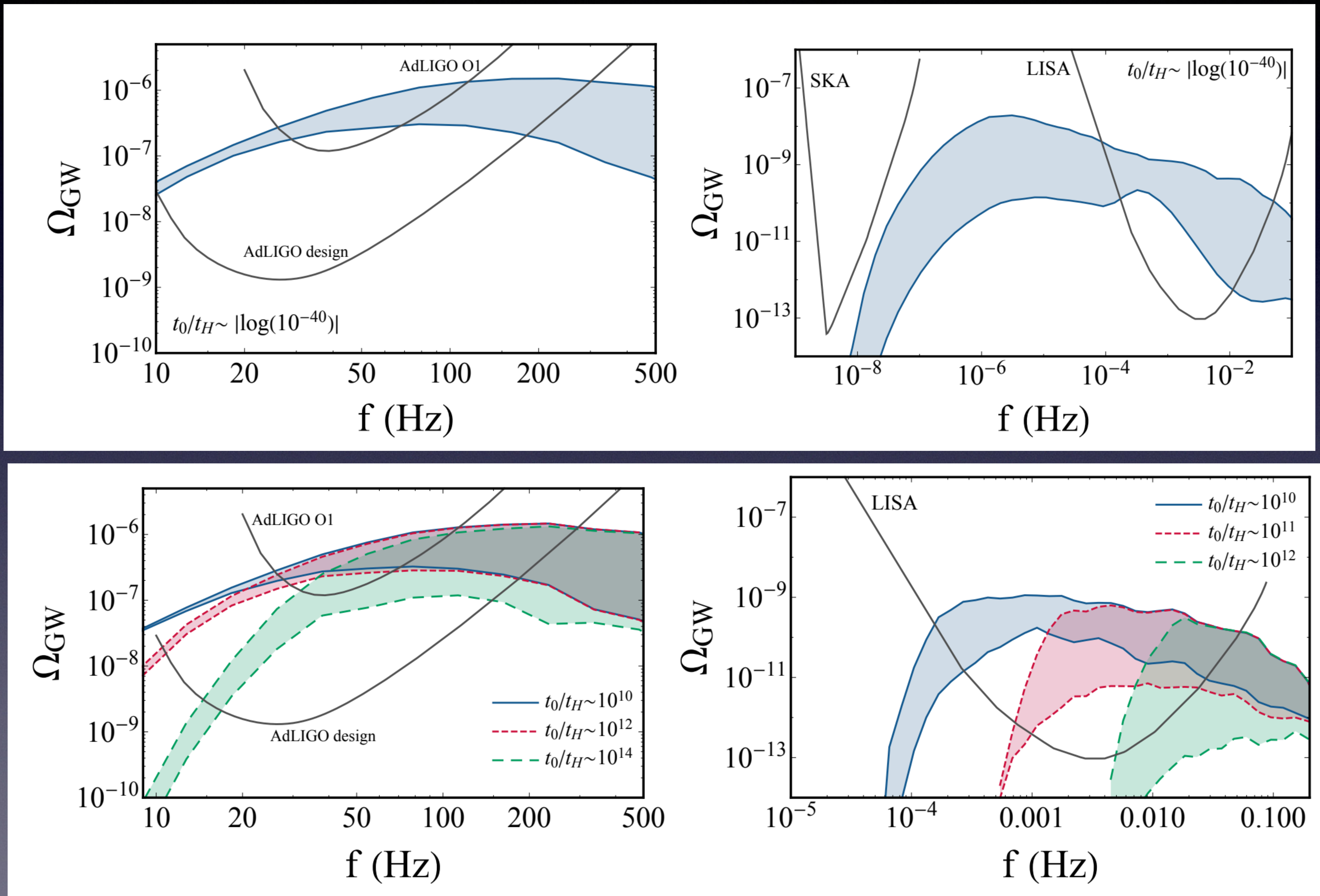

EB, et al 2018

Regge plane "holes"

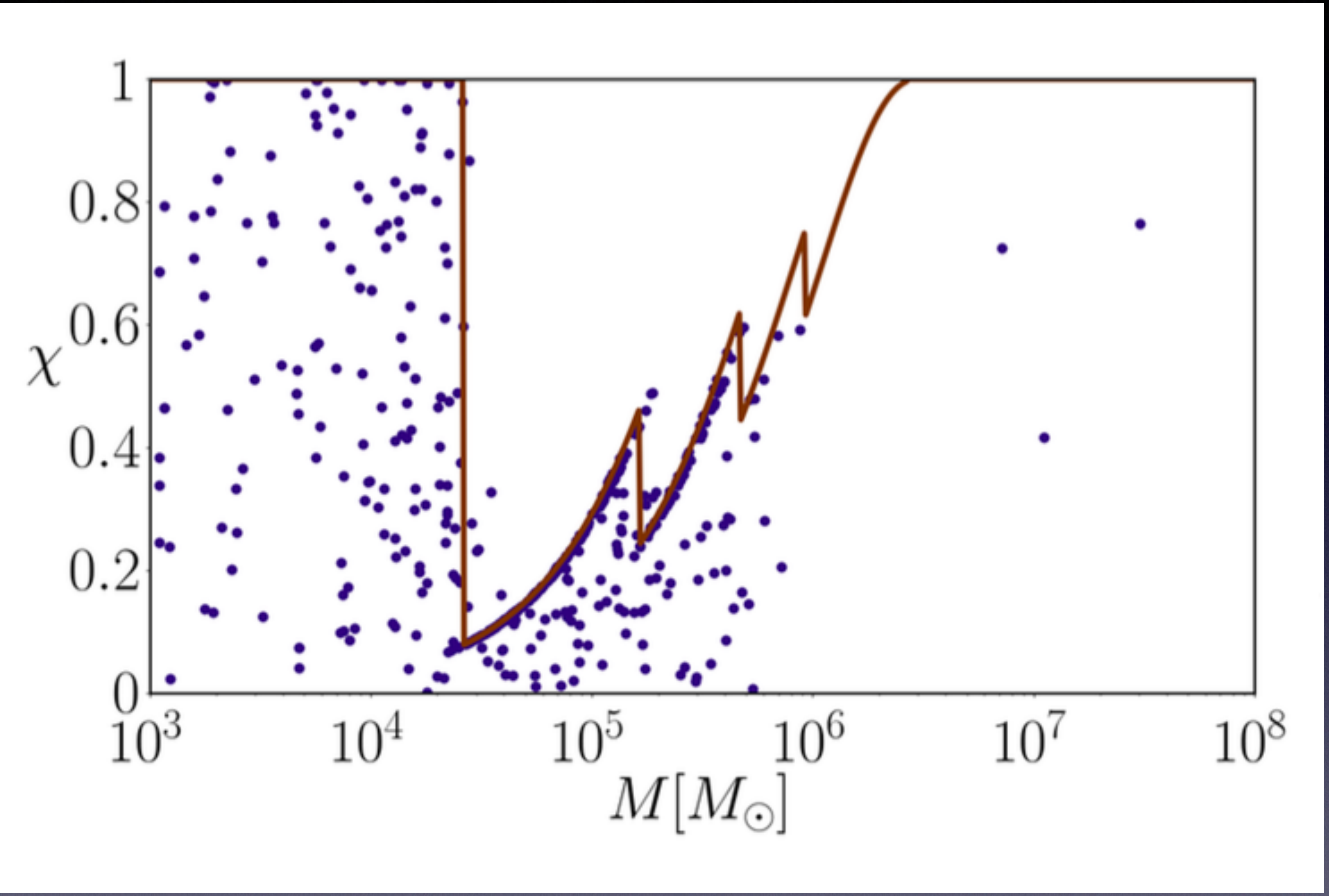

Brito EB, et al 2017

Look for "accumulation" near instability threshold
to avoid having to make assumptions
on astrophysical model

Conclusion

Gravitational waves have opened a new window on the Universe, and the LIGO/Virgo detections are just the beginning…